Ground-Based Observations for Validation (GBOV) of Copernicus Global Land Products

Algorithm Theoretical Basis Document - Energy products: RM1 (short wave radiation), LP1 (Top Of Canopy Reflectance), LP2 (Albedo)

Ref. : GBOV-ATBD-RM1-LP1-LP2

Version: 1.3

Date: 21/11/2019

Framework Contract ref.: 932059

Signatures

	Name	Company	Signature
Prepared by	Said Kharbouche, Rui Song, Jan-Peter Muller	University College London	
Reviewed by	Christophe Lerebourg	ACRI-ST	

Distribution list

Company	To
	Public Document

Changes Log

Version	Date	Changes
1.3	21/11/2019	Update at CP1 second release
1.2	05/12/2018	Minor correction
1.1	27/11/2018	Updated version for SC#2 closure
1.0	25/09/2018	Initial version delivered at the last milestone of the GBOV SC#2 – Component 1 – Year

Table of Content

List of Figures

List of Tables

1 Introduction

1.1 Context

The Copernicus Ground-Based Observations for Validation (GBOV) service aims to develop and distribute robust ground datasets from a selection of ground-based monitoring sites for a systematic and quantitative validation of EO land products. The EO land products of particular interest are those from the Copernicus Global Land Service (CGLS) biophysical and radiative variables[1]. The ATBD – Energy products deals with the energy/radiation aspects[2].

1.2 Scope of the Document

This document starts with a definition of the fundamental reference measurement (RM1) from the tower albedometers followed by a short description of the tower sites including their location and main measurement variables associated with each site. This is followed by an Algorithm Theoretical Basis Document (ATBD) on how the tower albedometer and shortwave radiation data from these sites, where available, can be employed to derive top-of-canopy albedo (LP2) and broadband reflectances (LP1) for validation of the CGLS albedo and Top of Canopy Reflectance (TOC-R).

1.3 Structure of the Document

This document contains the following chapters:

- This chapter introduces the document;
- Chapter 2 provides the scientific background to the algorithm and a description of the tower sites;
- Chapter 3 provides a detailed description of the algorithm;
- Chapter 4 provides examples of the application of the algorithm using tower data.
- Chapter 5 provides the processing chain and examples of upscaling the tower measurements to CGLS pixels;
- Chapter 6 presents the LP1 and LP2 uncertainty computation procedure;
- Chapter 7 Processing steps for upscaled TOC-R, DHR and BHR production
- Chapter 8 provides the scientific references cited in this document.
- Chapter 9 provides comparison of blue-sky-albedo (BSA) between CGLS products and in-situ retrievals

[1] https://land.copernicus.eu/global/themes/vegetation
[2] https://land.copernicus.eu/global/themes/Energy

1.4 Acronyms

The definition of the acronyms used in this document is provided hereafter:

ATBD	Algorithm Theoretical Basis Document
AOD	Aerosol Optical Depth
BHR	Bi-Hemispherical Reflectance
BRDF	Bidirectional Reflectance Distribution Function
BSRN	Baseline Surface Radiation Network
CGLS	Copernicus Global Land Service
DHR	Directional Hemispherical Reflectance
FLUXNET	A global network of energy and gas flux measurements made form tower sites
FoV	Field Of View
GBOV	Ground-Based Observations for Validation (GBOV) of Copernicus Global Land Products
IFOV	Instantaneous Field of View
LP	Land Product
JRC	Joint Research Centre
PAR	Photosynthetically Active Radiation
RM	Reference Measurement
SURFRAD	Surface Radiation Budget Network
SZA	Solar Zenith Angle
TOA	Top Of Atmosphere
WMO	World Meteorological Organization
TBC	To be Confirmed
TBD	To be Defined
TOC	Top Of Canopy
TOC-R	Top Of Canopy Reflectance

2 Scientific Background

2.1 Definition of Reference Measurement (RM1)

The Reference Measurement 1 (RM1), consists of the downward shortwave radiative flux (SW_IN), upward shortwave radiative flux (SW_OUT), and downward diffuse shortwave radiative flux (SW_DIF), which are employed to validate the energy-related Land Products (LPs) derived by the Copernicus Global Land Service.

Downward radiation is the sum of the direct and diffuse downwelling components of the solar radiation, upward radiation is the upwelling solar radiation reflected by the surface, and diffuse radiation is mainly the downward radiation that has been scattered by molecules (Rayleigh scattering), and particles in the atmosphere such as cloud droplets and aerosols (diffuse solar radiation). Shortwave relates to the part of the shortwave spectrum, typically understood as radiation in the spectral range between ca. 0.25 µm and 4.0 µm. A radiative flux is identical with the quantity measured by an ideal cosine-collector light-meter. In accordance with common usage in geophysical disciplines, flux implies per unit area. The unit of all the measurands in RM1 is W/m^2.

The shortwave radiation for validation purposes is measured by albedometers from the top of ground-based tower sites. A broadband albedometer essentially consist of two pyranometers, which measure total downward and upwelling shortwave radiation, respectively. Diffuse radiation is measured by an independent shaded pyranometer using a sun tracker to shield the sensor from direct sunlight. Figure 1 shows photos of Tumbarumba Flux tower, and configuration of the albedometers and other instruments.

Figure 1. Photos of 70m Tumbarumba Flux tower, and configuration of the albedometers (extreme right). Courtesy of Dr William Woodgate, CSIRO Australia

2.2 Overview of Tower Sites

Twenty tower sites have been selected for the first phase of the GBOV project. The sites are located over four continents as follows: Europe (7 sites), North America (11 sites), South

America (1 site), South-West Africa (1 site), Australia (2 sites), with the last 2 sites located in Antarctica at the South-Pole.

These sites belong to well established and "operational" networks: FLUXNET[3] (10 sites), SURFRAD[4] (7 sites), BSRN[5] (7 sites). Table 1 lists the key characteristics of the twenty selected sites including their associated network, geographic coordinates, start date timeframe, land cover type and other characteristics. For more clarification, Figure 2 shows the geographical distribution of the sites and, Figure 3 shows spaceborne pictures of the landscape (taken from Google Earth) for each site with overlapping pixel footprints of the finest grid of the CGLS products (1/112˚ x 1/112˚), the MODIS SIN BRDF/albedo product and, a circle of radius 500m around each tower site representing the projected Field of View (FOV) of an albedometer (Zuosen, private communication, 2012) from a tower altitude of 50m.

Table 1. List of tower sites with key characteristics: acronym, coordinates, network, frame date, spectral bands, tower height, vegetation height, footprint diameter and land cover type.

Station	Acronym	Lat	Lon	Network	Start year	Tower height [m]	Vegetation height [m]	Footprint diameter [m] see page 45	Land classification (IGBP)
Barrow, Alaska, US	US-BRW	71.323	-156.607	BSRN	2002	4		91	Snow and Ice
Boulder atmospheric observatory, Colorado, US	US-BAO	40.050	-105.004	BSRN	1995				Cropland Mosaics
Concordia Station	DOM	-75.1	123.383	BSRN	2006	2	0	46	Sonw and Ice
Cabauw, Netherland	NL-CAB	51.971	4.927	BSRN	2005	2	0	46	Grassland
Gobabeb, Namibia	NM-GOB	-23.561	15.042	BSRN	2012	2	0	46	Desert
Ny-Ålesund, Norway	NO-NYA	78.925	11.93	BSRN	1992	2	0	46	Tundra
South Pole Observatory, Antarctica	SPO	-90.000	59.000	BSRN	1999		0		Snow and Ice
ARM Southern Great Plains site, Oklahoma & Kansas, US	US-ARM	36.606	-97.489	FLUXNET	2006	2/2.55	0	46/58	Croplands
Brasschaat, Belgium	BE-Bra	51.309	4.521	FLUXNET	2010	40	21	434	Mixed Forest
Calperum, Australia	AU-Cpr	-34.003	140.588	FLUXNET	2010	20	3	389	Closed Shrublands
Gebesee, Germany	DE-Geb	51.100	10.914	FLUXNET	2004				Croplands
Grignon, France	FR-Gri	48.844	1.952	FLUXNET	2000	2.5/5.3		57/121	Croplands
Guyaflux, French Guiana	GF-Guy	5.279	-52.925	FLUXNET	2004	58	35	526	Evergreen Broadleaf
Hainich, Germany	DE-Hai	51.070	10.450	FLUXNET	2000	42	9	754	Mixed Forest
Niwot Ridge, Colorado, US	US-NR1	40.033	-105.546	FLUXNET	1998	25.5	13	286	Evergreen Needleleaf
Renon, Italy	IT-Ren	46.587	11.434	FLUXNET	2000				Evergreen Needleleaf
Tumbarumba, Australia	AU-Tum	-35.657	148.152	FLUXNET	2011	70	30	914	Evergreen Broadleaf
Bondville, Illinois, US	US-BON	40.052	-88.373	SURFRAD	1995	10		229	Croplands
Desert Rock, Nevada, US	US-DRA	36.624	-116.019	SURFRAD	1998	10		229	Open Shrublands
Goodwin Creek, Mississippi, US	US-GCM	34.255	-89.873	SURFRAD	1995	10		229	Deciduous Broadleaf
Fort Peck, Montana, US	US-FPK	48.308	-105.102	SURFRAD	1995	10		229	Grasslands
Rock Springs Penn, State University, US	US-PSU	40.720	-77.931	SURFRAD	1998	10		229	Deciduous Broadleaf
Sioux Falls, South Dakota, US	US-SXF	43.730	-96.620	SURFRAD	2003	10		229	Croplands
Table Mountain, Boulder, Colorado, US	US-TBL	40.125	-105.237	SURFRAD	1995	10		229	Bare soil and Rocks

[3] https://fluxnet.ornl.gov
[4] https://www.esrl.noaa.gov/gmd/grad/surfrad/
[5] http://bsrn.awi.de

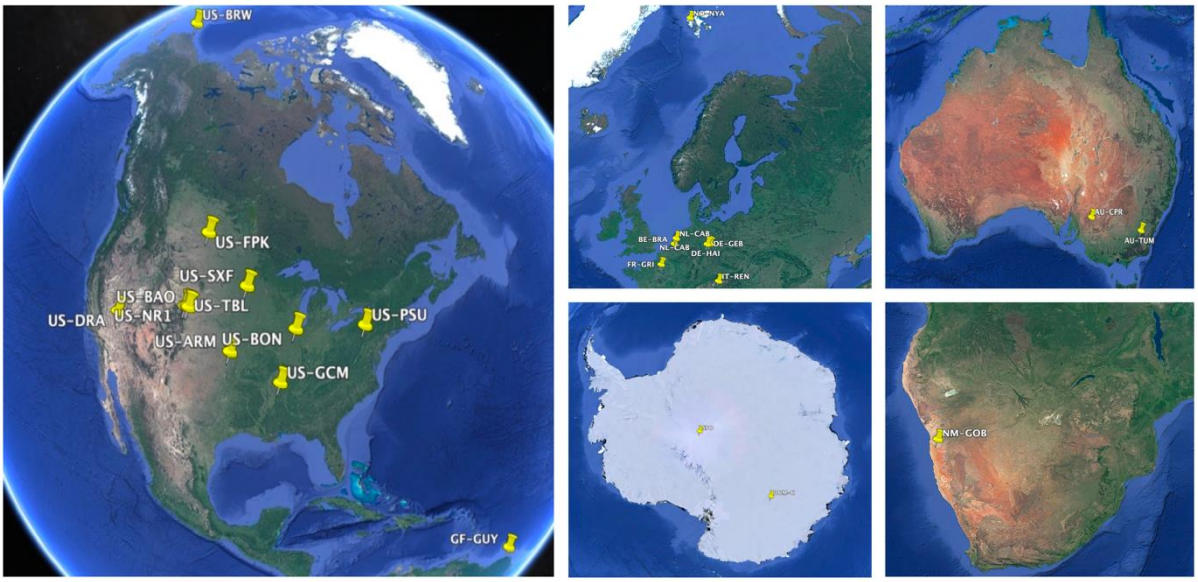

Figure 2. Geographical distribution of selected sites (Google Earth).

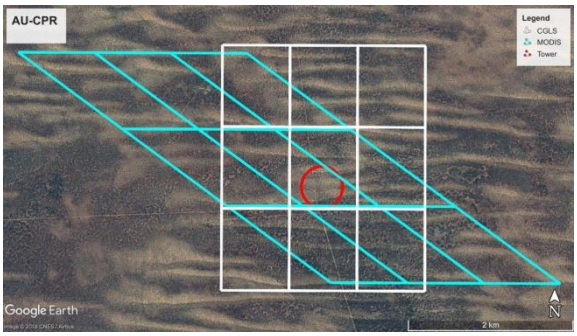

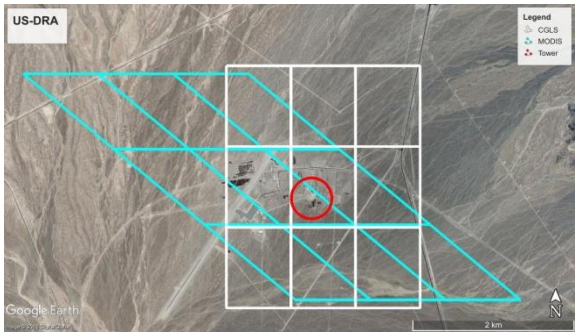

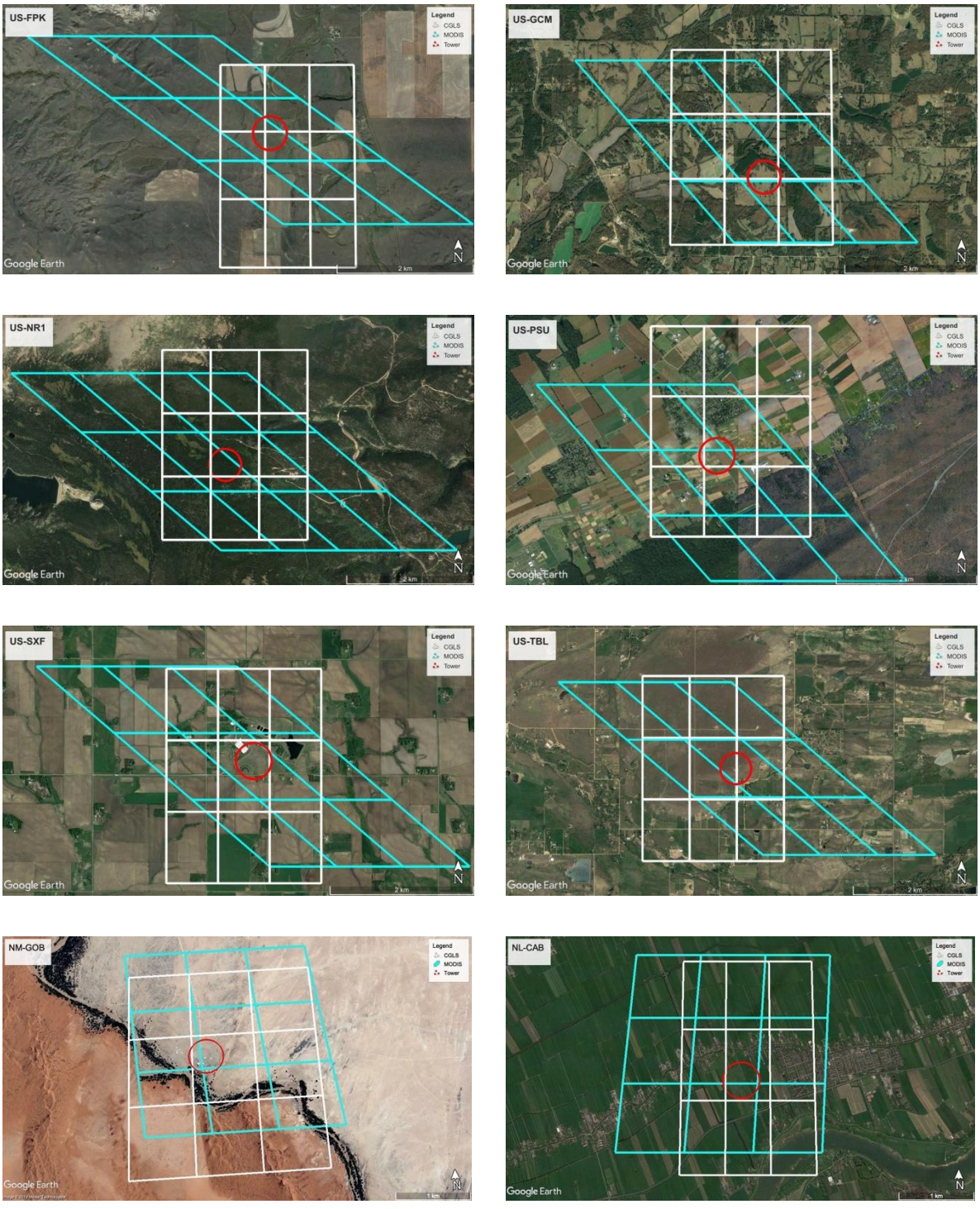

Figure 3. Overview of selected tower sites (taken using Google Earth). The white line represents CGLS Spot/VGT product pixel footprints of 1/112º, the MODIS SIN projection grid for 3 x 3 km pixels is shown in cyan and the red circle around the tower shows a 500m radius equivalent to a tower albedometer footprint from a tower of 50m in height. The site short-name is indicated and a nadir view employed. No standard VGT-CGLS data are produced above ±60˚of latitude so neither BSRN-BRW nor SPO are displayed. N.B. The MODIS SIN projection is more distorted in the Western hemisphere, the further the west one goes.

2.3 Tower data characteristics

The albedometer sensor types are not identical for many key characteristics, namely spectral bands, instantaneous field of view (IFOV) and tower height. In addition to these differences, data of each network are provided with different temporal frequency, variables, naming and format.

In this section, we focus only on the variables that are used for the derivation of LP1 (Surface Reflectance) and LP2 (Surface Albedo). Table 2 for each network provides the names of variables from the three Networks for the relevant measurands and their quality flags.

Table 2. Variables of interest with their equivalence in FLUXNET, SURFRAD and BSRN networks.

Variable	Description	Network		
		FLUXNET	SURFRAD	BSRN
down_total_sw	Downwelling total radiation shortwave [W/m^2]	SW_IN_F	dw_solar	SWD
down_total_sw_sigma	Uncertainty or quality flag of down_total_sw	SW_IN_F_QC	---	---
up_total_sw	Upwelling total radiation shortwave [w/m2]	SW_OUT_F	uw_solar	SWU
up_total_sw_sigma	Uncertainty or quality flag of up_total_sw	SW_OUT_F_QC	---	---
down_diffuse_sw	Downwelling diffuse radiation shortwave [w/m^2]	SW_DIF	diffuse	DIFF[6]
down_diffuse_sw_sigma	Uncertainty or quality flag for down_diffuse_sw	SW_DIF_QC	---	---
down_potential_ToA_SW	Downwelling potential Top-of-Atmosphere Radiance	SW_IN_POT	---	---
datetime	Date and time of measurements [yyymmddMMHHSS]	TIMESTAMP	Year,MM,DD,HH,MM	year,day, month,day, hour,min

[6] The BSRN report the standard deviation over the sampling period (1min with acquisition at 1 sec) and the maximum and minimum values (when available). An alternative can be to use the difference between SWD and the component sum DIR cosZ +DIF to estimate the uncertainty (or flag data).

tz	Time zone	Local	UTC	UTC
sza	Solar zenith angle [degree]	---	zen	

2.3.1 Estimation of diffuse radiation

Some FLUXNET sites do not measure downwelling diffuse shortwave radiation, which is an essential variable for calculating Bi-Hemispherical Reflectance (BHR). To deal with this obstacle, we propose to estimate the ratio of diffuse (β) using the potential Top of Atmosphere (TOA) radiance (*SW_IN_POT*) (W. Woodgate, private communication, 2018). For the actual variable, using names for FLUXNET only, this formula is as follows:

$$\beta = (SW\_IN\_POT - SW\_IN\_F) \ / \ SW\_IN\_POT \quad (1)$$

For tower sites which do not include such measurements or those with missing values in *SW_IN_POT*, they can be estimated based on the location and local time of the measurements. Firstly, the incidence of solar radiation on a surface of $\theta = 0°$ outside the Earth's atmosphere varies with the day of year number and can be computed from the solar constant as follows:

$$I_0 = I_{SC}(1.000110 + 0.034221\, cos\,\Gamma + 0.001280\, sin\,\Gamma + 0.000719\, cos\,2\Gamma + 0.000077\, sin\,2\Gamma) \quad (2)$$

where I_{SC} is the solar constant taken usually as 1367 W/m^2. Γ is the day angle in radians and is represented by

$$\Gamma = 2\pi(\frac{n-1}{365}) \quad (3)$$

SW_IN_POT is the radiation incident on the surface tangent to the outer surface of the atmosphere. It is a function of zenith angle, θ_{in}, thus, it is a function of latitude, time during the day and number of the day in the year. *SW_IN_POT* is given by:

$$SW\_IN\_POT = I_0 \cos\theta_{in} = I_0(cos\,\varphi\, cos\,\delta\, cos\,\omega + sin\,\varphi\, sin\,\delta) \quad (4)$$

where δ is the declination angle, ω is the hour angle and φ is the latitude.

A final linear or quadratic function needs to be obtained by fitting these to as many FLUXNET sites as possible which already have the diffuse component available. Note that we are not inserting the whole range of β, just when β is very low (DHR is usually defined when β=0) or very high (BHR is usually defined as $DIF/SWD = 1$). For example, Figure 4 plots β against *(SW_IN_POT – SW_IN_F) / SW_IN_POT* for the FLUXNET site of Hainich (DE-Hai); it shows there is a reasonable linear relationship but we only use the values for the grey area in this work.

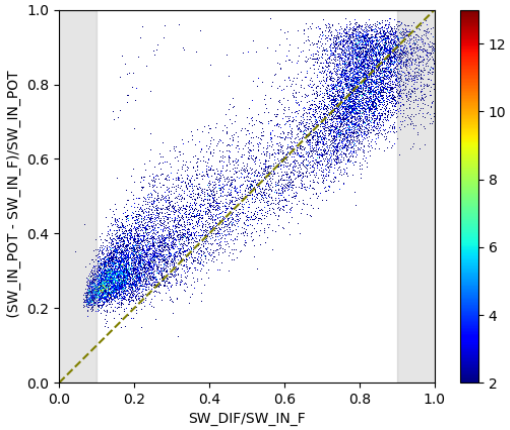

Figure 4. Ratio of diffuse (β) against (SW_IN_POT–SW_IN_F)/SW_IN_POT, over the FLUXNET site of Hainich (DE-Hai). The grey area represents our intervals of interest for β.

2.3.2 Time series of tower data

Time series of the selected tower sites were downloaded and analysed to check their consistency and continuity. Figure 5 shows the time series of some of these key variables for all selected FLUXNET, BSRN and SURFRAD sites between 1st January 2012 and 31st December 2018.

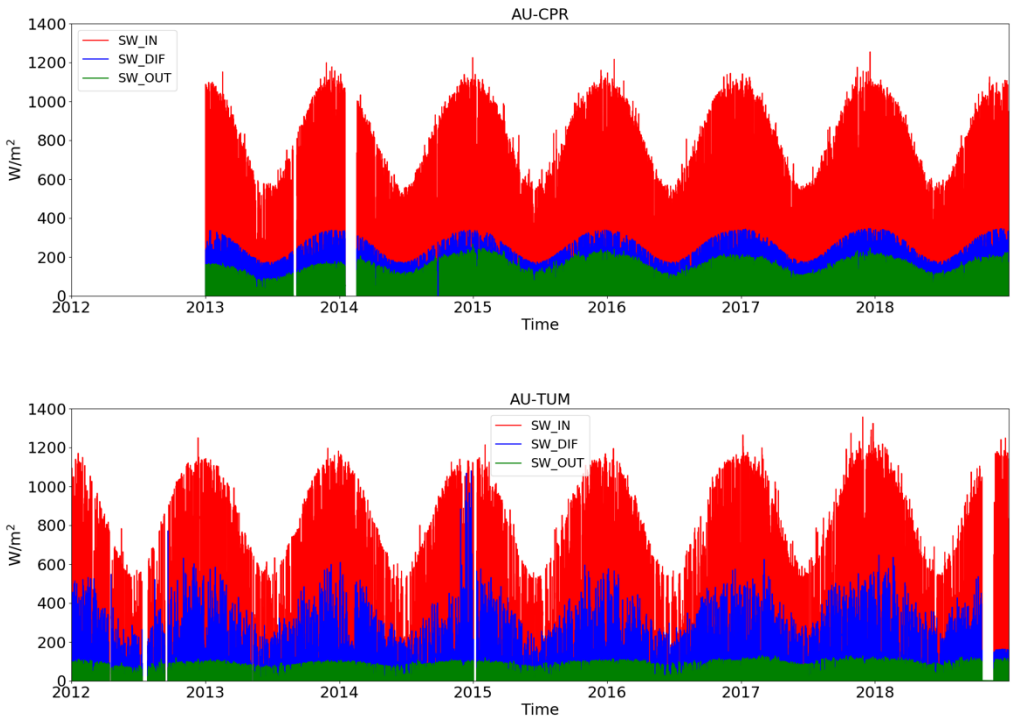

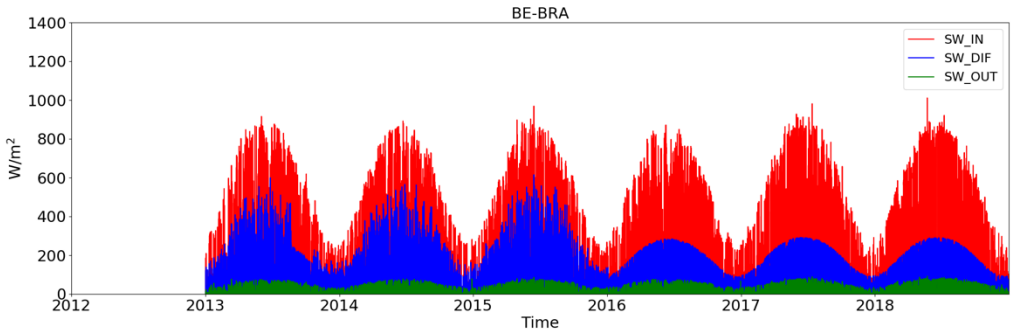

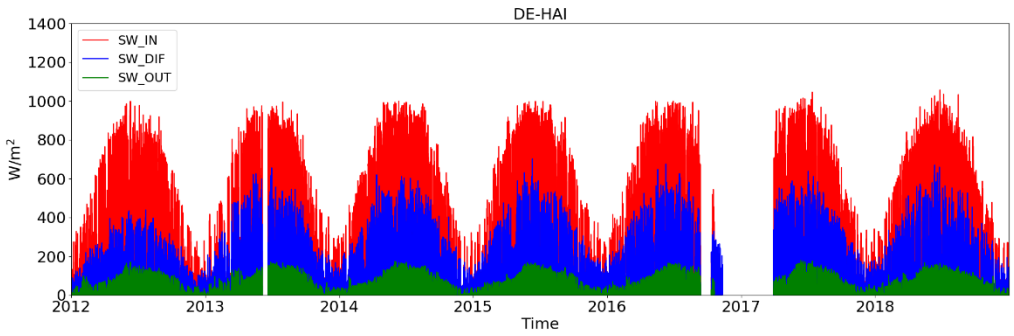

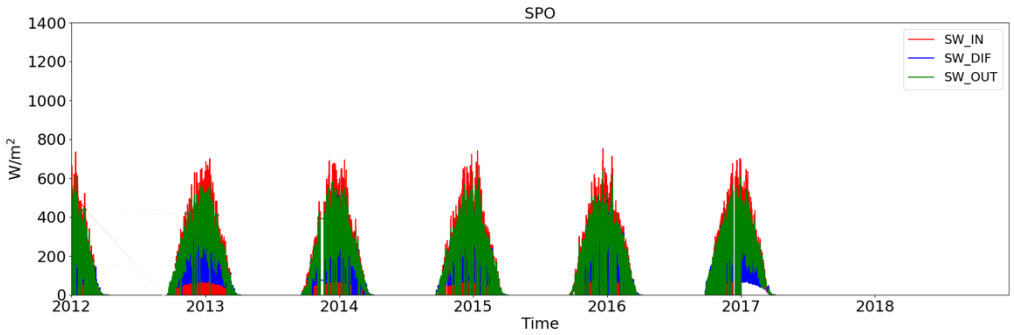

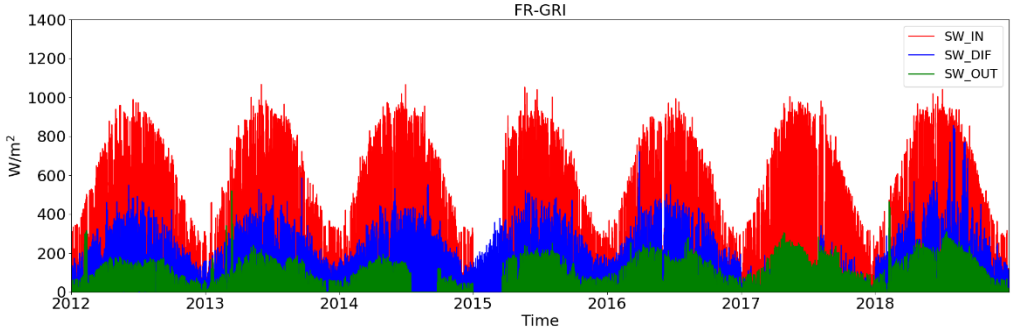

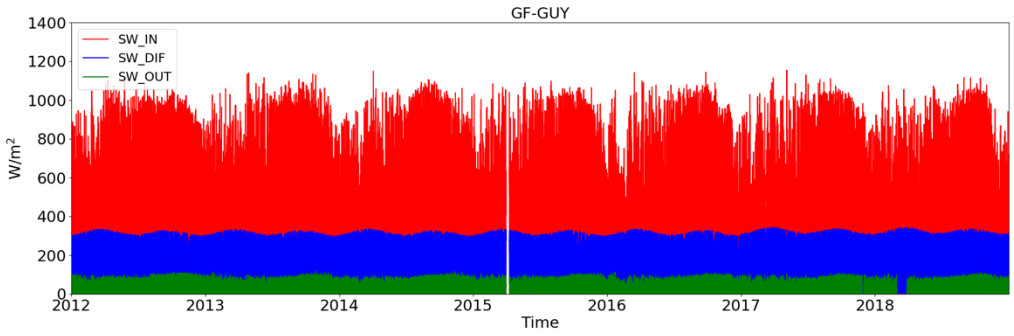

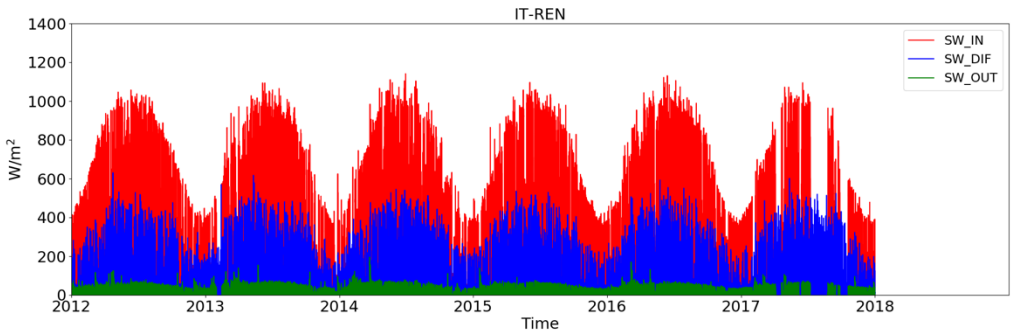

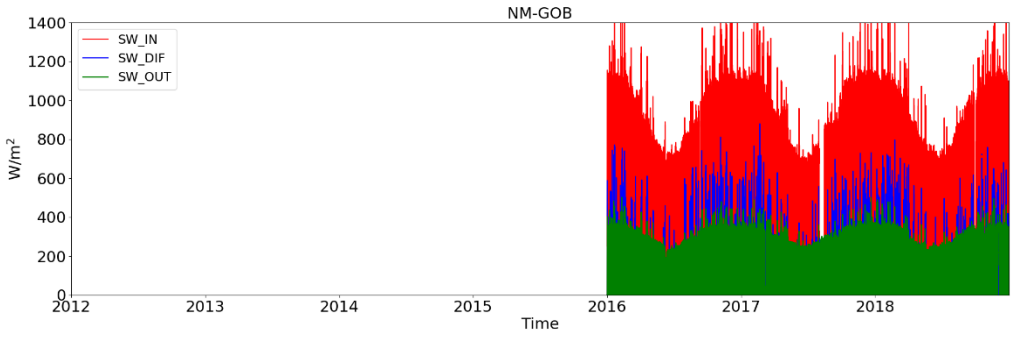

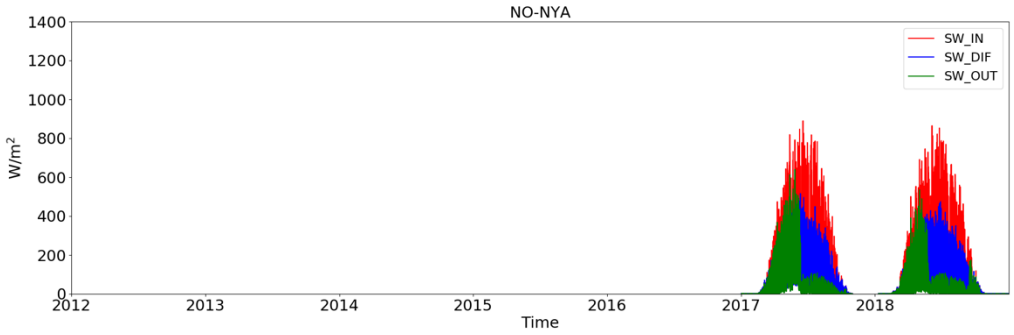

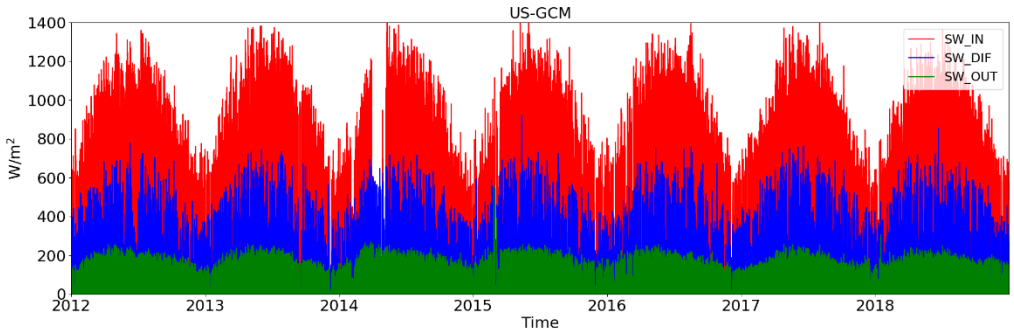

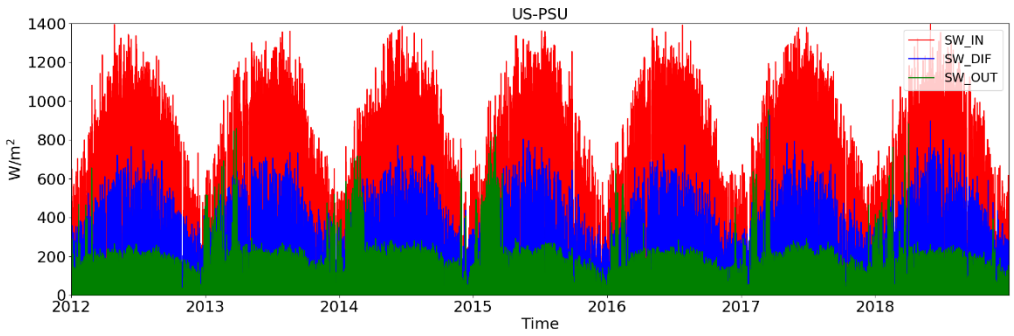

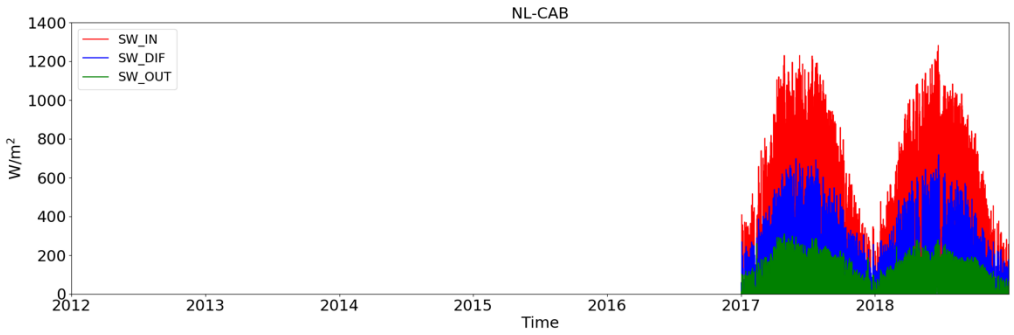

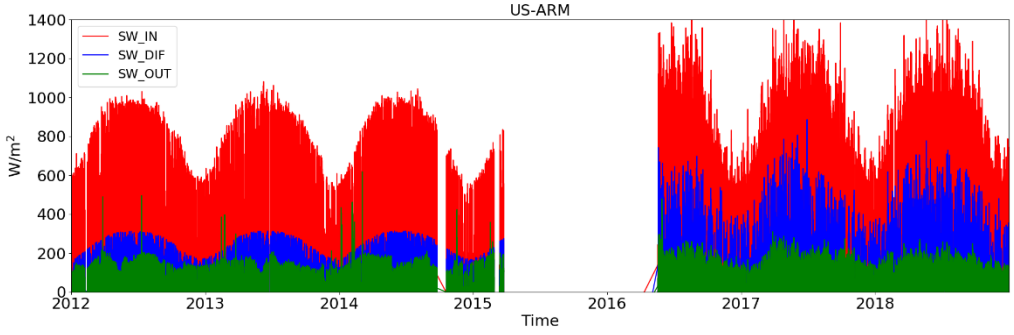

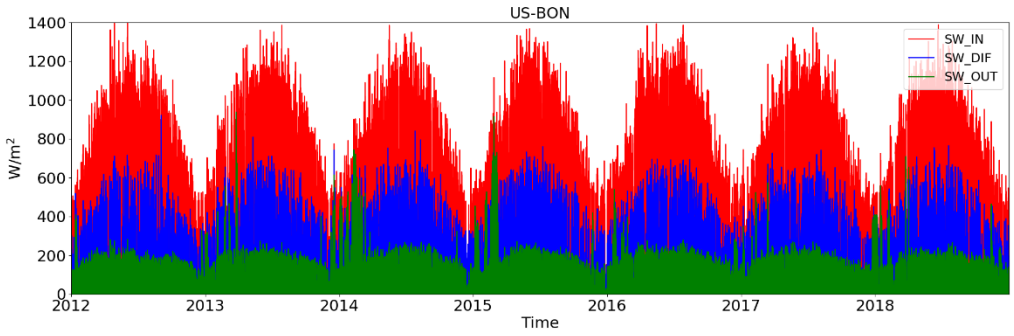

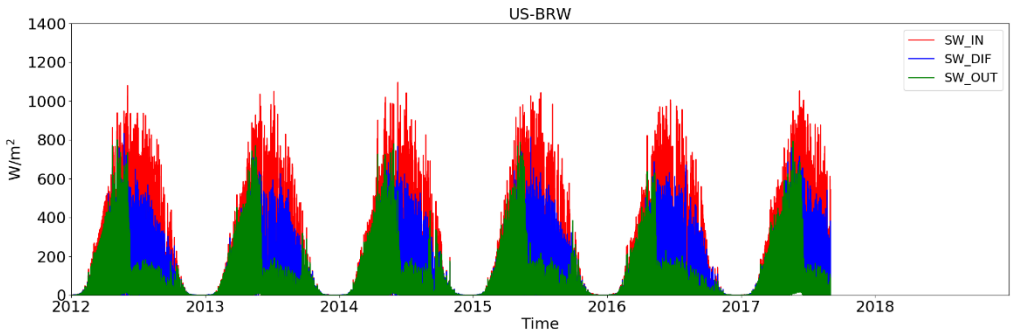

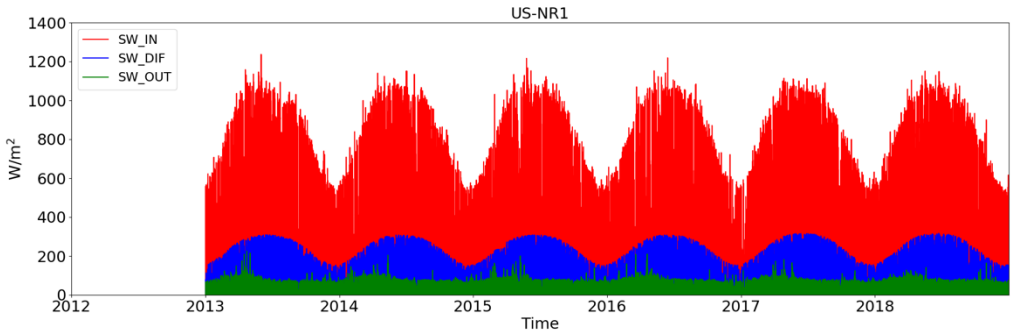

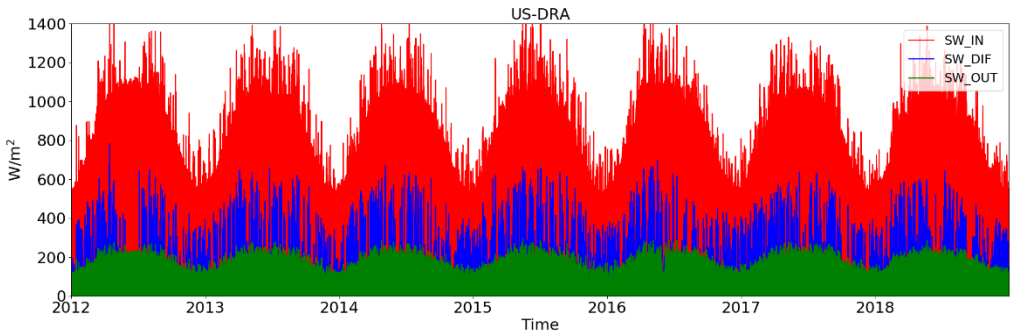

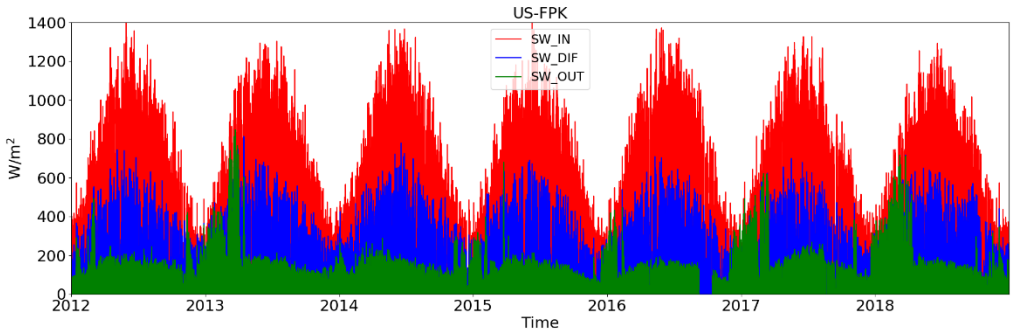

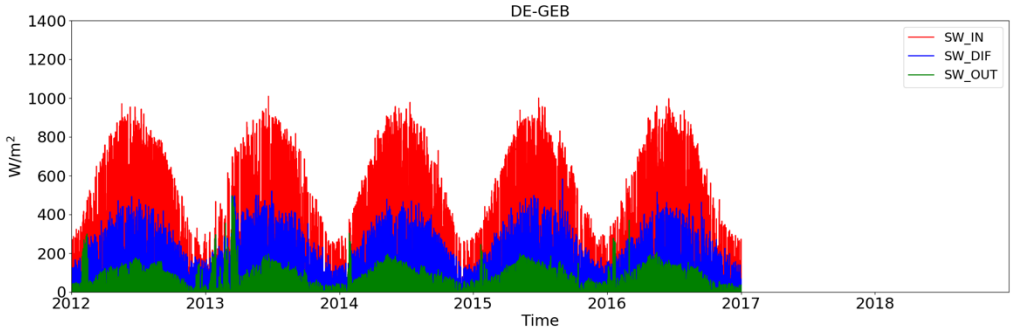

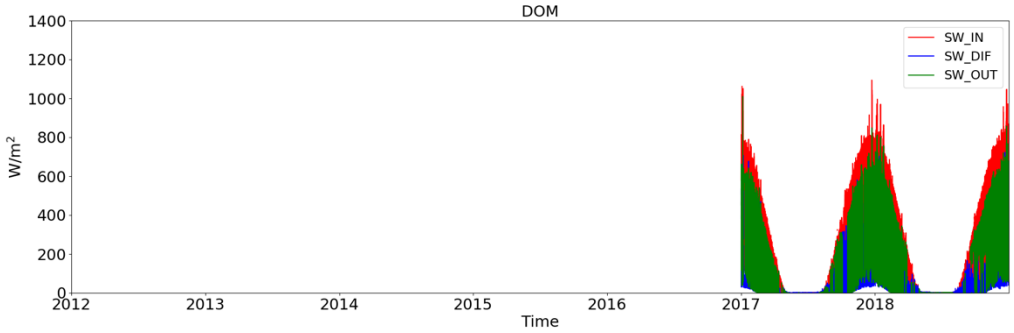

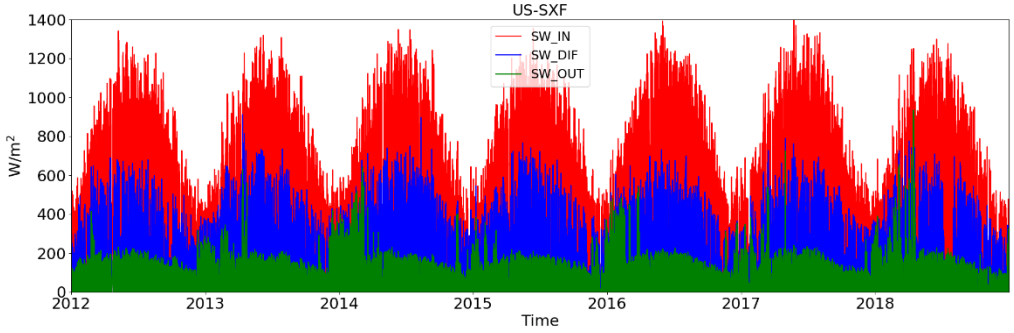

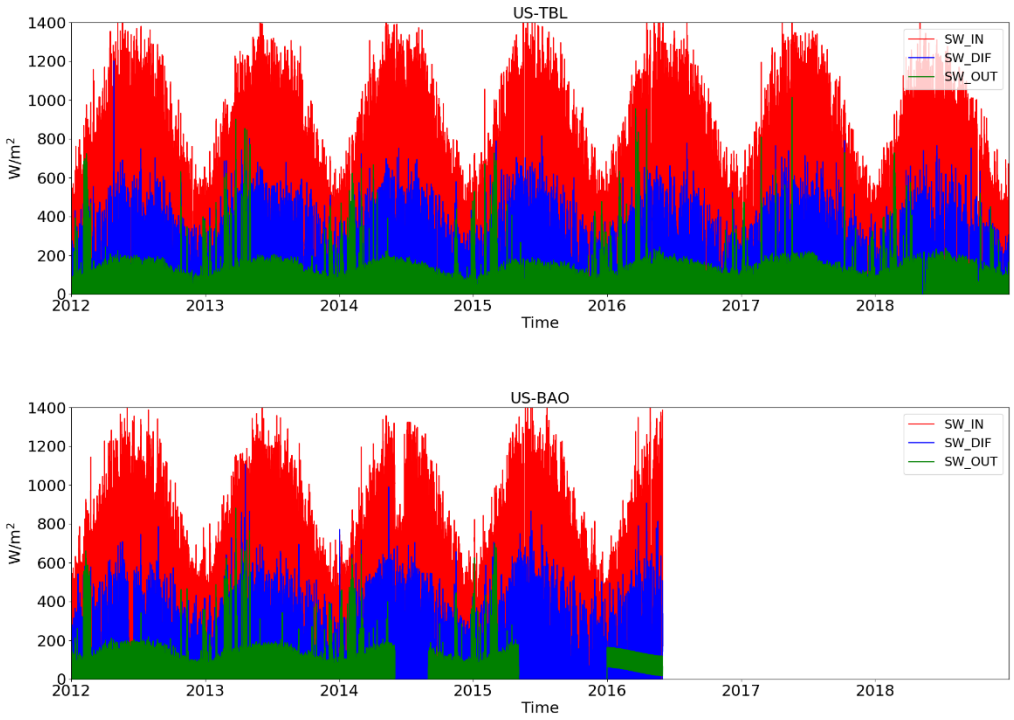

Figure 5. Time series of the RM1 for the selected sites showing all 3 quantities between 01.01.2012 and 31/12/2018. Diffuse radiation from US-NR1, GF-GUY and AU-CPR are calculated using the method described in Section 2.3.1.

After producing RM1, LP1 and LP2 for the selected 20 sites between 1st January 2012 and 31st December 2016, the GBOV project is producing an improved version of LP1 and LP2 products using new datasets covering the time period from 01/01/2017 to 31/12/2018. The Sensor invariant Atmospheric Correction (SIAC) method is now being employed as the atmospheric correction tool in producing upscaled LP1 and LP2 between 01/01/2017 and 31/12/2018. A detailed description about the SIAC method is introduced in Section 5.2.

2.3.3 Uncertainty of tower data

Currently, few studies have addressed the uncertainty of solar radiation observations. In summary, solar radiation estimated by a commercial pyranometer has an uncertainty of 5% (at a 95% confidence level) for daily values under ideal conditions (Reda, 2011). Table 3 gives details of the actual radiometers used at the selected sites with the manufacturer's quoted uncertainties and the temporal frequency that data is recorded at.

For Fluxnet sites, Cescatti et al. (2012) compared MODIS albedo retrievals at 500m with *in situ* measurements with varying footprints across the FLUXNET towers for sites which were deemed to be homogeneous. However, there were no detailed uncertainty calculations included in their work, but an expected accuracy of 4-7% in clear sky and 1-4% in overcast condition was given. In this particular case, the method developed by Román et al. (2009) was employed to select only those FLUXNET sites where the homogeneity met certain criteria

based on a semi-variogram analysis of higher resolution Landsat data only using sites where the spatial heterogeneity is low at scales of 1-3km. In this way, any issues related to heterogeneity and upscaling could be ignored. There are also a few other publications associated with the solar radiation measured at the Fluxnet network sites, where most of them estimate an overall uncertainty of 5%. For all the FLUXNET sites, Kipp & Zonen CNR1 & CNR4 albedometers were utilised. The daily uncertainties of CNR4 and CNR1 are provided in the Kipp & Zonen Instruction Manual. It is worth noting that previous studies have shown that solar radiation derived from the net radiometer CNR1 may have substantial errors.

At the SURFRAD sites, the SpectroSun SR-75 and Eppley 8-48 pyranometers are used to measure the global and diffuse solar radiation, respectively. The Eppley 8-48 is a World Meteorological Organization (WMO) second-class pyranometer that lacks thermal offset issues. The SpectroSum SR-75 provides an independent check for the sum of direct and diffuse solar radiation at the SURFRAD sites.

At the start of the BSRN programme, the uncertainties of global and diffuse solar radiation were estimated as 15 and 10 W/m^2, respectively. With the development of new sensors and methods of observation, the overall uncertainties have been reduced to 5 W/m^2 (3%) for global solar radiation and 3 W/m^2 (2%) for diffuse solar radiation.

In the process of upscaling surface reflectance and albedo from tower measurements onto the grid of CGLS products, errors are estimated by considering the uncertainty of albedometers.

Table 3. Summary of collected sites and their instrument type for solar radiation measurements.

Site	Network	Instrument type	Uncertainty	Sampling frequency	Time range
US-BAO	BSRN	Kipp & Zonen CMP21/22	Global: 2% or 5 W/m^2 Diffuse: 2% or 3 W/m^2	1minute	2012-2015
US-BRW	BSRN	Kipp & Zonen CMP21/22	Global: 2% or 5 W/m^2 Diffuse: 2% or 3 W/m^2	1minute	2013-2016
SPO	BSRN	Kipp & Zonen CMP21/22	Global: 2% or 5 W/m^2 Diffuse: 2% or 3 W/m^2	1minute	2013-2016
DOM	BSRN	Kipp & Zonen CMP21/22	Global: 2% or 5 W/m^2 Diffuse: 2% or 3 W/m^2	1minute	2017-2018
NL-CAB	BSRN	Kipp & Zonen CMP21/22	Global: 2% or 5 W/m^2 Diffuse: 2% or 3 W/m^2	1minute	2016-2018
NM-GOB	BSRN	Kipp & Zonen CMP21/22	Global: 2% or 5 W/m^2 Diffuse: 2% or 3 W/m^2	1minute	2016-2018
NO-NYA	BSRN	Kipp & Zonen CMP21/22	Global: 2% or 5 W/m^2 Diffuse: 2% or 3 W/m^2	1minute	2017-2018
US-BON	SURFRAD	Global: Pyranometer (SpectroSun SR-75) Diffuse: Pyranometer (Eppley 8-48)	Global: 2 - 5% Diffuse: 5 W/m^2	1minute	2013-2018
US-DRA	SURFRAD	Global: Pyranometer (SpectroSun SR-75) Diffuse: Pyranometer (Eppley 8-48)	Global: 2 - 5% Diffuse: 5 W/m^2	1minute	2013-2018
US-FPK	SURFRAD	Global: Pyranometer (SpectroSun SR-75) Diffuse: Pyranometer (Eppley 8-48)	Global: 2 - 5% Diffuse: 5 W/m^2	1minute	2013-2018
US-GCM	SURFRAD	Global: Pyranometer (SpectroSun SR-75) Diffuse: Pyranometer (Eppley 8-48)	Global: 2 - 5% Diffuse: 5 W/m^2	1minute	2013-2018

US-PSU	SURFRAD	Global: Pyranometer (SpectroSun SR-75) Diffuse: Pyranometer (Eppley 8-48)	Global: 2 - 5% Diffuse: 5 W/m^2	1minute	2013-2018
US-TBL	SURFRAD	Global: Pyranometer (SpectroSun SR-75) Diffuse: Pyranometer (Eppley 8-48)	Global: 2 - 5% Diffuse: 5 W/m^2	1minute	2013-2018
US-SXF	SURFRAD	Global: Pyranometer (SpectroSun SR-75) Diffuse: Pyranometer (Eppley 8-48)	Global: 2 - 5% Diffuse: 5 W/m^2	1minute	2013-2018
AU-CPR	Fluxnet	Kipp & Zonen CNR4	5%	30 minutes	2013-2018
AU-TUM	Fluxnet	Kipp & Zonen CNR4	5%	1 hour	2013-2018
BE-BRA	Fluxnet	Kipp & Zonen CNR4	5%	1 hour	2013-2018
DE-GEB	Fluxnet	Kipp & Zonen (version TBC)	-	30 minutes	2012-2015
DE-HAI	Fluxnet	Kipp & Zonen CNR1	10%	10 minutes	2012-2018
FR-GRI	Fluxnet	Kipp & Zonen CM7B (2012-December 2014) Kipp & Zonen CNR4 (March 2015 - now)	5%	10 minutes	2012-2018
GF-GUY	Fluxnet	Kipp & Zonen CNR1	10%	30 minutes	2012-2018
IT-REN	Fluxnet	Kipp & Zonen CNR1	10%	30 minutes	2012-2017
US-NR1	Fluxnet	Kipp & Zonen CNR1	10%	30 minutes	2013-2018
US-ARM	Fluxnet	Kipp & Zonen CNR4	5%	30 minutes	2012-2018

2.3.4 Data filtering

The shortwave solar radiation data contains noise which needs to be filtered out as far as possible. Several rules are applied to filter the shortwave solar radiation data before they can be further processed into surface reflectance and albedo. Firstly, radiation data with invalid values (i.e. zero or negative radiation values) need to be eliminated. Secondly, in order to use the Bidirectional Reflectance Distribution Function (BRDF) model which is based on a semi-empirical linear assumption, only data with solar zenith angle smaller than 75° are retained. For SURFRAD and for BSRN sites which are calculated from the location and date/time, the solar zenith angle is given directly as an independent variable. For FLUXNET sites, the solar zenith angle needs to be calculated from the local date and time. In summary, radiance data with a direct-to-diffuse ratio smaller than a threshold (β_{max}) are used to estimate the DHR, while data with this “diffuse ratio” larger than a threshold (β_{min}) is used to estimate the BHR.

3 Copernicus Global Land Surface product

The Copernicus Global Land Surface component in the framework of "GMES Initial Operations" (GIOGL) aims to provide several satellite-derived land products. Two of these products are Albedo and normalized Top of Canopy reflectance (TOC-R), which are both derived from the same Bidirectional Reflectance Distribution Function (BRDF). The BRDF is derived from level-1 data (Top of Atmosphere reflectance) product of VGT/Proba-V spaceborne sensors after performing inter-sensor calibration, cloud/snow masking and atmospheric correction. Figure 6 shows an overview of the published processing chain for Albedo and TOC-R production from the spaceborne instruments.

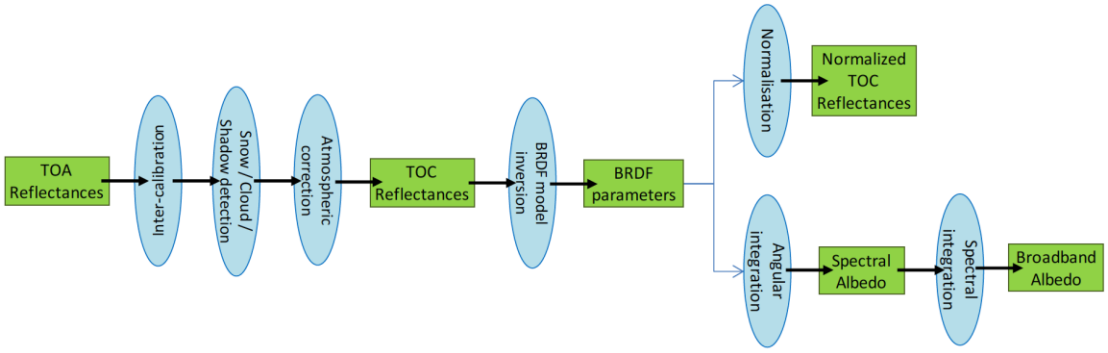

Figure 6. Flow chart of Albedo and TOC-R chain algorithm (after Lacaze 2014).

We now discuss more about the BRDF, Albedo and TOC-R creation. For an in depth description of all the processing stages we refer the reader to the ATBDs of TOC-R and Albedo (Lacaze 2014; Roujean 2014).

3.1 BRDF Creation

The BRDF employed is the semi-empirical linear model of (Roujean, 1992) where the reflectance is represented as follows:

$$R(\lambda,\ \theta_{in},\ \theta_{out},\ \varphi) = k_0(\lambda) + k_1(\lambda) f_1(\theta_{in},\ \theta_{out},\ \varphi) + k_2(\lambda) f_2(\theta_{in},\ \theta_{out},\ \varphi) \qquad (5)$$

where θ_{in} denotes solar zenith angle, θ_{out} denotes view zenith angle, φ_{in} denotes solar azimuth angle, φ_{out} denotes view azimuth angle, φ denotes relative azimuth angle ($\varphi_{in} - \varphi_{out}$). The three scalar values k_0, k_1 and k_2 are referred to as the BRDF parameters that are calculated for each spectral band, λ. The parameter k_0 is known as the isotropic contribution to the reflectance factor ($f_0 = 1$), with functions f_1 and f_2 representing the angular distribution related to geometric and volumetric surface scattering processes, respectively. f_1 and f_2 can be represented as follows:

$$f_1(\theta_{in}, \theta_{out}, \varphi) = \frac{1}{2\pi}[(\pi - \varphi)cos\varphi + sin\varphi]tan\theta_{in}tan\theta_{out} - \frac{1}{\pi}(tan\theta_{in} + tan\theta_{out} + \sqrt{tan^2\theta_{in} + tan^2\theta_{out} - 2tan\theta_{in}tan\theta_{in}cos\varphi}) \qquad (6)$$

for $\varphi \in [0, \pi]$

$$f_2\,(\theta_{in}, \theta_{out}, \varphi) = \frac{4}{3\pi}\frac{1}{cos\theta_{in} + cos\theta_{out}}\left[\left(\frac{\pi}{2} - \xi\right)cos\xi + sin\xi\right] - \frac{1}{3} \quad (7)$$

with $\xi = \arccos\left[cos\theta_{in}cos\theta_{in} + sin\theta_{in}\,sin\theta_{out}cos\varphi\right]$.

BRDF parameters (normalized coefficients k_i) are computed periodically (every 10-days) and globally (landmass) with a spatial resolution of 1/112°×1/112° (≈1km). BRDFs are produced for the four spectral narrow bands of VGT/Proba-V: B0 [450 ± 20nm], B1 [645 ± 35nm], B2 [835 ± 55nm] and SWIR [1665 ± 85nm].

Thus, for each pixel, cloud-free TOC reflectances are collected during a synthesis period of 30 days every 10 days to be used in the optimization of BRDF parameters (k_0, k_1, k_2) using least squares regression and reported at the centre of the synthesis period. Two weighting functions are applied to the collected TOC-R: temporal and angular weighting. Only the weighting temporal function is presented here because this function will be called in the processing of *in situ* data. Temporal weighting consists of weighting the TOC-R by means of its time difference to the end of the synthesis period:

$$w_{tmp}(t) = \exp\left(-0.5\,\frac{(t-t_0)^2}{(1.87\,\sigma_T)^2}\right)\ with\ \sigma_T = \frac{T}{\sqrt{7\,ln2}} \quad (8)$$

where t is the Julian day of the observation, t_0 is the Julian day of the central day of the synthesis period, and T is the length of the synthesis period (30 days), which is a compromise between the number of cloud-free observations available and the user requirements on the temporal resolution of the products.

Consider the following elements:

- F is the matrix containing the model kernels (f_0, f_1, f_2)
- R is the vector containing the observed surface reflectances (TOC-R)
- W is the diagonal matrix containing the weights (resulting from the temporal and angular weighting)
- K is the vector containing the BRDF parameters (k_0, k_1, k_2)

The BRDF parameters estimation aims to solve the equation:

$$(W \cdot F) \cdot K = W \cdot R \quad (9)$$

with

$$K = C \cdot A^T \cdot B \quad (10)$$

where $\mathrm{A} = \mathrm{W} \cdot \mathrm{F}$, $\mathrm{B} = \mathrm{W} \cdot \mathrm{R}$, and $\mathrm{C} = (\mathrm{A}^{\mathrm{T}} \cdot \mathrm{A})^{-1}$.

The main inputs for generating BRDF parameters are:

- TOA of SPOT/VGT and SPOT/PROBA-V at four bands: B0, B1, B2, SWIR;
- Viewing and solar azimuth angles [0, 360°];
- Viewing and solar zenith angles [0, 90°].

In addition, several other products are used as axillary data to perform atmospheric correction and geographic re-projection, namely:

- The digital elevation model used is GTOPO30 which is described at http://edc.usgs.gov/products/elevation/gtopo30/README.html. It is reformatted as a global product at 1/112°. (N.B. This is very poor quality compared to its successor, GMTED2010)
- The landcover map used is the GLC2000[7]. It is a global product at 1/112° resolution.
- A climatology of aerosol optical thickness derived from multi-years of MODIS products (MOD08_M3[8]). It is a global product at 1° resolution. See section 3.3.4 for the calculation of the climatology.
- The ozone data from EPTOMS (till 2005) and from TOAST (from 2006)[9], is accessible at ftp://ftp.orbit.nesdis.noaa.gov/pub/smcd/spb/ozone/toast/. They are daily global data at 1.25° in longitude and 1° resolution in latitude.
- Water vapour content and surface pressure come from NCEP data[10]. They are global data available 4 times per day at synoptic times.

In summary, the operational processing scheme of the BRDF algorithm comprises the following steps:

1. Inter-calibration of the 2 VGT sensors to a reference to have a consistent time series from 1999 to 2014.
2. Snow, cloud and cloud shadow detection
3. Atmospheric correction to remove the effects of water vapour, ozone, aerosols, and surface pressure.
4. Least squares regression to estimate BRDF parameters.

3.2 Albedo Creation

Two types of albedo are computed within the GIOGL land product: 1) Directional Hemispherical Reflectance (DHR), also known as Black-Sky-Albedo (BSA); and 2) Bi-Hemispherical Reflectance (BHR), also known as White-Sky-Albedo (WSA).

[7] http://bioval.jrc.ec.europa.eu/products/glc2000/glc2000.php
[8] http://modisatmos.gsfc.nasa.gov/MOD08_M3/index.html
[9] http://www.ospo.noaa.gov/Products/atmosphere/toast/index.html
[10] http://www.ncep.noaa.gov/

As Albedo (BHR and DHR) and TOC-R products are extracted from the same product (BRDF), they all have the same spatial resolution 1/112˚×1/112˚, and temporal resolution (every 10 days) and we can infer that they also have the same synthesis period, which is 30 days. However, Albedo products differ with TOC-R and BRDF in spectral bands, in such a way that the Albedo at the four original bands of VGT/Proba-V bands (B0, B1, B2, SWIR) are converted to Albedos over three broadbands: VIS[400nm, 700nm], NIR [700nm, 4000nm], SW [300nm, 4000nm]. Note that VIS, NIR and SW, refer to visible, near infra-red and shortwave, respectively.

DHR represents the integration of reflectance from all view angles for a given illumination (solar) geometry angle (Schaepman-Strub 2006):

$$DHR(\lambda,\theta_{in},\varphi) = \frac{1}{\pi}\int_{\theta_{out}=0}^{\frac{\pi}{2}}\int_{\varphi=0}^{2\pi} R(\lambda,\theta_{in},\theta_{out},\varphi)\, cos\theta_{out} sin\theta_{in} d\theta_{out} d\varphi \qquad (11)$$

Using Eq. (5) leads to:

$$DHR(\lambda,\theta_{in}) = \sum_{i=0,1,2} k_i(\lambda)\, I_i^{dhr}(\theta_{in}) \qquad (12)$$

with:

$$I_i^{dhr}(\theta_{in}) = \frac{1}{\pi}\int_{\theta_{out}=0}^{\frac{\pi}{2}}\int_{\varphi=0}^{2\pi} f_i\,(\lambda,\theta_{in},\theta_{out},\varphi) cos\theta_{out} sin\theta_{in} d\theta_{out} d\varphi \qquad (13)$$

$I_i^{dhr}(\theta_{in})$ were pre-computed for a set of solar zenith angles and stored in look-up tables (see Table 4). However, it can also be approximated by a 3-degree polynomial of solar zenith angle (Strahler, Muller et al., 1999).

On the other hand, BHR represents the integration of reflectance from all view and illumination angles. In other words, BHR is the integration of DHR over all illumination angles (Schaepman-Strub 2006):

$$BHR(\lambda) = \frac{1}{\pi}\int_{\theta_{in}=0}^{\frac{\pi}{2}}\int_{\varphi=0}^{2\pi} DHR(\lambda,\theta_{in},\varphi_{in}) cos\theta_{in} d\theta_{in} d\varphi \qquad (14)$$

Using Eq. (5) – (14) leads to:

$$BHR(\lambda) = \sum_{i=0,1,2} k_i(\lambda)\, I_i^{bhr} \qquad (15)$$

Table 4. Look-up table of directional-hemispherical and bi-hemispherical kernel integrals as a function of solar zenith angle for the Roujean BRDF model (Lacaze 2014).

θ_{in}	I_0^{dhr}	I_1^{dhr}	I_2^{dhr}

0°	1.0	-0.997910	-0.00894619
5°	1.0	-0.998980	-0.00837790
10°	1.0	-1.00197	-0.00665391
15°	1.0	-1.00702	-0.00371872
20°	1.0	-1.01438	0.000524714
25°	1.0	-1.02443	0.00621877
30°	1.0	-1.03773	0.0135606
35°	1.0	-1.05501	0.0228129
40°	1.0	-1.07742	0.0343240
45°	1.0	-1.10665	0.0485505
50°	1.0	-1.14526	0.0661051
55°	1.0	-1.19740	0.0878086
60°	1.0	-1.27008	0.114795
65°	1.0	-1.37595	0.148698
70°	1.0	-1.54059	0.191944
75°	1.0	-1.82419	0.248471
80°	1.0	-2.40820	0.325351
85°	1.0	-4.20369	0.438371
--	I_0^{bhr}	I_1^{bhr}	I_2^{bhr}
	1.0	-1.28159	0.0802838

with:

$$I_i^{bhr} = 2\int_0^{\frac{\pi}{2}} I_i^{dhr}(\theta_{in})cos\theta_{in}sin\theta_{in}\, d\theta_{in} \qquad (16)$$

I_i^{bhr} were computed and stored (see Table 4).

3.2.1 Narrow-to-broadband

The initial DHR and BHR are created at the four spectral bands of VGT/Proba-V (B0, B1, B2, SWIR), which are then converted to three broadbands (VIS, NIR, SW). The conversion from spectral albedo to broadband is performed using a linear combination of 4 different cases:

- Snow & BO not saturated & B2 not saturated
- Snow & BO saturated & B2 not saturated
- Snow & BO saturated B2 & saturated
- Snow free

The conversion is performed as follows:

$$BHR(bb) = c_0 + c_1 BHR(B0) + c_2 BHR(B1) + c_3 BHR(B2) + c_4 BHR(SWIR) \qquad (17)$$

$$DHR(bb) = c_0 + c_1 DHR(B0) + c_2 DHR(B1) + c_3 DHR(B2) + c_4 DHR(SWIR) \qquad (18)$$

Table 5 gives the coefficients that are deployed to convert albedo from narrow bands to broadband.

Table 5. Narrow to broadband conversion coefficients for the SPOT/VGT channels (Lacaze 2014).

Broadband	Cases	C_0	C_1 (B0)	C_2 (B1)	C_3 (B2)	C_4 (SWIR)
VIS	Snow	0.0284	0.57795	0.37077	--	--
	Snow & B0 saturated	0.0255	--	0.89055	0.06964	-0.31278
	Snow & (B0 and B2 saturated)	0.0792	--	--	1.01062	-1.82936
	Snow free	0.0010	0.50791	0.47503	--	--
NIR	Snow	0.0212	--	0.04437	0.55193	0.36701
	Snow & B0 saturated	0.0236	--	--	0.59939	0.28744
	Snow & (B0 and B2 saturated)	--	--	--	--	--
	Snow free	0.0140	--	0.00882	0.56868	0.35175
SW	Snow	0.0248	0.12171	0.26775	0.35725	0.08221
	Snow & B0 saturated	0.0266	--	0.39913	0.34290	0.05098
	Snow & (B0 and B2 saturated)	0.0525	--	--	0.76376	-0.65405
	Snow free	0.0097	0.18875	0.21475	0.34410	0.18457

3.3 Top of Canopy Reflectance (TOC-R)

Normalized Top of Canopy reflectance TOC-R is calculated using Eq. (5) with solar angles of 10:00 local time and with a nadir-equivalent view. TOC -R product is calculated on the global (landmass) with a 10-daily temporal sampling and 1/112˚×1/112˚ spatial resolution.

Note that the TOC-R is just an estimated response from a BRDF model for a given viewing/illumination geometry angle. Thus, the accuracy of the TOC-R will mainly depend on the accuracy of the retrieved BRDF parameters (k_0, k_1, k_2) and, obviously, on the BRDF model employed.

Table 6 summarizes the key characteristics of Albedo and TOC -R products of GEO-GL.

Table 6. Key characteristics of GIOGL VGT broadband & spectral products of Albedo & TOC-R respectively.

	Spatial resolution	Coverage	Temporal resolution	Synthesis Period	Spectral bands [nm]
Albedo/DHR	1/112˚×1/112˚	Global landmass	10-daily	30 days	VIS: [400, 700] NIR: [700, 4000] SW: [300, 4000]
Albedo/BHR	1/112˚×1/112˚	Global landmass	10-daily	30 days	VIS: [400, 700] NIR: [700, 4000] SW: [300, 4000]
TOC-R	1/112˚×1/112˚	Global landmass	10-daily	30 days	B0: [430, 470] B1: [610, 680] B2: [780, 890] SWIR: [1580,1750]

4 Tower data processing

4.1 Top-of-Canopy Reflectance (TOC-R): LP1

TOC-R represents the normalised top of canopy reflectance at 10:00 am local time at a nadir view angle for four spectral bands of VEGETATION and Proba-V (B0, B1, B2, and SWIR). However, TOC-R does not result from a direct measurement but from a BRDF function that requires a synthesis period of 30 days to optimize its three parameters (k_0, k_1, k_2).

TOC-R and measurements from ground-based albedometers differ in two main respects: spectral bands and instantaneous field of view (IFOV). The difference in spectral bands requires that the TOC-R needs to be converted to the albedometer shortwave. For this, we can use the same conversion coefficients from Table 5 for both cases of snow and snow-free. However, the difference in the IFOV requires further processing because, whilst the IFOV of TOC-R is supposed to be null, the IFOV of a ground-based albedometer is around 170˚.

Thus, we propose here a new approach for the validation of TOC-R. This proposed approach consists of computing BRDF parameters (k_0, k_1, k_2) using tower data, and then creating TOC-R using Eq. (5). Normally, to calculate BRDF parameters, a set of TOC reflectances at different angles and with very small IFOV is needed but all we can get from the tower albedometer is albedo. Note that tower albedo can be also considered as TOC but with a wider IFOV.

The idea here is to use BHR and DHR that are extracted from tower albedometer measurements to calculate BRDF parameters. So, for each day we collect a tower BHR (when $\beta \geq \beta_{\mathrm{bhr}}$) and DHR (when $\beta \leq \beta_{\mathrm{dhr}}$) over ±15 days by computing their associated temporal weights (Eq. (8)). Note that while BHR is intended to be defined as being stable over the day because it does not depend on solar angle, DHR varies with changes in solar angles. To have an idea about the variation of DHR with SZA during the day, Figure 7 shows a sample of a DHR time series for a single day over the Tumbarumba site. Similarly, Figure 8 shows a time series of BHR for a single day over the same site.

For each day we try to have a single BHR measurement and multiple DHR measurements for certain SZAs (0˚, 5˚, 10˚, … , 70˚) as those in the look-up table of Table 4. We limited our range of SZA in [0˚, 70˚] because linear BRDF model do not work for SZA ≥ 75˚ (Lacaze 2014).
Once BHR and DHRs are collected from tower measurements, we can compute the best values of (k_0, k_1, k_2) that fit the look-up table of Table 4 for DHR at different SZAs and formulae for BHR at any SZA. Nevertheless, we do not expect to have many BHR and DHR on some days because they require completely different cloud conditions. Note that at least three measurements (DHRs and BHR) are needed to estimate the three BRDF parameters but the estimation will be more accurate if DHRs refer to a wider range of solar zenith angles.

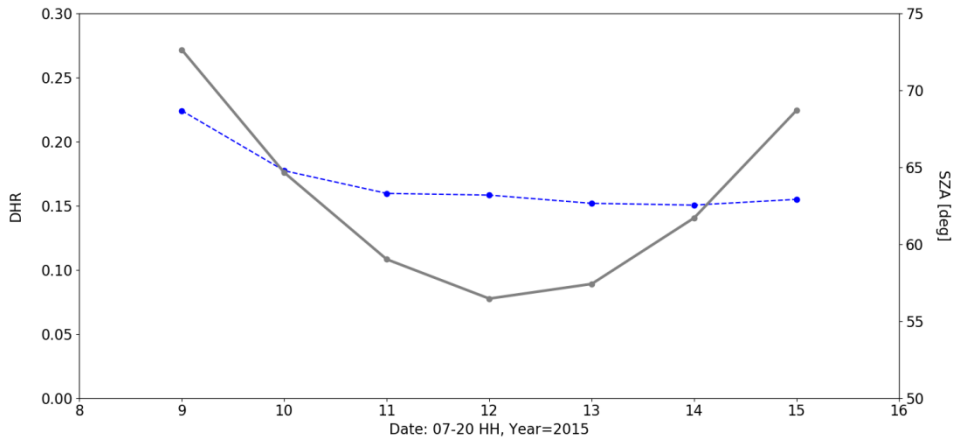

Figure 7.Variation of Tower DHR (in blue) during a single day at Tumbarumba site (2015-07-20).

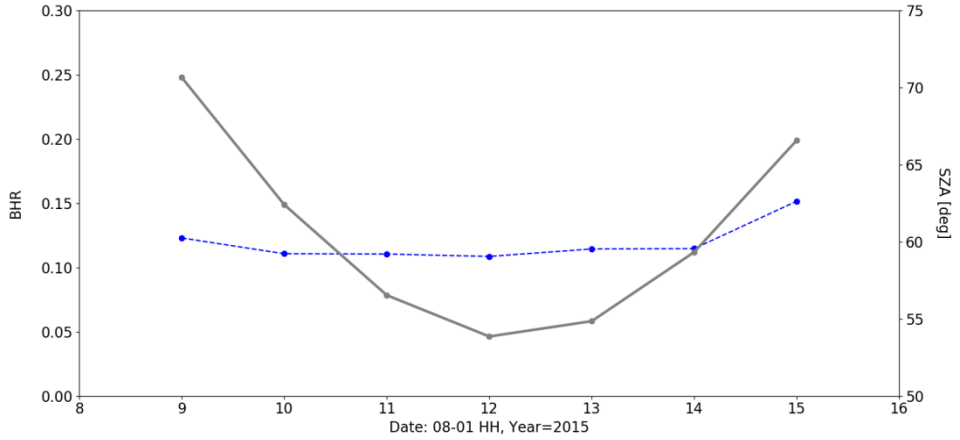

Figure 8.Variation of Tower BHR (in blue) during a single day at Tumbarumba site (2015-08-01).

Next, after computing the BRDF parameters, we can calculate reflectance with a nadir view and with solar angles at 10:00 local time. Finally, the temporal weighing function of TOC-R (Eq. (8)) within the same sliding time window (30 days) will be applied over those reflectances. However, the last step in the temporal weighing can be optional as the final user may wish to apply another temporal weighting function.
Consider the following elements:

- I is the matrix containing integrated model kernels (I_0, I_1, I_2) of Table 4;
- R is the vector containing the observed BHRs and DHRs;
- W is the diagonal matrix containing the weight;
- K is the vector containing the BRDF parameters (k_0, k_1, k_2).

The BRDF parameters estimation aims to solve:

$$(W \cdot I) \cdot K = W \cdot R \tag{19}$$

with:

$$K = C \cdot A^T \cdot B \tag{20}$$

where $A = W \cdot I$, $B = W \cdot R$, $C = (A^T \cdot A)^{-1}$.

To summarize, the processing chain of LP2 can be represented by a set of consecutive steps as follows:

- For each day in the time window (i.e. $T \epsilon t \pm 15$ days):
  - Collect BHRs: SW_OUT/SW_IN when SW_DIF/SW_IN = $\beta \geq \beta_{bhr}$
    - BHRs averaging
  - For each solar zenith angle in (0˚, 5˚…70˚):
    - Collect DHRs: SW_OUT/SW_IN when SW_DIF/SW_IN = $\beta \leq \beta_{dhr}$
  - Compute associated temporal weights for day t (i.e. Eq. (8))
- If the number of BHR and DHRs is sufficient:
  - Compute BRDF parameters (k0, k1, k2)
  - Compute reflectance (equation [1]) at view nadir and at 10:00 local time.

Figure 9 shows an example of TOC-R estimation using a tower's DHR for a given day at the tower site of Tumbarumba. The BRDF parameters that have been computed from those DHRs are used to calculate TOC-R. This figure also shows fitted DHR (for some SZAs) and a reflectance function (at view nadir). Similarly, Figure 10 shows TOC-R estimation over the tower site of Hainich using DHR samples from a single day. In order to have more samples per SZA for computing BRDF parameters in a single day, the diffuse ratio β_{max} is fixed at 25%. However, further experimentation may still be required to check for each tower station and by date the ability to collect samples (BHR and DHR) using finer diffuse thresholds ($\beta_{\max} \leq 10\%$ and $\beta_{\min} \geq 99\%$) but with wider observation (synthesis) period (i.e. 7 days, 15 days, 30 days) this should be possible. However, more tests need to be performed using the MODIS BRDF in order to test and verify this new approach.

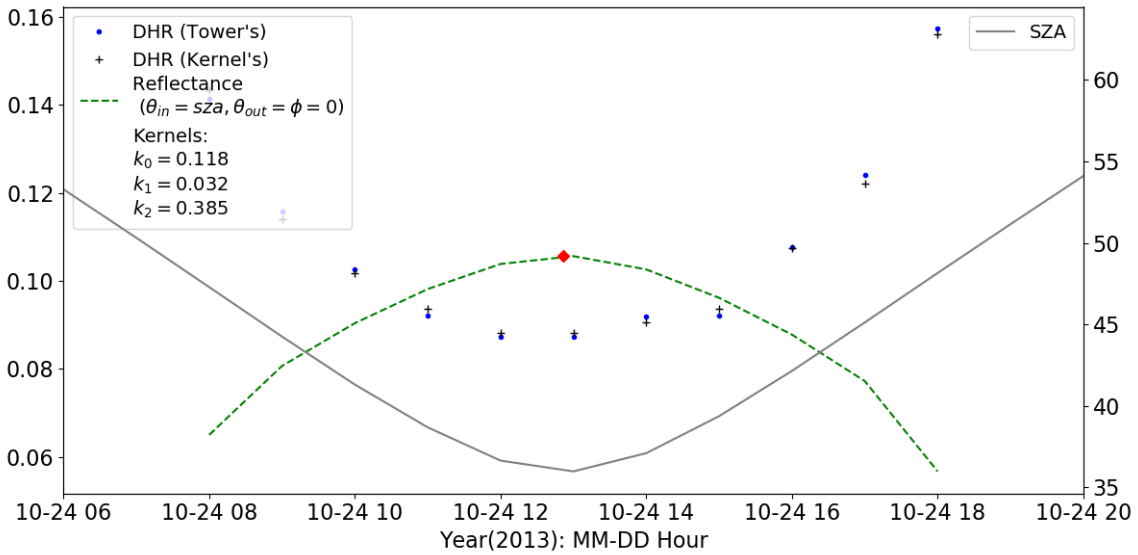

Figure 9. Estimation of TOC-R by Tower DHRs within ±15 days' time window: FLUXNET Tumbarumba site on 24th October 2013. BRDF parameters (k0,k1,k2) were calculated from Tower's DHR and then TOC-R is computed using the reflectance function at local solar noon and with a nadir view.

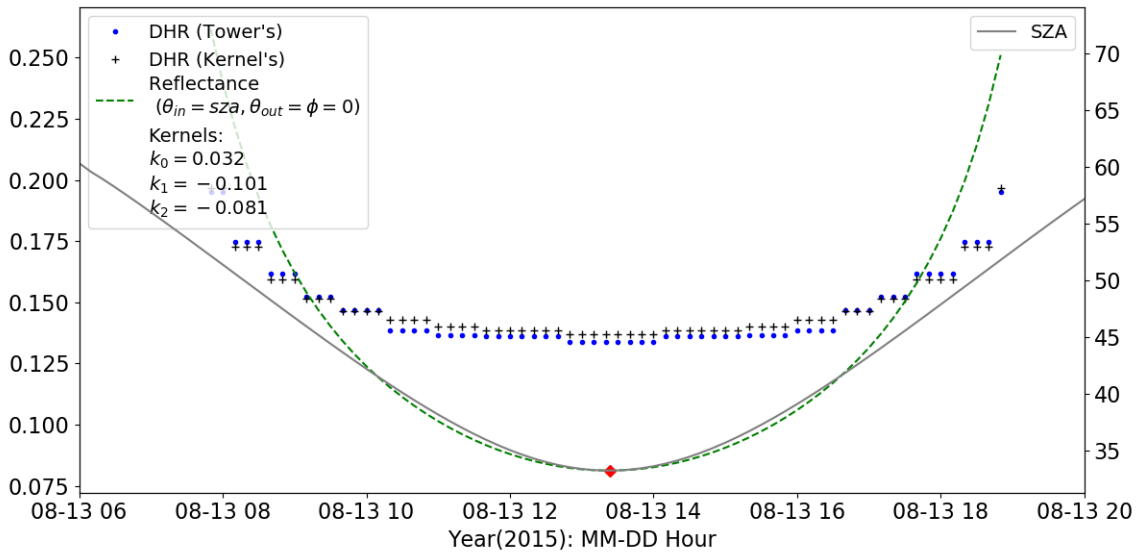

Figure 10.Estimation of TOC-R by Tower DHRs within ±15 days' time window: FLUXNET Hainich site on 13th August 2015. BRDF parameters (k0,k1,k2) are calculated from Tower's DHR and then TOC-R is computed using the reflectance function at local solar noon and at view nadir. Note the close agreement between the DHRs.

4.2 Surface Albedo from RM1 tower measurements (LP2)

BHR and DHR represent extreme cases that rarely exist in the physical "real world" because BHR requires uniform illumination from all angles and, DHR requires illumination from a single infinitesimally small point source. This is the reason why in all previous works of satellite-derived albedo validation against *in situ* data, BHR and DHR have been indirectly compared using a compromise value between BHR and DHR (Lucht 2000; Román 2010; Lewis 2011; Sanchez 2015). This compromise value is intended to represent *in situ* albedo, which is called Blue-Sky (or clear sky) albedo and can be computed as follows:

$$\text{BlueSkyAlbedo} = \beta * BHR + (1 - \beta) * DHR \qquad (21)$$

where β denotes the proportion of diffuse component in downwelling solar energy (at a given spectral band). Normally, β is provided by a ground-based station as a time variable with other measurements. If it is not available, a satellite aerosol product (e.g. MOD04/MYD04 of MODIS or the AOD retrieved as part of the GlobAlbedo product) can be used to estimate β but this is with high temporal and spatial uncertainties (Muller et al., 2012 GlobAlbedo validation report).

Blue sky albedo can be computed from satellite data (BHR and DHR) combined with β from tower data. Therefore, albedo at local solar noon can be used directly for comparison with ground-based albedo. However, this manner of inter-comparison has two major critical issues: 1) blue sky albedo is dominated by DHR because β is computed at local solar noon and, often, under cloud free conditions (low β); 2) there is no obvious method to use blue sky albedo assessment in a separate assessment of DHR and BHR. To overcome those issues, we propose

here a new strategy for ground-based albedo processing in order to provide a better estimation of DHR and BHR in-situ data, as shown in Figure 11.

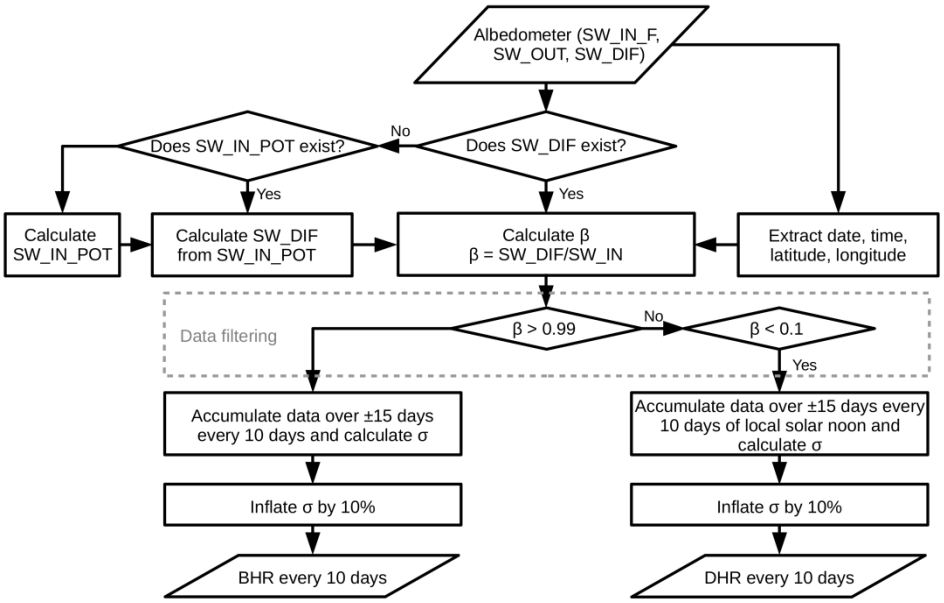

Figure 11.Flowchart illustrating the algorithm of estimating DHR and BHR from tower measurements.

4.2.1 Bi-Hemispherical Reflectance (BHR)

According to Eq. (21), BHR can be approximated by blue-sky-albedo when β tends towards 1. The highest values of β can only be reached under certain conditions, such as under thick unbroken Stratus clouds, just before sunrise, and just after sundown. We therefore postulate that the threshold of $\beta_{bhr} = 0.99$ can be adopted for masking undesirable measurements because the data showing $\beta \geq \beta_{bhr}$, for all sites, can be considered sufficient to perform the validation of satellite-derived BHR.

Once the data are filtered by the condition $\beta \geq \beta_{bhr}$, we compute the mean and the standard deviation (*st-dev*) over a sliding time window of 30 days using the same temporal weighting function as the one deployed by GIOGL (Eq. (8)). The effect of DHR in BHR *in situ* should be less than $1 - \beta_{bhr}$ (0.01%). Thus, the *st-dev* of the final BHR in-situ will be increased by $1 - \beta_{bhr}$ in order to represent this uncertainty.

Figure 12 shows an example of ground-based albedo (SW_IN/SW_OUT) at different stages of BHR *in situ* data creation from the data of FLUXNET Tumbarumba site in 2015.

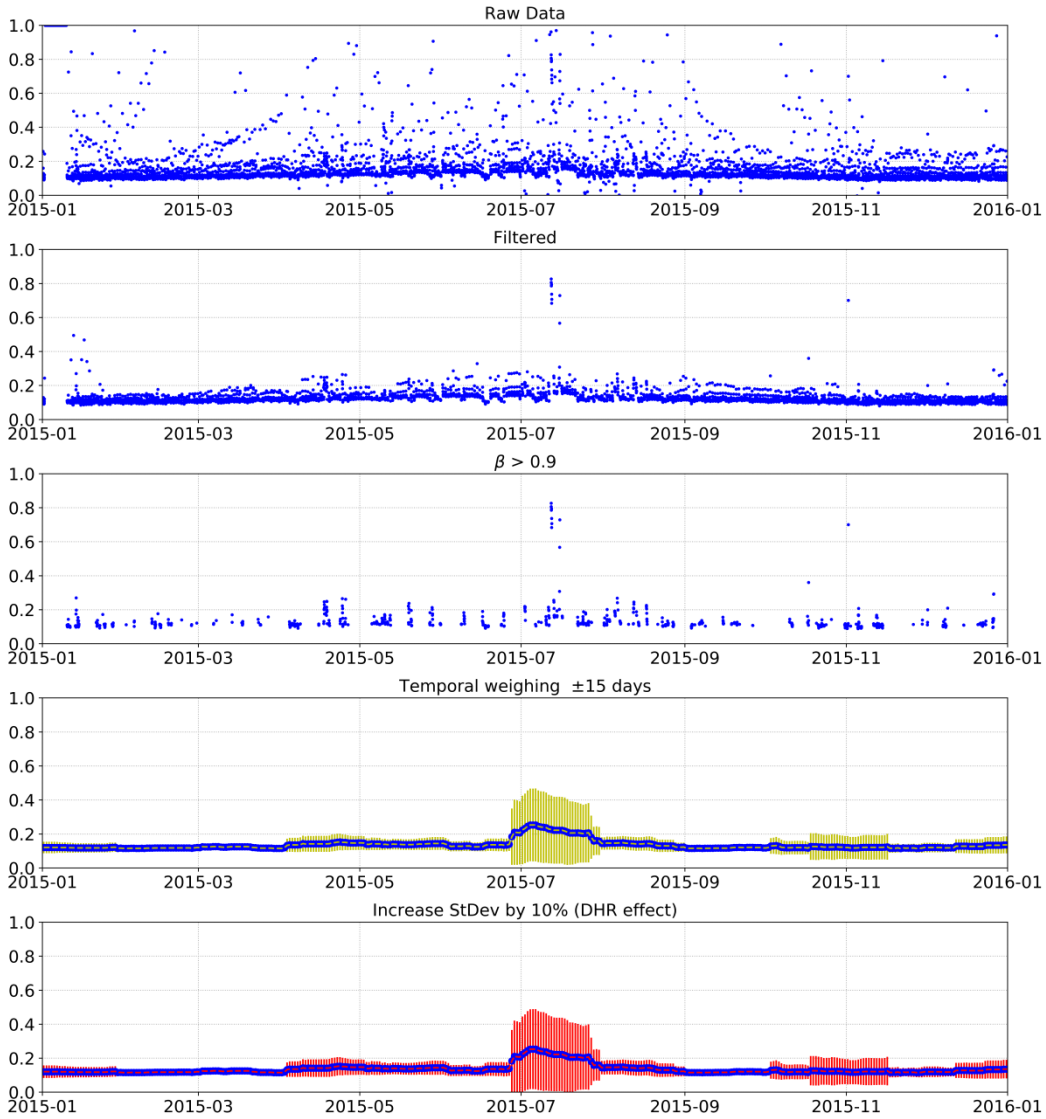

Figure 12.A sample of processed FLUXNET Tumbarumba tower data for producing in-situ BHR.

4.2.2 Directional Hemispherical Reflectance (DHR)

According to Eq. (21), DHR can be well approximated by a blue sky albedo when β tends towards 0. The lowest values of β can be reached under totally cloud free conditions with a very low level of aerosol at local solar noon. We have verified that a threshold of $\beta_{dhr} = 0.05$ can be used for masking undesired measurements because the data verifying $\beta \leq \beta_{dhr}$ at ±30min local solar noon, for all sites, can be considered sufficient to perform the validation of satellite-derived DHR. Note data working with a lower β_{dhr} than 0.05 drastically reduces the amount of remaining data because we consider only data in ±30min local solar noon and, also because β does not often reach a very low level due to broken cloud cover.

Once the ±30min local noon data are filtered by the condition $\beta \leq \beta_{dhr}$, we can compute the mean and standard deviation (*st-dev*) over a sliding time window of 30 days using the same temporal weighting function as the one deployed by GIOGL (Eq. (21)). The effect of BHR on

DHR in-situ should be less than $1 - \beta_{dhr}$ (0.05%). Thus, the *st-dev* of the final BHR in-situ is dilated by $1 - \beta_{dhr}$ in order to represent this uncertainty. Figure 13 shows an example of ground-based albedo (SW_IN/SW_OUT) at different stage of DHR in-situ data creation from the data of FLUXNET Tumbarumba site in 2015.

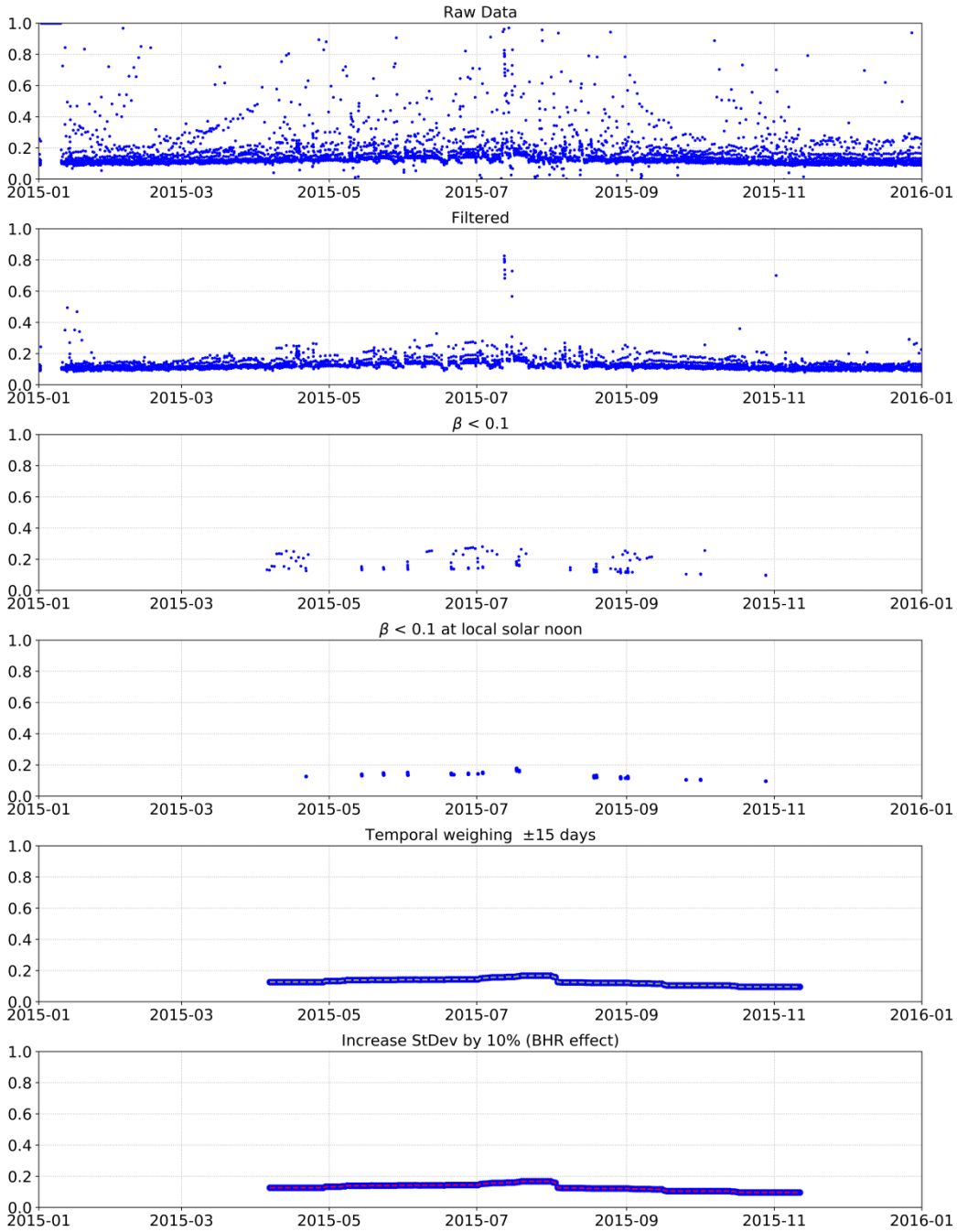

Figure 13.An example of processed FLUXNET Tumbarumba tower data showing the production of in situ DHR.

4.3 Comparison of surface albedo between CGLS and in-situ retrievals

In this section, the tower measured DHRs and BHRs between 01/01/2012 and 31/12/2016 are compared with the coarse-resolution 1/112º (≈1 km) CGLS products. The DHR intercomparison and BHR intercomparison at the selected 19 sites are shown in Figure 14 and Figure 15, respectively. The CGLS albedo products are directly extracted from the pixel which is closest to the corresponding tower station.

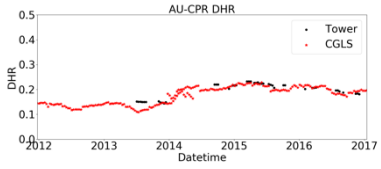

(a)

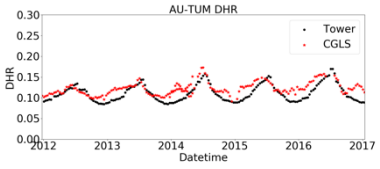

(b)

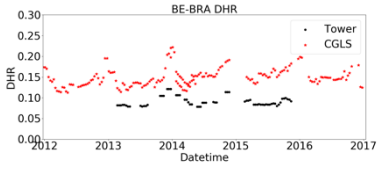

(c)

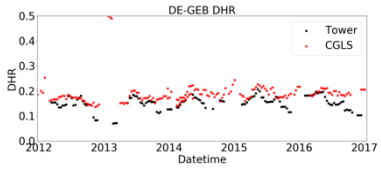

(d)

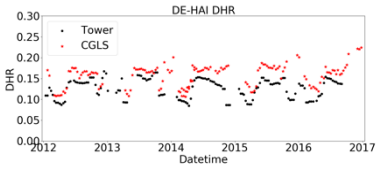

(e)

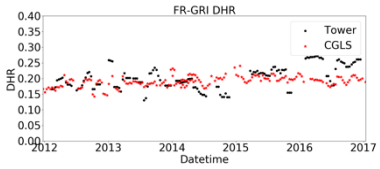

(f)

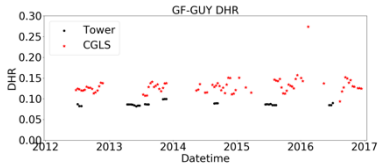

(g)

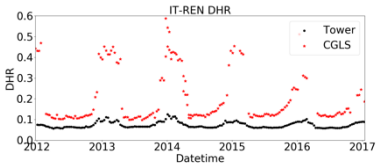

(h)

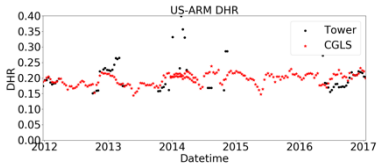

(i)

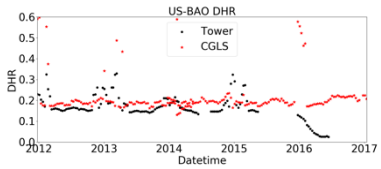

(j)

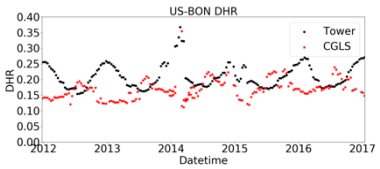

(k)

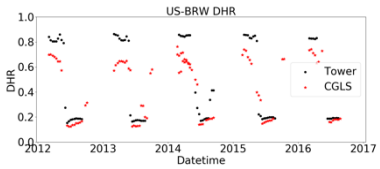

(l)

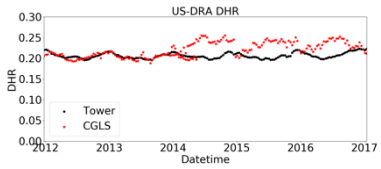

(m)

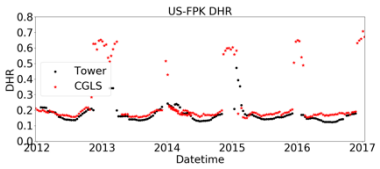

(n)

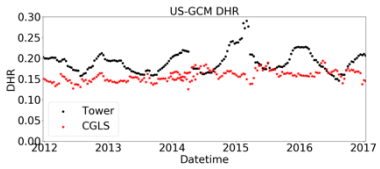

(o)

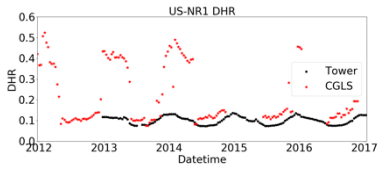

(p)

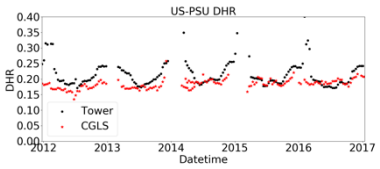

(q)

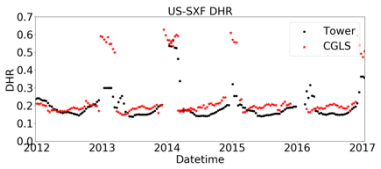

(r)

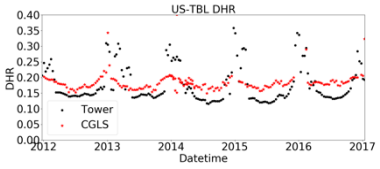

(s)

Figure 14.Intercomparison between tower measured DHRs and CGLS DHR products.

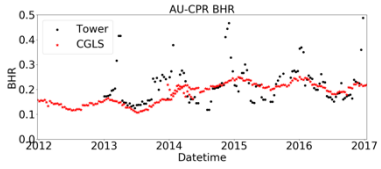

(a)

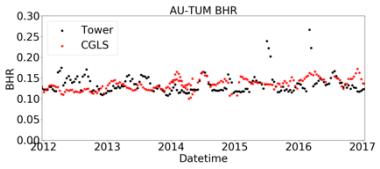

(b)

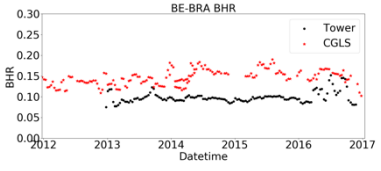

(c)

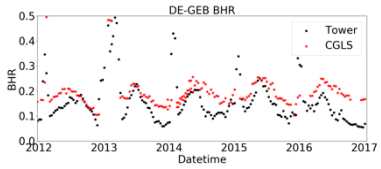

(d)

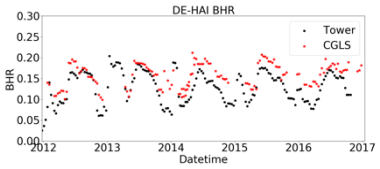

(e)

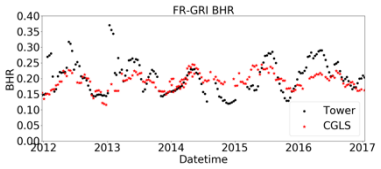

(f)

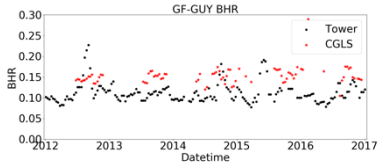

(g)

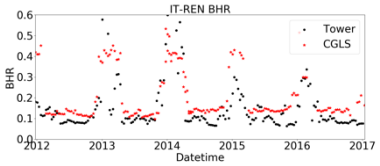

(h)

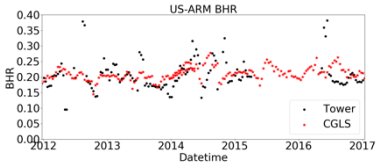

(i)

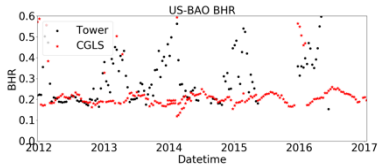

(j)

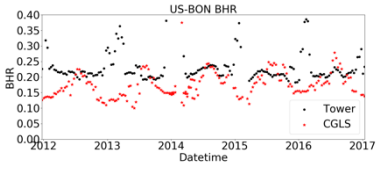

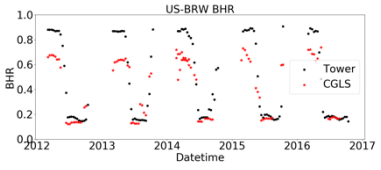

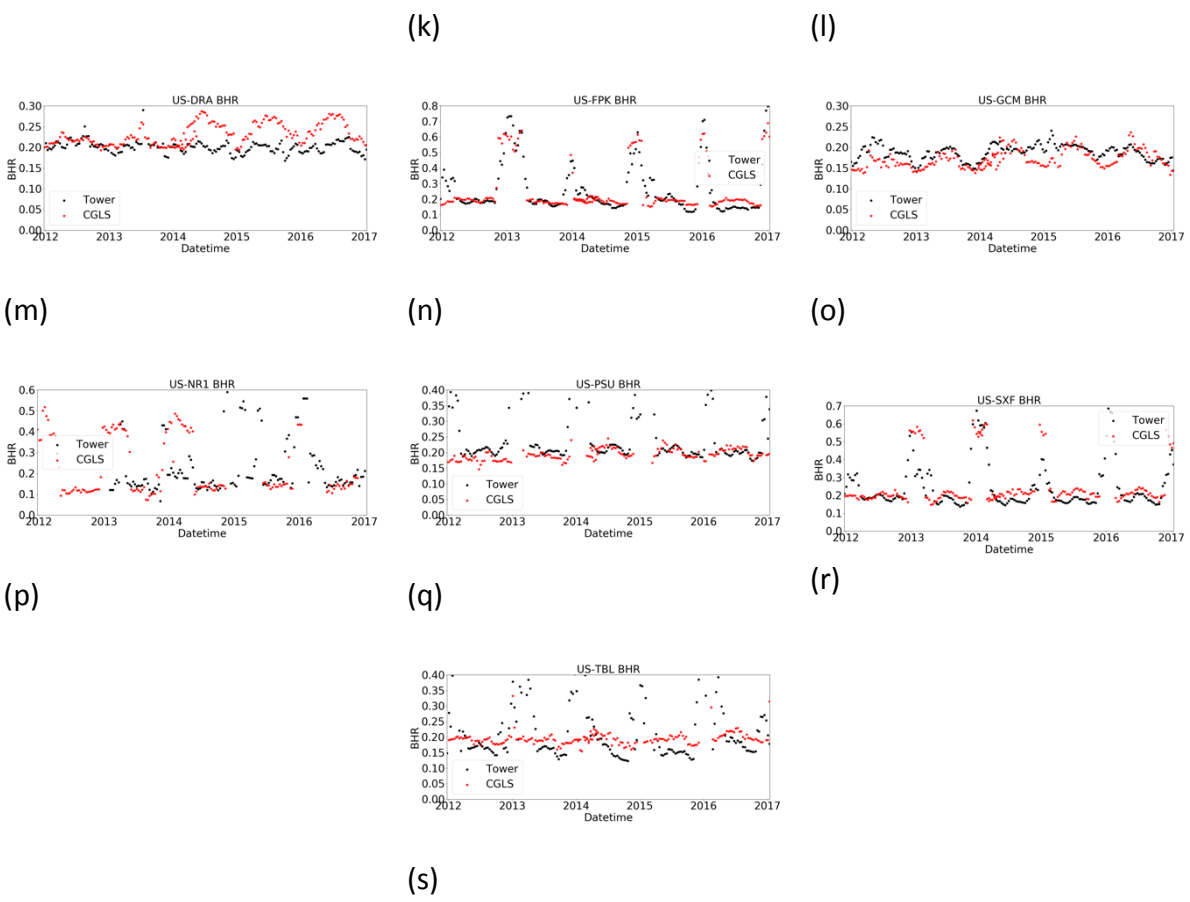

Figure 15.Intercomparison between tower measured BHRs and CGLS BHR products.

At stations such as the Tumbarumba and Fort Peck sites, the DHR intercomparison shows a good match in terms of absolute values and seasonal variations. The DHR mismatch at some other sites (e.g. the Brasschaat site) is likely due to the heterogeneity of the land surface at the satellite measurement scale. It is also worth noting that the Barrow site shows a better match during the snow-free season than the snow-covered season.

Generally speaking, the DHR retrievals show better agreement between satellite and in-situ measurements than the BHR retrievals. In our method for BHR retrievals, the illumination is assumed to be uniform from all angles when the diffuse ratio is larger than β_B. However, not all the tower data screened for BHR retrievals can meet this condition. This is the error source that may reduce the accuracy of BHR retrievals. For more comparisons between satellite and in-situ retrievals, please refer to Song et al. (2019).

In Annex B, a comparison of blue-sky-albedo (BSA) between CGLS products and in-situ retrievals is also displayed. The CGLS BSA values are calculated from Eq. (21) using CGLS DHR and BHR products, as well as β values measured from the tower at the central date. Tower BSA values are directly derived by calculating SW_{out}/SW_{in} at $\pm$ 1hour local solar noon.

5 Upscaling to CGLS pixel sizes

It is necessary for heterogeneous surfaces to upscale the in situ measurements of LP1 & LP2 to the resolution of the CGLS pixel size at 1/112º. The following section describes how this will be done using an example to illustrate the steps of upscaling LP1 and LP2 products from tower measurements to CGLS pixels. The tower measurements at the FLUXNET Hainich site are selected in order to demonstrate this upscaling process.

5.1 TOC-R from tower-derived BRDF to HR TOC-R (SW)

Upscaling TOC-R from towers measurements to CGLS grid consists of two major steps. Firstly, the TOC-R estimated from the tower-derived BRDF is compared with the TOC-R obtained from high resolution (HR) Earth observations (EO) using the same solar and view angles. Then, this "calibration factor" is used to upscale the TOC-R from the HR-EO scale to the coarse CGLS grid. Figure 16 shows a flowchart to illustrate the overall upscaling process.

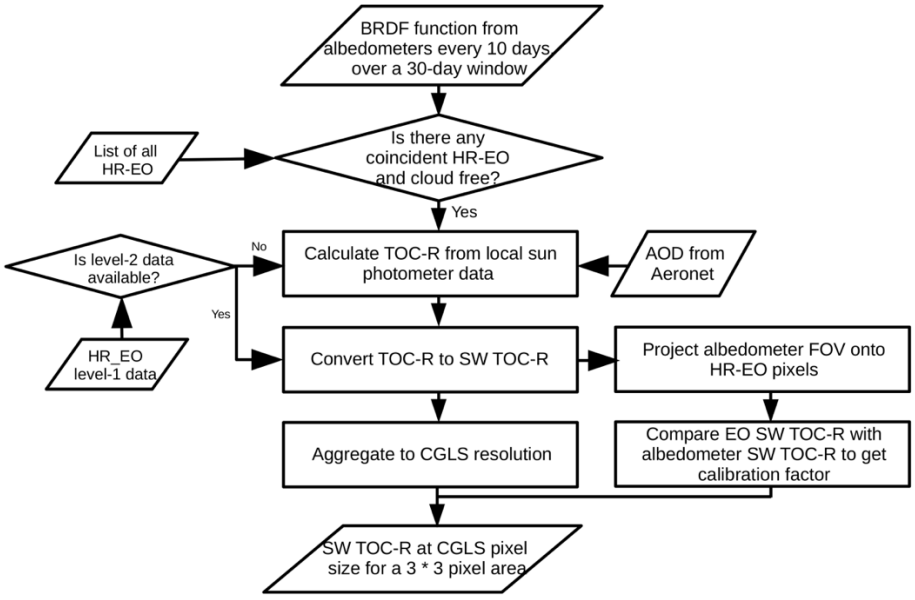

Figure 16.Flowchart illustrating the process of upscaling TOC-R.

5.1.1 Data Screening.

Using the formulae introduced in Section 4, a BRDF function can be derived from tower measurements every 10 days within a time window of ±15 days. Then, for the date on which the TOC-R from tower measurements is upscaled, a data screening process is carried out to find if there are any cloud-free HR-EO data available from the database. This includes Landsat-7 (2012-2016), Landsat-8 (from May 2013), Sentinel-2 (from June-2015) and Spot 4 and 5 (2012-2016).

Table 7. Selected 12 dates per annum for LP1 & LP2 upscaling between 01/01/2012 and 31/12/2016. This table includes the US-BRW, US-NR1, US-SXF, AU-TUM and US-ARM. For the coloured HR-EO dates, red indicates Sentinel-2, light blue Landsat-7, dark blue Landsat-8, and purple indicates interpolation is used and grey indicates no upscaling is needed.

US-BRW		US-NR1		US-SXF		AU-TUM		US-ARM	
CGLS dates	EO dates	CGLS dates	EO dates	CGLS dates	EO dates	CGLS dates	EO dates	CGLS dates	EO dates
								03/02/2012	01/02/2012
								22/02/2012	26/02/2012
								03/03/2012	04/03/2012
								23/04/2012	21/04/2012
								24/05/2012	23/05/2012
								03/06/2012	08/06/2012
								13/06/2012	13/06/2012
								03/08/2012	03/08/2012
								13/09/2012	12/09/2012
								13/10/2012	14/10/2012
								03/11/2012	30/10/2012
								13/11/2012	15/11/2012
CGLS dates	EO dates	CGLS dates	EO dates	CGLS dates	EO dates	CGLS dates	EO dates	CGLS dates	EO dates
03/06/2013	03/06/2013	23/06/2013	23/06/2013	13/06/2013	10/06/2013	24/01/2013	01/28/2013	03/02/2013	03/02/2013
13/06/2013	13/06/2013	03/07/2013	03/07/2013	23/06/2013	23/06/2013	13/02/2013	13/02/2013	21/02/2013	19/02/2013
23/06/2013	23/06/2013	13/07/2013	13/07/2013	03/07/2013	04/07/2013	03/03/2013	03/03/2013	03/03/2013	07/03/2013
03/07/2013	08/07/2013	24/07/2013	24/07/2013	13/07/2013	12/07/2013	13/03/2013	13/03/2013	23/04/2013	24/04/2013
13/07/2013	13/07/2013	03/08/2013	03/08/2013	24/07/2013	21/07/2013	03/04/2013	01/04/2013	03/06/2013	03/06/2013
24/07/2013	24/07/2013	13/08/2013	13/08/2013	03/08/2013	03/08/2013	23/04/2013	25/04/2013	03/08/2013	06/08/2013
03/08/2013	03/08/2013	24/08/2013	24/08/2013	13/08/2013	13/08/2013	24/05/2013	27/05/2013	13/09/2013	07/09/2013
13/08/2013	11/08/2013	03/09/2013	03/09/2013	24/08/2013	20/08/2013	03/08/2013	30/07/2013	23/09/2013	23/09/2013
24/08/2013	24/08/2013	13/09/2013	17/09/2013	03/09/2013	03/09/2013	13/08/2013	15/08/2013	13/10/2013	09/10/2013
03/09/2013	03/09/2013	23/09/2013	23/09/2013	13/09/2013	22/09/2013	03/09/2013	03/09/2013	24/10/2013	25/10/2013
13/09/2013	13/09/2013	03/10/2013	03/10/2013	03/10/2013	01/10/2013	03/11/2013	03/11/2013	03/11/2013	03/11/2013
23/09/2013	23/09/2013	24/10/2013	19/10/2013	13/10/2013	16/10/2013	23/11/2013	19/11/2013	23/11/2013	26/11/2013
CGLS dates	EO dates	CGLS dates	EO dates	CGLS dates	EO dates	CGLS dates	EO dates	CGLS dates	EO dates
03/06/2014	03/06/2014	03/06/2014	03/06/2014	13/04/2014	10/04/2014	03/01/2014	06/01/2014	13/02/2014	14/02/2014
13/06/2014	13/06/2014	13/06/2014	13/06/2014	24/05/2014	28/05/2014	24/01/2014	22/01/2014	13/03/2014	18/03/2014
23/06/2014	25/06/2014	23/06/2014	16/06/2014	23/06/2014	23/06/2014	03/02/2014	07/02/2014	23/04/2014	19/04/2014
03/07/2014	03/07/2014	03/07/2014	02/07/2014	03/07/2014	29/06/2014	21/02/2014	23/02/2014	03/05/2014	05/05/2014
13/07/2014	13/07/2014	13/07/2014	13/07/2014	13/07/2014	13/07/2014	03/08/2014	02/08/2014	03/07/2014	03/07/2014
24/07/2014	24/07/2014	24/07/2014	24/07/2014	24/07/2014	24/07/2014	03/09/2014	03/09/2014	13/07/2014	13/07/2014
03/08/2014	03/08/2014	03/08/2014	03/08/2014	03/08/2014	03/08/2014	23/09/2014	23/09/2014	24/07/2014	24/07/2014
13/08/2014	12/08/2014	13/08/2014	13/08/2014	13/08/2014	16/08/2014	03/10/2014	05/10/2014	24/08/2014	25/08/2014
24/08/2014	24/08/2014	24/08/2014	24/08/2014	03/09/2014	01/09/2014	24/10/2014	21/10/2014	03/09/2014	03/09/2014
03/09/2014	03/09/2014	03/09/2014	03/09/2014	13/09/2014	17/09/2014	03/11/2014	06/11/2014	13/09/2014	13/09/2014
13/09/2014	13/09/2014	13/09/2014	13/09/2014	24/10/2014	19/10/2014	23/11/2014	22/11/2014	23/09/2014	26/09/2014
23/09/2014	23/09/2014	23/09/2014	20/09/2014	03/11/2014	04/11/2014	03/12/2014	08/12/2014	24/10/2014	28/10/2014
CGLS dates	EO dates	CGLS dates	EO dates	CGLS dates	EO dates	CGLS dates	EO dates	CGLS dates	EO dates
03/06/2015	03/06/2015	24/01/2015	26/01/2015	22/02/2015	24/02/2015	13/03/2015	14/03/2015	21/02/2015	17/02/2015
13/06/2015	13/06/2015	03/06/2015	03/06/2015	24/03/2015	28/03/2015	03/04/2015	30/03/2015	03/06/2015	03/06/2015
23/06/2015	22/06/2015	13/06/2015	13/06/2015	13/04/2015	13/04/2015	13/04/2015	15/04/2015	13/06/2015	13/06/2015
03/07/2015	07/07/2015	23/06/2015	23/06/2015	03/05/2015	29/04/2015	23/04/2015	23/04/2015	23/06/2015	23/06/2015
13/07/2015	13/07/2015	03/07/2015	03/07/2015	13/07/2015	18/07/2015	03/05/2015	03/05/2015	03/07/2015	03/07/2015
24/07/2015	29/07/2015	13/07/2015	13/07/2015	03/08/2015	02/08/2015	13/05/2015	13/05/2015	13/07/2015	13/07/2015
03/08/2015	03/08/2015	24/07/2015	24/07/2015	13/08/2015	13/08/2015	24/05/2015	24/05/2015	24/07/2015	24/07/2015
13/08/2015	13/08/2015	03/08/2015	03/08/2015	24/08/2015	24/08/2015	03/06/2015	02/06/2015	03/08/2015	03/08/2015
24/08/2015	24/08/2015	24/08/2015	22/08/2015	13/09/2015	12/09/2015	13/06/2015	18/06/2015	13/08/2015	13/08/2015
03/09/2015	03/09/2015	13/10/2015	10/10/2015	03/10/2015	01/10/2015	23/06/2015	23/06/2015	24/08/2015	24/08/2015
13/09/2015	13/09/2015	24/10/2015	25/10/2015	24/10/2015	22/10/2015	24/08/2015	21/08/2015	03/09/2015	03/09/2015
23/09/2015	23/09/2015	13/11/2015	10/11/2015	03/11/2015	07/11/2015	24/10/2015	24/10/2015	13/09/2015	13/09/2015
CGLS dates	EO dates	CGLS dates	EO dates	CGLS dates	EO dates	CGLS dates	EO dates	CGLS dates	EO dates
03/06/2016	03/06/2016	13/06/2016	16/06/2016	03/05/2016	08/05/2016	13/02/2016	10/02/2016	13/06/2016	14/06/2016
13/06/2016	14/06/2016	23/06/2016	26/06/2016	13/05/2016	18/05/2016	13/03/2016	14/03/2016	23/06/2016	27/06/2016
23/06/2016	23/06/2016	03/07/2016	07/07/2016	03/06/2016	07/06/2016	13/04/2016	13/04/2016	03/07/2016	03/07/2016
03/07/2016	02/07/2016	13/07/2016	16/07/2016	13/06/2016	17/06/2016	23/04/2016	23/04/2016	13/07/2016	13/07/2016
13/07/2016	13/07/2016	24/07/2016	24/07/2016	23/06/2016	26/06/2016	03/06/2016	30/05/2016	24/07/2016	24/07/2016
24/07/2016	20/07/2016	03/08/2016	03/08/2016	13/07/2016	17/07/2016	13/06/2016	13/06/2016	03/08/2016	03/08/2016
03/08/2016	05/08/2016	13/09/2016	09/09/2016	24/07/2016	24/07/2016	23/06/2016	23/06/2016	13/08/2016	13/08/2016
13/08/2016	13/08/2016	23/09/2016	25/09/2016	03/08/2016	05/08/2016	03/07/2016	03/07/2016	24/08/2016	24/08/2016
24/08/2016	24/08/2016	13/10/2016	14/10/2016	03/09/2016	03/09/2016	13/07/2016	13/07/2016	03/09/2016	30/08/2016
03/09/2016	03/09/2016	24/10/2016	27/10/2016	03/10/2016	05/10/2016	24/07/2016	24/07/2016	13/09/2016	15/09/2016
13/09/2016	13/09/2016	03/11/2016	03/11/2016	24/10/2016	24/10/2016	24/10/2016	27/10/2016	23/09/2016	22/09/2016
23/09/2016	23/09/2016	13/11/2016	13/11/2016	03/11/2016	07/11/2016	03/11/2016	16/11/2016	03/10/2016	01/10/2016

Table 8. Selected 12 dates per annum for LP1 & LP2 upscaling between 01/01/2012 and 31/12/2016. This table includes the -BON, US-BAO, BE-BRA, AU-CPR and US-DRA. For the coloured HR-EO dates, red indicates Sentinel -2, light blue Landsat-7, dark blue Landsat-8, and purple indicates interpolation is used and grey indicates no upscaling is needed.

US-BON		US-BAO		BE-BRA		AU-CPR		US-DRA	
CGLS dates	EO dates	CGLS dates	EO dates	CGLS dates	EO dates	CGLS dates	EO dates	CGLS dates	EO dates
		13/04/2012	08/04/2012						
		23/04/2012	21/04/2012						
		13/05/2012	10/05/2012						
		24/05/2012	26/05/2012						
		13/06/2012	11/06/2012						
		23/06/2012	18/06/2012						
		03/07/2012	04/07/2012						
		13/07/2012	13/07/2012						
		24/07/2012	20/07/2012						
		03/08/2012	05/08/2012						
		13/08/2012	14/08/2012						
		24/08/2012	21/08/2012						
CGLS dates	EO dates	CGLS dates	EO dates	CGLS dates	EO dates	CGLS dates	EO dates	CGLS dates	EO dates
24/03/2013	20/03/2013	24/05/2013	21/05/2013	03/03/2013	05/03/2013	03/02/2013	03/02/2013	13/03/2013	11/03/2013
03/04/2013	05/04/2013	03/06/2013	06/06/2013	23/04/2013	22/04/2013	13/02/2013	16/02/2013	13/04/2013	12/04/2013
23/04/2013	22/04/2013	03/07/2013	29/06/2013	03/05/2013	01/05/2013	22/02/2013	22/02/2013	23/04/2013	20/04/2013
03/05/2013	29/04/2013	13/07/2013	08/07/2013	24/07/2013	19/07/2013	03/03/2013	04/03/2013	03/05/2013	28/04/2013
13/05/2013	15/05/2013	24/07/2013	24/07/2013	03/08/2013	04/08/2013	13/03/2013	13/03/2013	24/05/2013	22/05/2013
24/05/2013	24/05/2013	03/08/2013	31/07/2013	13/08/2013	13/08/2013	24/03/2013	20/03/2013	03/06/2013	07/06/2013
13/08/2013	18/08/2013	13/08/2013	16/08/2013	24/08/2013	24/08/2013	03/04/2013	05/04/2013	23/06/2013	23/06/2013
24/08/2013	28/08/2013	24/08/2013	24/08/2013	03/09/2013	03/09/2013	13/04/2013	13/04/2013	03/07/2013	09/07/2013
03/09/2013	04/09/2013	13/09/2013	17/09/2013	13/09/2013	13/09/2013	23/04/2013	23/04/2013	24/07/2013	25/07/2013
03/10/2013	06/10/2013	23/09/2013	26/09/2013	23/09/2013	06/09/2013	03/05/2013	03/05/2013	13/08/2013	10/08/2013
13/10/2013	13/10/2013	24/10/2013	19/10/2013	03/10/2013	07/10/2013	13/05/2013	13/05/2013	23/09/2013	27/09/2013
03/11/2013	07/11/2013	13/11/2013	13/11/2013	13/10/2013	13/10/2013	24/05/2013	24/05/2013	13/10/2013	13/10/2013
CGLS dates	EO dates	CGLS dates	EO dates	CGLS dates	EO dates	CGLS dates	EO dates	CGLS dates	EO dates
13/04/2014	09/04/2014	13/03/2014	12/03/2014	03/02/2014	05/02/2014	03/04/2014	31/03/2014	13/03/2014	14/03/2014
23/04/2014	25/04/2014	24/03/2014	21/03/2014	13/03/2014	09/03/2014	03/05/2014	03/05/2014	24/03/2014	22/03/2014
03/05/2014	03/05/2014	03/04/2014	03/04/2014	03/04/2014	01/04/2014	13/05/2014	13/05/2014	03/04/2014	07/04/2014
13/05/2014	11/05/2014	03/06/2014	03/06/2014	13/04/2014	11/04/2014	03/08/2014	06/08/2014	23/04/2014	23/04/2014
24/07/2014	21/07/2014	13/06/2014	09/06/2014	24/05/2014	19/05/2014	24/08/2014	22/08/2014	03/05/2014	09/05/2014
03/08/2014	30/07/2014	23/06/2014	23/06/2014	03/06/2014	06/06/2014	03/09/2014	07/09/2014	24/05/2014	25/05/2014
13/08/2014	13/08/2014	03/07/2014	03/07/2014	03/07/2014	03/07/2014	23/09/2014	23/09/2014	13/07/2014	12/07/2014
24/08/2014	24/08/2014	13/07/2014	13/07/2014	13/07/2014	13/07/2014	13/10/2014	09/10/2014	13/08/2014	13/08/2014
03/09/2014	03/09/2014	24/07/2014	24/07/2014	24/07/2014	24/07/2014	24/10/2014	25/10/2014	24/08/2014	29/08/2014
23/09/2014	23/09/2014	13/08/2014	13/08/2014	03/08/2014	03/08/2014	13/11/2014	10/11/2014	03/09/2014	06/09/2014
24/10/2014	25/10/2014	23/09/2014	20/09/2014	13/08/2014	13/08/2014	23/11/2014	26/11/2014	23/09/2014	22/09/2014
03/11/2014	03/11/2014	03/10/2014	06/10/2014	13/09/2014	17/09/2014	13/12/2014	12/12/2014	03/10/2014	30/09/2014
CGLS dates	EO dates	CGLS dates	EO dates	CGLS dates	EO dates	CGLS dates	EO dates	CGLS dates	EO dates
03/07/2015	30/06/2015	21/02/2015	21/02/2015	13/02/2015	15/02/2015	03/02/2015	29/01/2015	13/03/2015	09/03/2015
13/07/2015	13/07/2015	22/02/2015	22/02/2015	13/03/2015	12/03/2015	03/04/2015	03/04/2015	24/03/2015	25/03/2015
24/07/2015	24/07/2015	03/03/2015	03/03/2015	23/06/2015	23/06/2015	03/06/2015	06/06/2015	13/04/2015	10/04/2015
03/08/2015	02/08/2015	13/03/2015	13/03/2015	03/07/2015	01/07/2015	24/07/2015	24/07/2015	23/04/2015	26/04/2015
13/08/2015	13/08/2015	24/03/2015	24/03/2015	13/07/2015	13/07/2015	13/08/2015	09/08/2015	24/05/2015	28/05/2015
24/08/2015	25/08/2015	03/04/2015	31/03/2015	24/07/2015	24/07/2015	23/09/2015	26/09/2015	13/06/2015	13/06/2015
03/09/2015	03/09/2015	13/04/2015	13/04/2015	03/08/2015	03/08/2015	13/10/2015	11/10/2015	03/07/2015	29/06/2015
13/09/2015	13/09/2015	23/04/2015	23/04/2015	24/08/2015	22/08/2015	13/11/2015	13/11/2015	13/07/2015	15/07/2015
23/09/2015	23/09/2015	03/05/2015	03/05/2015	03/09/2015	03/09/2015	23/11/2015	24/11/2015	13/08/2015	16/08/2015
03/10/2015	03/10/2015	13/05/2015	11/05/2015	13/09/2015	11/09/2015	03/12/2015	29/11/2015	13/09/2015	09/09/2015
13/10/2015	13/10/2015	24/05/2015	24/05/2015	23/09/2015	27/09/2015	13/12/2015	13/12/2015	03/10/2015	03/10/2015
24/10/2015	24/10/2015	03/06/2015	03/06/2015	03/10/2015	01/10/2015	24/12/2015	24/12/2015	13/10/2015	11/10/2015
CGLS dates	EO dates	CGLS dates	EO dates	CGLS dates	EO dates	CGLS dates	EO dates	CGLS dates	EO dates
03/04/2016	05/04/2016			13/03/2016	14/03/2016	03/01/2016	03/01/2016	13/04/2016	16/04/2016
13/04/2016	14/04/2016			13/06/2016	09/06/2016	13/01/2016	13/01/2016	23/04/2016	26/04/2016
23/04/2016	23/04/2016			23/06/2016	23/06/2016	03/02/2016	01/02/2016	13/05/2016	09/05/2016
24/05/2016	23/05/2016			03/07/2016	03/07/2016	13/02/2016	12/02/2016	03/06/2016	30/05/2016
03/06/2016	08/06/2016			13/07/2016	13/07/2016	03/03/2016	04/03/2016	13/06/2016	18/06/2016
13/06/2016	17/06/2016			24/07/2016	20/07/2016	24/03/2016	20/03/2016	23/06/2016	23/06/2016
13/07/2016	10/07/2016			03/08/2016	03/08/2016	13/09/2016	12/09/2016	03/07/2016	01/07/2016
03/08/2016	04/08/2016			13/08/2016	16/08/2016	13/10/2016	14/10/2016	13/07/2016	17/07/2016
03/09/2016	05/09/2016			24/08/2016	24/08/2016	24/10/2016	29/10/2016	24/07/2016	28/07/2016
13/09/2016	12/09/2016			03/09/2016	03/09/2016	13/11/2016	15/11/2016	03/08/2016	04/08/2016
23/09/2016	21/09/2016			13/09/2016	08/09/2016	03/12/2016	01/12/2016	13/08/2016	17/08/2016
13/10/2016	13/10/2016			23/09/2016	25/09/2016	13/12/2016	18/12/2016	24/08/2016	24/08/2016

Table 9. Selected 12 dates per annum for LP1 & LP2 upscaling between 01/01/2012 and 31/12/2016. This table includes the US-FPK, DE-GEB, US-GCM, FR-GRI and GF-GUY. For the coloured HR-EO dates, red indicates Sentinel-2, light blue Landsat-7, dark blue Landsat-8, and purple indicates interpolation is used and grey indicates no upscaling is needed.

US-FPK		DE-GEB		US-GCM		FR-GRI		GF-GUY	
CGLS dates	EO dates	CGLS dates	EO dates	CGLS dates	EO dates	CGLS dates	EO dates	CGLS dates	EO dates
		03/07/2012	03/07/2012			13/03/2012	15/03/2012	03/09/2012	05/09/2012
		13/07/2012	13/07/2012			24/03/2012	25/03/2012	13/09/2012	13/09/2012
		24/07/2012	24/07/2012			03/05/2012	24/05/2012	23/09/2012	23/09/2012
		03/08/2012	03/08/2012			24/05/2012	28/05/2012	03/10/2012	03/10/2012
		13/08/2012	13/08/2012			23/06/2012	23/06/2012	13/10/2012	13/10/2012
		24/08/2012	22/08/2012			24/07/2012	24/07/2012	24/10/2012	24/10/2012
		03/09/2012	29/08/2012			03/08/2012	03/08/2012	03/11/2012	03/11/2012
		13/09/2012	13/09/2012			13/08/2012	09/08/2012	13/11/2012	13/11/2012
		23/09/2012	23/09/2012			24/08/2012	24/08/2012	23/11/2012	23/11/2012
		03/10/2012	30/09/2012			03/09/2012	01/09/2012	03/12/2012	03/12/2012
		13/10/2012	09/10/2012			13/09/2012	15/09/2012	13/12/2012	13/12/2012
		24/10/2012	24/10/2012			23/09/2012	19/09/2012	24/12/2012	24/12/2012
CGLS dates	EO dates	CGLS dates	EO dates	CGLS dates	EO dates	CGLS dates	EO dates	CGLS dates	EO dates
03/07/2013	06/07/2013	13/06/2013	13/06/2013	03/03/2013	04/03/2013	03/07/2013	03/07/2013	13/06/2013	13/06/2013
13/07/2013	13/07/2013	23/06/2013	23/06/2013	13/03/2013	13/03/2013	13/07/2013	10/07/2013	23/06/2013	23/06/2013
24/07/2013	22/07/2013	03/07/2013	03/07/2013	24/03/2013	20/03/2013	24/07/2013	19/07/2013	03/07/2013	03/07/2013
03/08/2013	07/08/2013	13/07/2013	16/07/2013	03/04/2013	05/04/2013	03/08/2013	04/08/2013	13/07/2013	13/07/2013
13/08/2013	13/08/2013	24/07/2013	24/07/2013	23/04/2013	21/04/2013	13/08/2013	13/08/2013	24/07/2013	24/07/2013
24/08/2013	24/08/2013	03/08/2013	01/08/2013	03/05/2013	30/04/2013	24/08/2013	20/08/2013	03/08/2013	03/08/2013
03/09/2013	03/09/2013	13/08/2013	16/08/2013	13/05/2013	15/05/2013	03/09/2013	04/09/2013	13/08/2013	16/08/2013
13/09/2013	15/09/2013	24/08/2013	24/08/2013	24/05/2013	24/05/2013	13/09/2013	13/09/2013	24/08/2013	27/08/2013
23/09/2013	24/09/2013	03/09/2013	03/09/2013	03/07/2013	02/07/2013	23/09/2013	23/09/2013	03/09/2013	03/09/2013
03/10/2013	01/10/2013	13/09/2013	13/09/2013	13/07/2013	11/07/2013	03/10/2013	07/10/2013	13/09/2013	13/09/2013
13/10/2013	13/10/2013	23/09/2013	23/09/2013	24/08/2013	28/08/2013	13/10/2013	13/10/2013	23/09/2013	23/09/2013
24/10/2013	26/10/2013	03/10/2013	03/10/2013	03/09/2013	04/09/2013	03/11/2013	30/10/2013	03/10/2013	03/10/2013
CGLS dates	EO dates	CGLS dates	EO dates	CGLS dates	EO dates	CGLS dates	EO dates	CGLS dates	EO dates
24/03/2014	19/03/2014	13/06/2014	13/06/2014	13/02/2014	27/02/2014	03/02/2014	03/02/2014	23/06/2014	23/06/2014
03/04/2014	04/04/2014	23/06/2014	23/06/2014	03/03/2014	08/03/2014	13/02/2014	12/02/2014	03/07/2014	03/07/2014
23/04/2014	20/04/2014	03/07/2014	03/07/2014	24/03/2014	24/03/2014	03/03/2014	07/03/2014	13/07/2014	13/07/2014
13/05/2014	13/05/2014	13/07/2014	13/07/2014	13/04/2014	09/04/2014	13/03/2014	16/03/2014	24/07/2014	24/07/2014
03/06/2014	03/06/2014	24/07/2014	19/07/2014	03/07/2014	05/07/2014	13/04/2014	17/04/2014	03/08/2014	03/08/2014
13/06/2014	13/06/2014	03/08/2014	03/08/2014	13/07/2014	14/07/2014	24/05/2014	19/05/2014	13/08/2014	13/08/2014
23/06/2014	23/06/2014	13/08/2014	13/08/2014	24/07/2014	24/07/2014	13/06/2014	12/06/2014	24/08/2014	24/08/2014
03/07/2014	03/07/2014	24/08/2014	24/08/2014	03/08/2014	30/07/2014	24/07/2014	24/07/2014	03/09/2014	03/09/2014
03/08/2014	01/08/2014	03/09/2014	03/09/2014	24/08/2014	22/08/2014	03/08/2014	03/08/2014	13/09/2014	13/09/2014
24/08/2014	26/08/2014	13/09/2014	13/09/2014	03/09/2014	03/09/2014	13/08/2014	13/08/2014	23/09/2014	23/09/2014
03/09/2014	03/09/2014	23/09/2014	23/09/2014	13/09/2014	16/09/2014	03/09/2014	03/09/2014	03/10/2014	03/10/2014
23/09/2014	26/09/2014	03/10/2014	03/10/2014	24/10/2014	25/10/2014	03/10/2014	01/10/2014	13/10/2014	13/10/2014
CGLS dates	EO dates	CGLS dates	EO dates	CGLS dates	EO dates	CGLS dates	EO dates	CGLS dates	EO dates
13/03/2015	13/03/2015	13/06/2015	13/06/2015	03/02/2015	07/02/2015	23/04/2015	27/04/2015	23/06/2015	27/06/2015
24/03/2015	29/03/2015	23/06/2015	23/06/2015	13/02/2015	14/02/2015	03/06/2015	06/06/2015	03/07/2015	03/07/2015
03/04/2015	07/04/2015	03/07/2015	03/07/2015	03/05/2015	05/05/2015	13/06/2015	13/06/2015	13/07/2015	13/07/2015
13/05/2015	09/05/2015	13/07/2015	13/07/2015	24/07/2015	24/07/2015	03/07/2015	30/06/2015	24/07/2015	24/07/2015
03/06/2015	01/06/2015	24/07/2015	24/07/2015	03/08/2015	02/08/2015	13/07/2015	16/07/2015	03/08/2015	03/08/2015
13/06/2015	17/06/2015	03/08/2015	03/08/2015	13/08/2015	09/08/2015	24/07/2015	24/07/2015	13/08/2015	13/08/2015
23/06/2015	26/06/2015	13/08/2015	13/08/2015	24/08/2015	25/08/2015	03/08/2015	01/08/2015	24/08/2015	24/08/2015
24/07/2015	19/07/2015	24/08/2015	23/08/2015	03/10/2015	05/10/2015	24/08/2015	26/08/2015	03/09/2015	03/09/2015
03/08/2015	04/08/2015	03/09/2015	03/09/2015	24/10/2015	21/10/2015	03/09/2015	03/09/2015	13/09/2015	13/09/2015
24/08/2015	20/08/2015	13/09/2015	13/09/2015	13/11/2015	13/11/2015	13/09/2015	13/09/2015	23/09/2015	23/09/2015
13/09/2015	14/09/2015	23/09/2015	28/09/2015	23/11/2015	22/11/2015	23/09/2015	27/09/2015	03/10/2015	03/10/2015
03/10/2015	30/09/2015	03/10/2015	03/10/2015	13/12/2015	08/12/2015	03/10/2015	04/10/2015	13/10/2015	13/10/2015
CGLS dates	EO dates	CGLS dates	EO dates	CGLS dates	EO dates	CGLS dates	EO dates	CGLS dates	EO dates
24/03/2016	20/04/2016			24/03/2016	29/03/2016				
03/05/2016	02/05/2016			03/04/2016	05/04/2016				
13/05/2016	18/05/2016			03/05/2016	06/05/2016				
13/06/2016	12/06/2016			13/05/2016	13/05/2016				
23/06/2016	19/06/2016			03/06/2016	03/06/2016				
03/07/2016	28/06/2016			03/09/2016	03/09/2016				
13/07/2016	09/07/2016			13/09/2016	12/09/2016				
24/07/2016	21/07/2016			23/09/2016	23/09/2016				
03/08/2016	30/07/2016			03/10/2016	07/10/2016				
24/08/2016	22/08/2016			24/10/2016	23/10/2016				
13/09/2016	16/09/2016			03/11/2016	30/10/2016				
23/09/2016	27/09/2016			13/11/2016	15/11/2016				

Table 10. Selected 12 dates per annum for LP1 & LP2 upscaling between 01/01/2012 and 31/12/2016. This table includes the DE-HAI, IT-REN, US-PSU, US-TBL. For the coloured HR-EO dates, red indicates Sentinel-2, light blue Landsat-7, dark blue Landsat-8, and purple indicates interpolation is used and grey indicates no upscaling is needed.

DE-HAI		IT-REN		US-PSU		US-TBL	
CGLS dates	EO dates	CGLS dates	EO dates	CGLS dates	EO dates	CGLS dates	EO dates
13/03/2012	15/03/2012	13/03/2012	14/03/2012				
24/03/2012	24/03/2012	13/04/2012	09/04/2012				
03/05/2012	02/05/2012	24/05/2012	24/05/2012				
13/05/2012	13/05/2012	03/06/2012	03/06/2012				
24/05/2012	25/05/2012	13/06/2012	13/06/2012				
03/06/2012	03/06/2012	23/06/2012	24/06/2012				
23/06/2012	22/06/2012	03/07/2012	07/07/2012				
24/08/2012	29/08/2012	13/07/2012	13/07/2012				
23/09/2012	23/09/2012	24/07/2012	23/07/2012				
03/10/2012	03/10/2012	03/08/2012	08/08/2012				
13/10/2012	16/10/2012	13/08/2012	17/08/2012				
24/10/2012	24/10/2012	24/08/2012	24/08/2012				
CGLS dates	EO dates	CGLS dates	EO dates	CGLS dates	EO dates	CGLS dates	EO dates
03/07/2013	07/07/2013	03/06/2013	07/06/2013	23/04/2013	23/04/2013	03/06/2013	06/06/2013
13/07/2013	13/07/2013	13/06/2013	16/06/2013	03/05/2013	03/05/2013	23/06/2013	22/06/2013
24/07/2013	24/07/2013	23/06/2013	23/06/2013	13/05/2013	14/05/2013	03/07/2013	08/07/2013
03/08/2013	01/08/2013	03/07/2013	02/07/2013	24/05/2013	24/05/2013	24/07/2013	24/07/2013
13/08/2013	16/08/2013	13/07/2013	18/07/2013	03/06/2013	03/06/2013	03/08/2013	31/07/2013
24/08/2013	24/08/2013	24/07/2013	25/07/2013	13/06/2013	15/06/2013	13/08/2013	09/08/2013
03/09/2013	03/09/2013	03/08/2013	03/08/2013	23/06/2013	23/06/2013	24/08/2013	24/08/2013
13/09/2013	13/09/2013	13/08/2013	10/08/2013	03/07/2013	03/07/2013	03/09/2013	03/09/2013
23/09/2013	23/09/2013	24/08/2013	24/08/2013	13/07/2013	17ls/07/2013	13/09/2013	17/09/2013
03/10/2013	03/10/2013	03/09/2013	04/09/2013	24/07/2013	24/07/2013	23/09/2013	26/09/2013
13/10/2013	13/10/2013	13/09/2013	13/09/2013	03/08/2013	03/08/2013	24/10/2013	19/10/2013
24/10/2013	24/10/2013	13/10/2013	17/10/2013	13/08/2013	13/08/2013	13/11/2013	13/11/2013
CGLS dates	EO dates	CGLS dates	EO dates	CGLS dates	EO dates	CGLS dates	EO dates
22/02/2014	25/02/2014	03/04/2014	31/03/2014	03/07/2014	03/07/2014	22/02/2014	24/02/2014
13/03/2014	13/03/2014	13/04/2014	16/04/2014	13/07/2014	13/07/2014	03/03/2014	05/03/2014
24/03/2014	20/03/2014	13/05/2014	09/05/2014	24/07/2014	24/07/2014	13/03/2014	12/03/2014
13/05/2014	16/05/2014	24/05/2014	24/05/2014	03/08/2014	05/08/2014	24/03/2014	21/03/2014
24/05/2014	25/05/2014	13/06/2014	13/06/2014	13/08/2014	13/08/2014	03/06/2014	03/06/2014
03/06/2014	08/06/2014	23/06/2014	23/06/2014	24/08/2014	24/08/2014	13/06/2014	16/06/2014
03/07/2014	03/07/2014	03/07/2014	03/07/2014	03/09/2014	03/09/2014	03/07/2014	02/07/2014
13/07/2014	13/07/2014	03/08/2014	06/08/2014	13/09/2014	13/09/2014	13/07/2014	13/07/2014
24/07/2014	26/07/2014	24/08/2014	29/08/2014	23/09/2014	23/09/2014	24/07/2014	24/07/2014
03/08/2014	03/08/2014	03/09/2014	07/09/2014	03/10/2014	03/10/2014	13/08/2014	12/08/2014
23/09/2014	28/09/2014	23/09/2014	23/09/2014	13/10/2014	13/10/2014	23/09/2014	20/09/2014
03/10/2014	06/10/2014	03/10/2014	30/09/2014	24/10/2014	24/10/2014	03/10/2014	06/10/2014
CGLS dates	EO dates	CGLS dates	EO dates	CGLS dates	EO dates	CGLS dates	EO dates
23/04/2015	24/04/2015	13/03/2015	18/03/2015	03/07/2015	03/07/2015	03/04/2015	31/03/2015
13/05/2015	10/05/2015	03/04/2015	03/04/2015	13/07/2015	13/07/2015	13/05/2015	11/05/2015
03/06/2015	04/06/2015	23/04/2015	19/04/2015	24/07/2015	23/07/2015	03/06/2015	03/06/2015
13/06/2015	13/06/2015	24/05/2015	28/05/2015	03/08/2015	03/08/2015	23/06/2015	19/06/2015
23/06/2015	23/06/2015	03/06/2015	06/06/2015	13/08/2015	13/08/2015	03/07/2015	28/06/2015
03/07/2015	03/07/2015	13/06/2015	13/06/2015	24/08/2015	24/08/2015	13/07/2015	13/07/2015
13/07/2015	13/07/2015	13/07/2015	15/07/2015	03/09/2015	03/09/2015	24/07/2015	24/07/2015
24/07/2015	24/07/2015	03/08/2015	31/07/2015	13/09/2015	13/09/2015	03/08/2015	30/07/2015
03/08/2015	07/08/2015	13/08/2015	09/08/2015	23/09/2015	23/09/2015	13/08/2015	15/08/2015
24/08/2015	23/08/2015	03/09/2015	01/09/2015	03/10/2015	03/10/2015	24/08/2015	24/08/2015
03/09/2015	30/08/2015	23/09/2015	26/09/2015	13/10/2015	11/10/2015	13/10/2015	10/10/2015
03/10/2015	01/10/2015	13/10/2015	12/10/2015	24/10/2015	24/10/2015	24/10/2015	25/10/2015
CGLS dates	EO dates	CGLS dates	EO dates	CGLS dates	EO dates	CGLS dates	EO dates
				03/07/2016	03/07/2016	13/03/2016	10/03/2016
				13/07/2016	13/07/2016	03/05/2016	04/05/2016
				24/07/2016	24/07/2016	13/05/2016	13/05/2016
				03/08/2016	03/08/2016	24/05/2016	29/05/2016
				13/08/2016	13/08/2016	13/06/2016	14/06/2016
				24/08/2016	24/08/2016	23/06/2016	23/06/2016
				03/09/2016	03/09/2016	03/07/2016	07/07/2016
				13/09/2016	13/09/2016	13/07/2016	16/07/2016
				23/09/2016	27/09/2016	24/07/2016	24/07/2016
				03/10/2016	03/10/2016	13/08/2016	17/08/2016

				13/10/2016	13/10/2016	24/08/2016	25/08/2016
				24/10/2016	24/10/2016	13/09/2016	14/09/2016

- Table 10 list the selected 12 dates per annum for upscaling LP1 and LP2 at the 19 sites between 01/01/2012 and 31/12/2016. The 12 upscaling dates per annum are chosen from the CGLS dates such that the upscaled LP1 and LP2 are comparable with the CGLS products. The HR-EO dates are selected within the ± 5day-window of the upscaling dates.

Table 7. Selected 12 dates per annum for LP1 & LP2 upscaling between 01/01/2012 and 31/12/2016. This table includes the US-BRW, US-NR1, US-SXF, AU-TUM and US-ARM. For the coloured HR-EO dates, red indicates Sentinel-2, light blue Landsat-7, dark blue Landsat-8, and purple indicates interpolation is used and grey indicates no upscaling is needed.

US-BRW		US-NR1		US-SXF		AU-TUM		US-ARM	
CGLS dates	EO dates	CGLS dates	EO dates	CGLS dates	EO dates	CGLS dates	EO dates	CGLS dates	EO dates
								03/02/2012	01/02/2012
								22/02/2012	26/02/2012
								03/03/2012	04/03/2012
								23/04/2012	21/04/2012
								24/05/2012	23/05/2012
								03/06/2012	08/06/2012
								13/06/2012	13/06/2012
								03/08/2012	03/08/2012
								13/09/2012	12/09/2012
								13/10/2012	14/10/2012
								03/11/2012	30/10/2012
								13/11/2012	15/11/2012
CGLS dates	EO dates	CGLS dates	EO dates	CGLS dates	EO dates	CGLS dates	EO dates	CGLS dates	EO dates
03/06/2013	03/06/2013	23/06/2013	23/06/2013	13/06/2013	10/06/2013	24/01/2013	01/28/2013	03/02/2013	03/02/2013
13/06/2013	13/06/2013	03/07/2013	03/07/2013	23/06/2013	23/06/2013	13/02/2013	13/02/2013	21/02/2013	19/02/2013
23/06/2013	23/06/2013	13/07/2013	13/07/2013	03/07/2013	04/07/2013	03/03/2013	03/03/2013	03/03/2013	07/03/2013
03/07/2013	08/07/2013	24/07/2013	24/07/2013	13/07/2013	12/07/2013	13/03/2013	13/03/2013	23/04/2013	24/04/2013
13/07/2013	13/07/2013	03/08/2013	03/08/2013	24/07/2013	21/07/2013	03/04/2013	01/04/2013	03/06/2013	03/06/2013
24/07/2013	24/07/2013	13/08/2013	13/08/2013	03/08/2013	03/08/2013	23/04/2013	25/04/2013	03/08/2013	06/08/2013
03/08/2013	03/08/2013	24/08/2013	24/08/2013	13/08/2013	13/08/2013	24/05/2013	27/05/2013	13/09/2013	07/09/2013
13/08/2013	11/08/2013	03/09/2013	03/09/2013	24/08/2013	20/08/2013	03/08/2013	30/07/2013	23/09/2013	23/09/2013
24/08/2013	24/08/2013	13/09/2013	17/09/2013	03/09/2013	03/09/2013	13/08/2013	15/08/2013	13/10/2013	09/10/2013
03/09/2013	03/09/2013	23/09/2013	23/09/2013	13/09/2013	22/09/2013	03/09/2013	03/09/2013	24/10/2013	25/10/2013
13/09/2013	13/09/2013	03/10/2013	03/10/2013	03/10/2013	01/10/2013	03/11/2013	03/11/2013	03/11/2013	03/11/2013
23/09/2013	23/09/2013	24/10/2013	19/10/2013	13/10/2013	16/10/2013	23/11/2013	19/11/2013	23/11/2013	26/11/2013
CGLS dates	EO dates	CGLS dates	EO dates	CGLS dates	EO dates	CGLS dates	EO dates	CGLS dates	EO dates
03/06/2014	03/06/2014	03/06/2014	03/06/2014	13/04/2014	10/04/2014	03/01/2014	06/01/2014	13/02/2014	14/02/2014
13/06/2014	13/06/2014	13/06/2014	13/06/2014	24/05/2014	28/05/2014	24/01/2014	22/01/2014	13/03/2014	18/03/2014
23/06/2014	25/06/2014	23/06/2014	16/06/2014	23/06/2014	23/06/2014	03/02/2014	07/02/2014	23/04/2014	19/04/2014
03/07/2014	03/07/2014	03/07/2014	02/07/2014	03/07/2014	29/06/2014	21/02/2014	23/02/2014	03/05/2014	05/05/2014
13/07/2014	13/07/2014	13/07/2014	13/07/2014	13/07/2014	13/07/2014	03/08/2014	02/08/2014	03/07/2014	03/07/2014
24/07/2014	24/07/2014	24/07/2014	24/07/2014	24/07/2014	24/07/2014	03/09/2014	03/09/2014	13/07/2014	13/07/2014
03/08/2014	03/08/2014	03/08/2014	03/08/2014	03/08/2014	03/08/2014	23/09/2014	23/09/2014	24/07/2014	24/07/2014
13/08/2014	12/08/2014	13/08/2014	13/08/2014	13/08/2014	16/08/2014	03/10/2014	05/10/2014	24/08/2014	25/08/2014
24/08/2014	24/08/2014	24/08/2014	24/08/2014	03/09/2014	01/09/2014	24/10/2014	21/10/2014	03/09/2014	03/09/2014
03/09/2014	03/09/2014	03/09/2014	03/09/2014	13/09/2014	17/09/2014	03/11/2014	06/11/2014	13/09/2014	13/09/2014
13/09/2014	13/09/2014	13/09/2014	13/09/2014	24/10/2014	19/10/2014	23/11/2014	22/11/2014	23/09/2014	26/09/2014
23/09/2014	23/09/2014	23/09/2014	20/09/2014	03/11/2014	04/11/2014	03/12/2014	08/12/2014	24/10/2014	28/10/2014
CGLS dates	EO dates	CGLS dates	EO dates	CGLS dates	EO dates	CGLS dates	EO dates	CGLS dates	EO dates
03/06/2015	03/06/2015	24/01/2015	26/01/2015	22/02/2015	24/02/2015	13/03/2015	14/03/2015	21/02/2015	17/02/2015
13/06/2015	13/06/2015	03/06/2015	03/06/2015	24/03/2015	28/03/2015	03/04/2015	30/03/2015	03/06/2015	03/06/2015
23/06/2015	22/06/2015	13/06/2015	13/06/2015	13/04/2015	13/04/2015	13/04/2015	15/04/2015	13/06/2015	13/06/2015
03/07/2015	07/07/2015	23/06/2015	23/06/2015	03/05/2015	29/04/2015	23/04/2015	23/04/2015	23/06/2015	23/06/2015
13/07/2015	13/07/2015	03/07/2015	03/07/2015	13/07/2015	18/07/2015	03/05/2015	03/05/2015	03/07/2015	03/07/2015
24/07/2015	29/07/2015	13/07/2015	13/07/2015	03/08/2015	02/08/2015	13/05/2015	13/05/2015	13/07/2015	13/07/2015
03/08/2015	03/08/2015	24/07/2015	24/07/2015	13/08/2015	13/08/2015	24/05/2015	24/05/2015	24/07/2015	24/07/2015
13/08/2015	13/08/2015	03/08/2015	03/08/2015	24/08/2015	24/08/2015	03/06/2015	02/06/2015	03/08/2015	03/08/2015
24/08/2015	24/08/2015	24/08/2015	22/08/2015	13/09/2015	12/09/2015	13/06/2015	18/06/2015	13/08/2015	13/08/2015
03/09/2015	03/09/2015	13/10/2015	10/10/2015	03/10/2015	01/10/2015	23/06/2015	23/06/2015	24/08/2015	24/08/2015
13/09/2015	13/09/2015	24/10/2015	25/10/2015	24/10/2015	22/10/2015	24/08/2015	21/08/2015	03/09/2015	03/09/2015
23/09/2015	23/09/2015	13/11/2015	10/11/2015	03/11/2015	07/11/2015	24/10/2015	24/10/2015	13/09/2015	13/09/2015
CGLS dates	EO dates	CGLS dates	EO dates	CGLS dates	EO dates	CGLS dates	EO dates	CGLS dates	EO dates
03/06/2016	03/06/2016	13/06/2016	16/06/2016	03/05/2016	08/05/2016	13/02/2016	10/02/2016	13/06/2016	14/06/2016
13/06/2016	14/06/2016	23/06/2016	26/06/2016	13/05/2016	18/05/2016	13/03/2016	14/03/2016	23/06/2016	27/06/2016
23/06/2016	23/06/2016	03/07/2016	07/07/2016	03/06/2016	07/06/2016	13/04/2016	13/04/2016	03/07/2016	03/07/2016
03/07/2016	02/07/2016	13/07/2016	16/07/2016	13/06/2016	17/06/2016	23/04/2016	23/04/2016	13/07/2016	13/07/2016
13/07/2016	13/07/2016	24/07/2016	24/07/2016	23/06/2016	26/06/2016	03/06/2016	30/05/2016	24/07/2016	24/07/2016
24/07/2016	20/07/2016	03/08/2016	03/08/2016	13/07/2016	17/07/2016	13/06/2016	13/06/2016	03/08/2016	03/08/2016
03/08/2016	05/08/2016	13/09/2016	09/09/2016	24/07/2016	24/07/2016	23/06/2016	23/06/2016	13/08/2016	13/08/2016
13/08/2016	13/08/2016	23/09/2016	25/09/2016	03/08/2016	05/08/2016	03/07/2016	03/07/2016	24/08/2016	24/08/2016
24/08/2016	24/08/2016	13/10/2016	14/10/2016	03/09/2016	03/09/2016	13/07/2016	13/07/2016	03/09/2016	30/08/2016
03/09/2016	03/09/2016	24/10/2016	27/10/2016	03/10/2016	05/10/2016	24/07/2016	24/07/2016	13/09/2016	15/09/2016
13/09/2016	13/09/2016	03/11/2016	03/11/2016	24/10/2016	24/10/2016	24/10/2016	27/10/2016	23/09/2016	22/09/2016
23/09/2016	23/09/2016	13/11/2016	13/11/2016	03/11/2016	07/11/2016	03/11/2016	16/11/2016	03/10/2016	01/10/2016

Table 8. Selected 12 dates per annum for LP1 & LP2 upscaling between 01/01/2012 and 31/12/2016. This table includes the -BON, US-BAO, BE-BRA, AU-CPR and US-DRA. For the coloured HR-EO dates, red indicates Sentinel -2, light blue Landsat-7, dark blue Landsat-8, and purple indicates interpolation is used and grey indicates no upscaling is needed.

US-BON		US-BAO		BE-BRA		AU-CPR		US-DRA	
CGLS dates	EO dates	CGLS dates	EO dates	CGLS dates	EO dates	CGLS dates	EO dates	CGLS dates	EO dates
		13/04/2012	08/04/2012						
		23/04/2012	21/04/2012						
		13/05/2012	10/05/2012						
		24/05/2012	26/05/2012						
		13/06/2012	11/06/2012						
		23/06/2012	18/06/2012						
		03/07/2012	04/07/2012						
		13/07/2012	13/07/2012						
		24/07/2012	20/07/2012						
		03/08/2012	05/08/2012						
		13/08/2012	14/08/2012						
		24/08/2012	21/08/2012						
CGLS dates	EO dates	CGLS dates	EO dates	CGLS dates	EO dates	CGLS dates	EO dates	CGLS dates	EO dates
24/03/2013	20/03/2013	24/05/2013	21/05/2013	03/03/2013	05/03/2013	03/02/2013	03/02/2013	13/03/2013	11/03/2013
03/04/2013	05/04/2013	03/06/2013	06/06/2013	23/04/2013	22/04/2013	13/02/2013	16/02/2013	13/04/2013	12/04/2013
23/04/2013	22/04/2013	03/07/2013	29/06/2013	03/05/2013	01/05/2013	22/02/2013	22/02/2013	23/04/2013	20/04/2013
03/05/2013	29/04/2013	13/07/2013	08/07/2013	24/07/2013	19/07/2013	03/03/2013	04/03/2013	03/05/2013	28/04/2013
13/05/2013	15/05/2013	24/07/2013	24/07/2013	03/08/2013	04/08/2013	13/03/2013	13/03/2013	24/05/2013	22/05/2013
24/05/2013	24/05/2013	03/08/2013	31/07/2013	13/08/2013	13/08/2013	24/03/2013	20/03/2013	03/06/2013	07/06/2013
13/08/2013	18/08/2013	13/08/2013	16/08/2013	24/08/2013	24/08/2013	03/04/2013	05/04/2013	23/06/2013	23/06/2013
24/08/2013	28/08/2013	24/08/2013	24/08/2013	03/09/2013	03/09/2013	13/04/2013	13/04/2013	03/07/2013	09/07/2013
03/09/2013	04/09/2013	13/09/2013	17/09/2013	13/09/2013	13/09/2013	23/04/2013	23/04/2013	24/07/2013	25/07/2013
03/10/2013	06/10/2013	23/09/2013	26/09/2013	23/09/2013	06/09/2013	03/05/2013	03/05/2013	13/08/2013	10/08/2013
13/10/2013	13/10/2013	24/10/2013	19/10/2013	03/10/2013	07/10/2013	13/05/2013	13/05/2013	23/09/2013	27/09/2013
03/11/2013	07/11/2013	13/11/2013	13/11/2013	13/10/2013	13/10/2013	24/05/2013	24/05/2013	13/10/2013	13/10/2013
CGLS dates	EO dates	CGLS dates	EO dates	CGLS dates	EO dates	CGLS dates	EO dates	CGLS dates	EO dates
13/04/2014	09/04/2014	13/03/2014	12/03/2014	03/02/2014	05/02/2014	03/04/2014	31/03/2014	13/03/2014	14/03/2014
23/04/2014	25/04/2014	24/03/2014	21/03/2014	13/03/2014	09/03/2014	03/05/2014	03/05/2014	24/03/2014	22/03/2014
03/05/2014	03/05/2014	03/04/2014	03/04/2014	03/04/2014	01/04/2014	13/05/2014	13/05/2014	03/04/2014	07/04/2014
13/05/2014	11/05/2014	03/06/2014	03/06/2014	13/04/2014	11/04/2014	03/08/2014	06/08/2014	23/04/2014	23/04/2014
24/07/2014	21/07/2014	13/06/2014	09/06/2014	24/05/2014	19/05/2014	24/08/2014	22/08/2014	03/05/2014	09/05/2014
03/08/2014	30/07/2014	23/06/2014	23/06/2014	03/06/2014	06/06/2014	03/09/2014	07/09/2014	24/05/2014	25/05/2014
13/08/2014	13/08/2014	03/07/2014	03/07/2014	03/07/2014	03/07/2014	23/09/2014	23/09/2014	13/07/2014	12/07/2014
24/08/2014	24/08/2014	13/07/2014	13/07/2014	13/07/2014	13/07/2014	13/10/2014	09/10/2014	13/08/2014	13/08/2014
03/09/2014	03/09/2014	24/07/2014	24/07/2014	24/07/2014	24/07/2014	24/10/2014	25/10/2014	24/08/2014	29/08/2014
23/09/2014	23/09/2014	13/08/2014	13/08/2014	03/08/2014	03/08/2014	13/11/2014	10/11/2014	03/09/2014	06/09/2014
24/10/2014	25/10/2014	23/09/2014	20/09/2014	13/08/2014	13/08/2014	23/11/2014	26/11/2014	23/09/2014	22/09/2014
03/11/2014	03/11/2014	03/10/2014	06/10/2014	13/09/2014	17/09/2014	13/12/2014	12/12/2014	03/10/2014	30/09/2014
CGLS dates	EO dates	CGLS dates	EO dates	CGLS dates	EO dates	CGLS dates	EO dates	CGLS dates	EO dates
03/07/2015	30/06/2015	21/02/2015	21/02/2015	13/02/2015	15/02/2015	03/02/2015	29/01/2015	13/03/2015	09/03/2015
13/07/2015	13/07/2015	22/02/2015	22/02/2015	13/03/2015	12/03/2015	03/04/2015	03/04/2015	24/03/2015	25/03/2015
24/07/2015	24/07/2015	03/03/2015	03/03/2015	23/06/2015	23/06/2015	03/06/2015	06/06/2015	13/04/2015	10/04/2015
03/08/2015	02/08/2015	13/03/2015	13/03/2015	03/07/2015	01/07/2015	24/07/2015	24/07/2015	23/04/2015	26/04/2015
13/08/2015	13/08/2015	24/03/2015	24/03/2015	13/07/2015	13/07/2015	13/08/2015	09/08/2015	24/05/2015	28/05/2015
24/08/2015	25/08/2015	03/04/2015	31/03/2015	24/07/2015	24/07/2015	23/09/2015	26/09/2015	13/06/2015	13/06/2015
03/09/2015	03/09/2015	13/04/2015	13/04/2015	03/08/2015	03/08/2015	13/10/2015	11/10/2015	03/07/2015	29/06/2015
13/09/2015	13/09/2015	23/04/2015	23/04/2015	24/08/2015	22/08/2015	13/11/2015	13/11/2015	13/07/2015	15/07/2015
23/09/2015	23/09/2015	03/05/2015	03/05/2015	03/09/2015	03/09/2015	23/11/2015	24/11/2015	13/08/2015	16/08/2015
03/10/2015	03/10/2015	13/05/2015	11/05/2015	13/09/2015	11/09/2015	03/12/2015	29/11/2015	13/09/2015	09/09/2015
13/10/2015	13/10/2015	24/05/2015	24/05/2015	23/09/2015	27/09/2015	13/12/2015	13/12/2015	03/10/2015	03/10/2015
24/10/2015	24/10/2015	03/06/2015	03/06/2015	03/10/2015	01/10/2015	24/12/2015	24/12/2015	13/10/2015	11/10/2015
CGLS dates	EO dates	CGLS dates	EO dates	CGLS dates	EO dates	CGLS dates	EO dates	CGLS dates	EO dates
03/04/2016	05/04/2016			13/03/2016	14/03/2016	03/01/2016	03/01/2016	13/04/2016	16/04/2016
13/04/2016	14/04/2016			13/06/2016	09/06/2016	13/01/2016	13/01/2016	23/04/2016	26/04/2016
23/04/2016	23/04/2016			23/06/2016	23/06/2016	03/02/2016	01/02/2016	13/05/2016	09/05/2016
24/05/2016	23/05/2016			03/07/2016	03/07/2016	13/02/2016	12/02/2016	03/06/2016	30/05/2016
03/06/2016	08/06/2016			13/07/2016	13/07/2016	03/03/2016	04/03/2016	13/06/2016	18/06/2016
13/06/2016	17/06/2016			24/07/2016	20/07/2016	24/03/2016	20/03/2016	23/06/2016	23/06/2016
13/07/2016	10/07/2016			03/08/2016	03/08/2016	13/09/2016	12/09/2016	03/07/2016	01/07/2016
03/08/2016	04/08/2016			13/08/2016	16/08/2016	13/10/2016	14/10/2016	13/07/2016	17/07/2016
03/09/2016	05/09/2016			24/08/2016	24/08/2016	24/10/2016	29/10/2016	24/07/2016	28/07/2016
13/09/2016	12/09/2016			03/09/2016	03/09/2016	13/11/2016	15/11/2016	03/08/2016	04/08/2016
23/09/2016	21/09/2016			13/09/2016	08/09/2016	03/12/2016	01/12/2016	13/08/2016	17/08/2016
13/10/2016	13/10/2016			23/09/2016	25/09/2016	13/12/2016	18/12/2016	24/08/2016	24/08/2016

Table 9. Selected 12 dates per annum for LP1 & LP2 upscaling between 01/01/2012 and 31/12/2016. This table includes the US-FPK, DE-GEB, US-GCM, FR-GRI and GF-GUY. For the coloured HR-EO dates, red indicates Sentinel-2, light blue Landsat-7, dark blue Landsat-8, and purple indicates interpolation is used and grey indicates no upscaling is needed.

US-FPK		DE-GEB		US-GCM		FR-GRI		GF-GUY	
CGLS dates	EO dates	CGLS dates	EO dates	CGLS dates	EO dates	CGLS dates	EO dates	CGLS dates	EO dates
		03/07/2012	03/07/2012			13/03/2012	15/03/2012	03/09/2012	05/09/2012
		13/07/2012	13/07/2012			24/03/2012	25/03/2012	13/09/2012	13/09/2012
		24/07/2012	24/07/2012			03/05/2012	24/05/2012	23/09/2012	23/09/2012
		03/08/2012	03/08/2012			24/05/2012	28/05/2012	03/10/2012	03/10/2012
		13/08/2012	13/08/2012			23/06/2012	23/06/2012	13/10/2012	13/10/2012
		24/08/2012	22/08/2012			24/07/2012	24/07/2012	24/10/2012	24/10/2012
		03/09/2012	29/08/2012			03/08/2012	03/08/2012	03/11/2012	03/11/2012
		13/09/2012	13/09/2012			13/08/2012	09/08/2012	13/11/2012	13/11/2012
		23/09/2012	23/09/2012			24/08/2012	24/08/2012	23/11/2012	23/11/2012
		03/10/2012	30/09/2012			03/09/2012	01/09/2012	03/12/2012	03/12/2012
		13/10/2012	09/10/2012			13/09/2012	15/09/2012	13/12/2012	13/12/2012
		24/10/2012	24/10/2012			23/09/2012	19/09/2012	24/12/2012	24/12/2012
CGLS dates	EO dates	CGLS dates	EO dates	CGLS dates	EO dates	CGLS dates	EO dates	CGLS dates	EO dates
03/07/2013	06/07/2013	13/06/2013	13/06/2013	03/03/2013	04/03/2013	03/07/2013	03/07/2013	13/06/2013	13/06/2013
13/07/2013	13/07/2013	23/06/2013	23/06/2013	13/03/2013	13/03/2013	13/07/2013	10/07/2013	23/06/2013	23/06/2013
24/07/2013	22/07/2013	03/07/2013	03/07/2013	24/03/2013	20/03/2013	24/07/2013	19/07/2013	03/07/2013	03/07/2013
03/08/2013	07/08/2013	13/07/2013	16/07/2013	03/04/2013	05/04/2013	03/08/2013	04/08/2013	13/07/2013	13/07/2013
13/08/2013	13/08/2013	24/07/2013	24/07/2013	23/04/2013	21/04/2013	13/08/2013	13/08/2013	24/07/2013	24/07/2013
24/08/2013	24/08/2013	03/08/2013	01/08/2013	03/05/2013	30/04/2013	24/08/2013	20/08/2013	03/08/2013	03/08/2013
03/09/2013	03/09/2013	13/08/2013	16/08/2013	13/05/2013	15/05/2013	03/09/2013	04/09/2013	13/08/2013	16/08/2013
13/09/2013	15/09/2013	24/08/2013	24/08/2013	24/05/2013	24/05/2013	13/09/2013	13/09/2013	24/08/2013	27/08/2013
23/09/2013	24/09/2013	03/09/2013	03/09/2013	03/07/2013	02/07/2013	23/09/2013	23/09/2013	03/09/2013	03/09/2013
03/10/2013	01/10/2013	13/09/2013	13/09/2013	13/07/2013	11/07/2013	03/10/2013	07/10/2013	13/09/2013	13/09/2013
13/10/2013	13/10/2013	23/09/2013	23/09/2013	24/08/2013	28/08/2013	13/10/2013	13/10/2013	23/09/2013	23/09/2013
24/10/2013	26/10/2013	03/10/2013	03/10/2013	03/09/2013	04/09/2013	03/11/2013	30/10/2013	03/10/2013	03/10/2013
CGLS dates	EO dates	CGLS dates	EO dates	CGLS dates	EO dates	CGLS dates	EO dates	CGLS dates	EO dates
24/03/2014	19/03/2014	13/06/2014	13/06/2014	13/02/2014	27/02/2014	03/02/2014	03/02/2014	23/06/2014	23/06/2014
03/04/2014	04/04/2014	23/06/2014	23/06/2014	03/03/2014	08/03/2014	13/02/2014	12/02/2014	03/07/2014	03/07/2014
23/04/2014	20/04/2014	03/07/2014	03/07/2014	24/03/2014	24/03/2014	03/03/2014	07/03/2014	13/07/2014	13/07/2014
13/05/2014	13/05/2014	13/07/2014	13/07/2014	13/04/2014	09/04/2014	13/03/2014	16/03/2014	24/07/2014	24/07/2014
03/06/2014	03/06/2014	24/07/2014	19/07/2014	03/07/2014	05/07/2014	13/04/2014	17/04/2014	03/08/2014	03/08/2014
13/06/2014	13/06/2014	03/08/2014	03/08/2014	13/07/2014	14/07/2014	24/05/2014	19/05/2014	13/08/2014	13/08/2014
23/06/2014	23/06/2014	13/08/2014	13/08/2014	24/07/2014	24/07/2014	13/06/2014	12/06/2014	24/08/2014	24/08/2014
03/07/2014	03/07/2014	24/08/2014	24/08/2014	03/08/2014	30/07/2014	24/07/2014	24/07/2014	03/09/2014	03/09/2014
03/08/2014	01/08/2014	03/09/2014	03/09/2014	24/08/2014	22/08/2014	03/08/2014	03/08/2014	13/09/2014	13/09/2014
24/08/2014	26/08/2014	13/09/2014	13/09/2014	03/09/2014	03/09/2014	13/08/2014	13/08/2014	23/09/2014	23/09/2014
03/09/2014	03/09/2014	23/09/2014	23/09/2014	13/09/2014	16/09/2014	03/09/2014	03/09/2014	03/10/2014	03/10/2014
23/09/2014	26/09/2014	03/10/2014	03/10/2014	24/10/2014	25/10/2014	03/10/2014	01/10/2014	13/10/2014	13/10/2014
CGLS dates	EO dates	CGLS dates	EO dates	CGLS dates	EO dates	CGLS dates	EO dates	CGLS dates	EO dates
13/03/2015	13/03/2015	13/06/2015	13/06/2015	03/02/2015	07/02/2015	23/04/2015	27/04/2015	23/06/2015	27/06/2015
24/03/2015	29/03/2015	23/06/2015	23/06/2015	13/02/2015	14/02/2015	03/06/2015	06/06/2015	03/07/2015	03/07/2015
03/04/2015	07/04/2015	03/07/2015	03/07/2015	03/05/2015	05/05/2015	13/06/2015	13/06/2015	13/07/2015	13/07/2015
13/05/2015	09/05/2015	13/07/2015	13/07/2015	24/07/2015	24/07/2015	03/07/2015	30/06/2015	24/07/2015	24/07/2015
03/06/2015	01/06/2015	24/07/2015	24/07/2015	03/08/2015	02/08/2015	13/07/2015	16/07/2015	03/08/2015	03/08/2015
13/06/2015	17/06/2015	03/08/2015	03/08/2015	13/08/2015	09/08/2015	24/07/2015	24/07/2015	13/08/2015	13/08/2015
23/06/2015	26/06/2015	13/08/2015	13/08/2015	24/08/2015	25/08/2015	03/08/2015	01/08/2015	24/08/2015	24/08/2015
24/07/2015	19/07/2015	24/08/2015	23/08/2015	03/10/2015	05/10/2015	24/08/2015	26/08/2015	03/09/2015	03/09/2015
03/08/2015	04/08/2015	03/09/2015	03/09/2015	24/10/2015	21/10/2015	03/09/2015	03/09/2015	13/09/2015	13/09/2015
24/08/2015	20/08/2015	13/09/2015	13/09/2015	13/11/2015	13/11/2015	13/09/2015	13/09/2015	23/09/2015	23/09/2015
13/09/2015	14/09/2015	23/09/2015	28/09/2015	23/11/2015	22/11/2015	23/09/2015	27/09/2015	03/10/2015	03/10/2015
03/10/2015	30/09/2015	03/10/2015	03/10/2015	13/12/2015	08/12/2015	03/10/2015	04/10/2015	13/10/2015	13/10/2015
CGLS dates	EO dates	CGLS dates	EO dates	CGLS dates	EO dates	CGLS dates	EO dates	CGLS dates	EO dates
24/03/2016	20/04/2016			24/03/2016	29/03/2016				
03/05/2016	02/05/2016			03/04/2016	05/04/2016				
13/05/2016	18/05/2016			03/05/2016	06/05/2016				
13/06/2016	12/06/2016			13/05/2016	13/05/2016				
23/06/2016	19/06/2016			03/06/2016	03/06/2016				
03/07/2016	28/06/2016			03/09/2016	03/09/2016				
13/07/2016	09/07/2016			13/09/2016	12/09/2016				
24/07/2016	21/07/2016			23/09/2016	23/09/2016				
03/08/2016	30/07/2016			03/10/2016	07/10/2016				
24/08/2016	22/08/2016			24/10/2016	23/10/2016				

13/09/2016	16/09/2016			03/11/2016	30/10/2016				
23/09/2016	27/09/2016			13/11/2016	15/11/2016				

Table 10. Selected 12 dates per annum for LP1 & LP2 upscaling between 01/01/2012 and 31/12/2016. This table includes the DE-HAI, IT-REN, US-PSU, US-TBL. For the coloured HR-EO dates, red indicates Sentinel-2, light blue Landsat-7, dark blue Landsat-8, and purple indicates interpolation is used and grey indicates no upscaling is needed.

DE-HAI		IT-REN		US-PSU		US-TBL	
CGLS dates	EO dates	CGLS dates	EO dates	CGLS dates	EO dates	CGLS dates	EO dates
13/03/2012	15/03/2012	13/03/2012	14/03/2012				
24/03/2012	24/03/2012	13/04/2012	09/04/2012				
03/05/2012	02/05/2012	24/05/2012	24/05/2012				
13/05/2012	13/05/2012	03/06/2012	03/06/2012				
24/05/2012	25/05/2012	13/06/2012	13/06/2012				
03/06/2012	03/06/2012	23/06/2012	24/06/2012				
23/06/2012	22/06/2012	03/07/2012	07/07/2012				
24/08/2012	29/08/2012	13/07/2012	13/07/2012				
23/09/2012	23/09/2012	24/07/2012	23/07/2012				
03/10/2012	03/10/2012	03/08/2012	08/08/2012				
13/10/2012	16/10/2012	13/08/2012	17/08/2012				
24/10/2012	24/10/2012	24/08/2012	24/08/2012				
CGLS dates	EO dates	CGLS dates	EO dates	CGLS dates	EO dates	CGLS dates	EO dates
03/07/2013	07/07/2013	03/06/2013	07/06/2013	23/04/2013	23/04/2013	03/06/2013	06/06/2013
13/07/2013	13/07/2013	13/06/2013	16/06/2013	03/05/2013	03/05/2013	23/06/2013	22/06/2013
24/07/2013	24/07/2013	23/06/2013	23/06/2013	13/05/2013	14/05/2013	03/07/2013	08/07/2013
03/08/2013	01/08/2013	03/07/2013	02/07/2013	24/05/2013	24/05/2013	24/07/2013	24/07/2013
13/08/2013	16/08/2013	13/07/2013	18/07/2013	03/06/2013	03/06/2013	03/08/2013	31/07/2013
24/08/2013	24/08/2013	24/07/2013	25/07/2013	13/06/2013	15/06/2013	13/08/2013	09/08/2013
03/09/2013	03/09/2013	03/08/2013	03/08/2013	23/06/2013	23/06/2013	24/08/2013	24/08/2013
13/09/2013	13/09/2013	13/08/2013	10/08/2013	03/07/2013	03/07/2013	03/09/2013	03/09/2013
23/09/2013	23/09/2013	24/08/2013	24/08/2013	13/07/2013	17ls/07/2013	13/09/2013	17/09/2013
03/10/2013	03/10/2013	03/09/2013	04/09/2013	24/07/2013	24/07/2013	23/09/2013	26/09/2013
13/10/2013	13/10/2013	13/09/2013	13/09/2013	03/08/2013	03/08/2013	24/10/2013	19/10/2013
24/10/2013	24/10/2013	13/10/2013	17/10/2013	13/08/2013	13/08/2013	13/11/2013	13/11/2013
CGLS dates	EO dates	CGLS dates	EO dates	CGLS dates	EO dates	CGLS dates	EO dates
22/02/2014	25/02/2014	03/04/2014	31/03/2014	03/07/2014	03/07/2014	22/02/2014	24/02/2014
13/03/2014	13/03/2014	13/04/2014	16/04/2014	13/07/2014	13/07/2014	03/03/2014	05/03/2014
24/03/2014	20/03/2014	13/05/2014	09/05/2014	24/07/2014	24/07/2014	13/03/2014	12/03/2014
13/05/2014	16/05/2014	24/05/2014	24/05/2014	03/08/2014	05/08/2014	24/03/2014	21/03/2014
24/05/2014	25/05/2014	13/06/2014	13/06/2014	13/08/2014	13/08/2014	03/06/2014	03/06/2014
03/06/2014	08/06/2014	23/06/2014	23/06/2014	24/08/2014	24/08/2014	13/06/2014	16/06/2014
03/07/2014	03/07/2014	03/07/2014	03/07/2014	03/09/2014	03/09/2014	03/07/2014	02/07/2014
13/07/2014	13/07/2014	03/08/2014	06/08/2014	13/09/2014	13/09/2014	13/07/2014	13/07/2014
24/07/2014	26/07/2014	24/08/2014	29/08/2014	23/09/2014	23/09/2014	24/07/2014	24/07/2014
03/08/2014	03/08/2014	03/09/2014	07/09/2014	03/10/2014	03/10/2014	13/08/2014	12/08/2014
23/09/2014	28/09/2014	23/09/2014	23/09/2014	13/10/2014	13/10/2014	23/09/2014	20/09/2014
03/10/2014	06/10/2014	03/10/2014	30/09/2014	24/10/2014	24/10/2014	03/10/2014	06/10/2014
CGLS dates	EO dates	CGLS dates	EO dates	CGLS dates	EO dates	CGLS dates	EO dates
23/04/2015	24/04/2015	13/03/2015	18/03/2015	03/07/2015	03/07/2015	03/04/2015	31/03/2015
13/05/2015	10/05/2015	03/04/2015	03/04/2015	13/07/2015	13/07/2015	13/05/2015	11/05/2015
03/06/2015	04/06/2015	23/04/2015	19/04/2015	24/07/2015	23/07/2015	03/06/2015	03/06/2015
13/06/2015	13/06/2015	24/05/2015	28/05/2015	03/08/2015	03/08/2015	23/06/2015	19/06/2015
23/06/2015	23/06/2015	03/06/2015	06/06/2015	13/08/2015	13/08/2015	03/07/2015	28/06/2015
03/07/2015	03/07/2015	13/06/2015	13/06/2015	24/08/2015	24/08/2015	13/07/2015	13/07/2015
13/07/2015	13/07/2015	13/07/2015	15/07/2015	03/09/2015	03/09/2015	24/07/2015	24/07/2015
24/07/2015	24/07/2015	03/08/2015	31/07/2015	13/09/2015	13/09/2015	03/08/2015	30/07/2015
03/08/2015	07/08/2015	13/08/2015	09/08/2015	23/09/2015	23/09/2015	13/08/2015	15/08/2015
24/08/2015	23/08/2015	03/09/2015	01/09/2015	03/10/2015	03/10/2015	24/08/2015	24/08/2015
03/09/2015	30/08/2015	23/09/2015	26/09/2015	13/10/2015	11/10/2015	13/10/2015	10/10/2015
03/10/2015	01/10/2015	13/10/2015	12/10/2015	24/10/2015	24/10/2015	24/10/2015	25/10/2015
CGLS dates	EO dates	CGLS dates	EO dates	CGLS dates	EO dates	CGLS dates	EO dates
				03/07/2016	03/07/2016	13/03/2016	10/03/2016
				13/07/2016	13/07/2016	03/05/2016	04/05/2016
				24/07/2016	24/07/2016	13/05/2016	13/05/2016
				03/08/2016	03/08/2016	24/05/2016	29/05/2016

				13/08/2016	13/08/2016	13/06/2016	14/06/2016
				24/08/2016	24/08/2016	23/06/2016	23/06/2016
				03/09/2016	03/09/2016	03/07/2016	07/07/2016
				13/09/2016	13/09/2016	13/07/2016	16/07/2016
				23/09/2016	27/09/2016	24/07/2016	24/07/2016
				03/10/2016	03/10/2016	13/08/2016	17/08/2016
				13/10/2016	13/10/2016	24/08/2016	25/08/2016
				24/10/2016	24/10/2016	13/09/2016	14/09/2016

In total, there are still 415 missing dates (≈45%) of HR-EO datasets out of a total of 924(=18*4*12+5*12).

Table 11. HR-EO availability between 01/01/2012 and 31/12/2016 for individual sites.

Site	Time range	HR-EO data available (12 p.a.)	Missing data
US-BAO	2012-2015	Landsat7, Landsat8, SPOT	20/48
US-BRW	2013-2016	Landsat8, Sentinel2	38/48
US-BON	2013-2016	Landsat7, Landsat8, SPOT, Sentinel2	16/48
US-DRA	2013-2016	Landsat7, Landsat8, Sentinel2	6/48
US-FPK	2013-2016	Landsat7, Landsat8, Sentinel2	10/48
US-GCM	2013-2016	Landsat7, Landsat8, Sentinel2	7/48
US-PSU	2013-2016	Landsat8	40/48
US-TBL	2013-2016	Landsat8, Sentinel2	11/48
US-SXF	2013-2016	Landsat8, SPOT, Sentinel2	15/48
AU-CPR	2013-2016	Landsat7, Landsat8, Sentinel2	14/48
AU-TUM	2013-2016	Landsat7, Landsat8, Sentinel2	16/48
BE-BRA	2013-2016	Landsat7, Landsat8, Sentinel2	25/48
DE-GEB	2012-2015	Landsat7, Landsat8, Sentinel2	38/48
DE-HAI	2012-2015	Landsat7, Landsat8, SPOT, Sentinel2	23/48
FR-GRI	2012-2015	Landsat7, Landsat8, SPOT, Sentinel2	22/48
GF-GUY	2012-2015	Landsat7, Landsat8	46/48
IT-REN	2012-2015	Landsat7, Landsat8, SPOT	17/48
US-NR1	2013-2016	Landsat8, Sentinel2	28/48
US-ARM	2012-2016	Landsat7, Landsat8, Sentinel2	23/60

Similarly, the LP1 and LP2 upscaling dates and the corresponding HR-EO dates for all the selected sites are listed in Table 13 for the period between 01/01/2016 and 31/12/2018.

Table 12. Selected 12 dates per annum for LP1 & LP2 upscaling between 01/01/2017 and 31/12/2018. For the coloured HR-EO dates, red indicates Sentinel-2, light blue Landsat-7, dark blue Landsat-8, and purple

IT-REN		NM-GOB		US-SXF		AU-TUM		US-ARM	
CGLS dates	EO dates	CGLS dates	EO dates	CGLS dates	EO dates	CGLS dates	EO dates	CGLS dates	EO dates
2016-05-03	2016-05-07	2016-01-03	2016-01-05						
2016-05-24	2016-05-22	2016-03-13	2016-03-09						
2016-07-13	2016-07-10	2016-03-24	2016-03-25						
2016-08-24	2016-08-27	2016-04-13	2016-04-10						
2016-09-13	2016-09-12	2016-05-13	2016-05-12						
2016-09-23	2016-09-26	2016-06-13	2016-06-13						
2016-10-03	2016-10-05	2016-07-13	2016-07-15						
2016-10-13	2016-10-16	2016-08-13	2016-08-16						
2016-11-03	2016-10-30	2016-09-13	2016-09-17						
2016-11-13	2016-11-15	2016-10-24	2016-10-19						
2016-12-03	2016-12-01	2016-11-23	2016-11-20						
2016-12-13	2016-12-17	2016-12-13	2016-12-11						
CGLS dates	EO dates	CGLS dates	EO dates	CGLS dates	EO dates	CGLS dates	EO dates	CGLS dates	EO dates
2017-05-13	2017-05-17	2017-01-13	2017-01-10	2017-02-13	2017-02-12	2017-01-13	2017-01-15	2017-01-13	2017-01-11
2017-06-13	2017-06-13	2017-02-13	2017-02-09	2017-02-22	2017-02-22	2017-01-24	2017-01-28	2017-03-03	2017-03-01
2017-06-23	2017-06-26	2017-03-13	2017-03-11	2017-05-13	2017-05-13	2017-02-13	2017-02-14	2017-03-24	2017-03-21
2017-07-13	2017-07-18	2017-04-13	2017-04-10	2017-06-03	2017-06-02	2017-02-22	2017-02-24	2017-04-13	2017-04-10
2017-08-03	2017-07-31	2017-05-13	2017-05-10	2017-07-03	2017-07-02	2017-03-13	2017-03-09	2017-05-24	2017-05-20
2017-08-24	2017-08-27	2017-06-13	2017-06-09	2017-07-13	2017-07-17	2017-03-24	2017-03-26	2017-06-13	2017-06-09
2017-09-03	2017-09-03	2017-07-03	2017-07-04	2017-10-13	2017-10-10	2017-04-13	2017-04-18	2017-07-24	2017-07-19
2017-09-13	2017-09-13	2017-08-13	2017-08-13	2017-10-24	2017-10-20	2017-05-03	2017-05-08	2017-08-03	2017-08-08
2017-09-23	2017-09-21	2017-09-13	2017-09-12	2017-11-13	2017-11-09	2017-07-24	2017-07-29	2017-08-24	2017-08-23
2017-10-03	2017-10-06	2017-10-13	2017-10-17	2017-11-23	2017-11-19	2017-09-03	2017-08-31	2017-10-03	2017-10-02
2017-10-24	2017-10-19	2017-11-13	2017-11-11	2017-12-03	2017-11-29	2017-09-23	2017-09-20	2017-10-24	2017-10-22
2017-11-03	2017-10-31	2017-12-13	2017-12-11	2017-12-24	2017-12-19	2017-10-03	2017-10-02	2017-12-03	2017-12-06
CGLS dates	EO dates	CGLS dates	EO dates	CGLS dates	EO dates	CGLS dates	EO dates	CGLS dates	EO dates
		2018-01-13	2018-01-15	2018-02-03	2018-01-31	2018-01-13	2018-01-10	2018-02-13	2018-02-09
		2018-02-13	2018-02-14	2018-03-13	2018-03-14	2018-02-13	2018-02-12	2018-03-13	2018-03-11
		2018-03-13	2018-03-11	2018-04-23	2018-04-23	2018-03-03	2018-02-27	2018-04-03	2018-04-05
		2018-04-13	2018-04-10	2018-05-03	2018-05-07	2018-03-24	2018-03-19	2018-04-13	2018-04-15
		2018-05-13	2018-05-15	2018-05-24	2018-05-28	2018-04-03	2018-03-31	2018-05-03	2018-04-30
		2018-06-13	2018-06-14	2018-07-03	2018-07-02	2018-04-13	2018-04-18	2018-06-13	2018-06-14
		2018-07-13	2018-07-14	2018-07-13	2018-07-12	2018-05-03	2018-05-05	2018-07-03	2018-06-29
		2018-08-13	2018-08-18	2018-08-03	2018-08-06	2018-06-03	2018-06-04	2018-07-24	2018-07-19
		2018-09-13	2018-09-12	2018-09-13	2018-09-12	2018-09-03	2018-09-05	2018-08-03	2018-07-29
		2018-10-13	2018-10-12	2018-10-24	2018-10-20	2018-10-03	2018-09-30	2018-09-03	2018-09-02
		2018-11-03	2018-11-06	2018-11-13	2018-11-14	2018-11-03	2018-10-30	2018-09-23	2018-09-22
		2018-12-24	2018-12-26	2018-12-13	2018-12-14	2018-12-03	2018-12-01	2018-10-24	2018-10-22

US-BON		AU-CPR		BE-BRA		US-GCM		NO-NYA	
CGLS dates	EO dates	CGLS dates	CGLS dates	CGLS dates	EO dates	CGLS dates	EO dates	CGLS dates	EO dates
2017-02-03	2017-02-03	2017-01-13	2017-01-17	2017-03-24	2017-03-27	2017-02-03	2017-01-31	2017-05-13	2017-05-12
2017-02-13	2017-02-12	2017-01-24	2017-01-27	2017-04-13	2017-04-09	2017-02-21	2017-02-19	2017-05-24	2017-05-24
2017-03-03	2017-03-02	2017-03-03	2017-03-08	2017-05-03	2017-05-06	2017-03-03	2017-03-02	2017-06-03	2017-06-03
2017-03-24	2017-03-22	2017-03-13	2017-03-18	2017-05-13	2017-05-13	2017-03-24	2017-03-23	2017-06-13	2017-06-13
2017-05-13	2017-05-10	2017-03-24	2017-03-28	2017-05-24	2017-05-26	2017-04-03	2017-04-01	2017-06-23	2017-06-21
2017-05-24	2017-05-26	2017-05-03	2017-05-07	2017-08-13	2017-08-13	2017-05-03	2017-05-03	2017-07-03	2017-07-03
2017-06-13	2017-06-10	2017-06-23	2017-06-26	2017-08-24	2017-08-29	2017-05-24	2017-05-26	2017-07-13	2017-07-18
2017-07-24	2017-07-25	2017-07-03	2017-07-06	2017-09-03	2017-09-03	2017-09-13	2017-09-18	2017-07-24	2017-07-24
2017-08-13	2017-08-14	2017-07-24	2017-07-21	2017-09-13	2017-09-13	2017-10-13	2017-10-08	2017-08-03	2017-08-02
2017-09-03	2017-08-29	2017-08-24	2017-08-20	2017-09-23	2017-09-25	2017-10-24	2017-10-28	2017-08-13	2017-08-12
2017-10-13	2017-10-08	2017-10-03	2017-09-29	2017-10-13	2017-10-18	2017-11-13	2017-11-17	2017-08-24	2017-08-24
2017-11-23	2017-11-22	2017-10-24	2017-10-29	2017-11-03	2017-10-30	2017-12-13	2017-12-12	2017-09-03	2017-09-03
CGLS dates	EO dates	CGLS dates	CGLS dates	CGLS dates	EO dates	CGLS dates	EO dates	CGLS dates	EO dates

2018-03-03	2018-03-02	2018-01-13	2018-01-17	2018-02-03	2018-02-05	2018-02-03	2018-01-31	2018-06-03	2018-06-07
2018-03-24	2018-03-22	2018-01-24	2018-01-27	2018-02-22	2018-02-23	2018-03-03	2018-03-02	2018-06-13	2018-06-11
2018-04-13	2018-04-11	2018-02-13	2018-02-11	2018-04-23	2018-04-21	2018-03-13	2018-03-12	2018-06-23	2018-06-22
2018-04-23	2018-04-26	2018-02-22	2018-02-26	2018-05-13	2018-05-09	2018-03-24	2018-03-22	2018-07-03	2018-07-03
2018-06-03	2018-06-05	2018-03-03	2018-03-08	2018-05-24	2018-05-21	2018-04-13	2018-04-16	2018-07-13	2018-07-15
2018-06-13	2018-06-15	2018-03-13	2018-03-18	2018-06-23	2018-06-27	2018-05-03	2018-05-06	2018-07-24	2018-07-24
2018-07-24	2018-07-25	2018-03-24	2018-03-28	2018-07-13	2018-07-15	2018-06-13	2018-06-10	2018-08-03	2018-07-30
2018-08-03	2018-08-04	2018-04-03	2018-04-07	2018-07-24	2018-07-25	2018-07-03	2018-07-05	2018-08-13	2018-08-12
2018-09-13	2018-09-13	2018-04-13	2018-04-17	2018-08-03	2018-08-06	2018-10-13	2018-10-18	2018-08-24	2018-08-20
2018-09-23	2018-09-23	2018-04-23	2018-04-27	2018-09-13	2018-09-18	2018-10-24	2018-10-28	2018-09-03	2018-09-03
2018-10-13	2018-10-18	2018-05-13	2018-05-12	2018-10-03	2018-09-30	2018-11-13	2018-11-17	2018-09-13	2018-09-13
2018-10-28	2018-10-24	2018-08-13	2018-08-10	2018-10-13	2018-10-10	2018-12-03	2018-12-02	2018-09-23	2018-09-23

US-FPK		NL-CAB		DE-HAI		FR-GRI		GF-GUY	
CGLS dates	EO dates	CGLS dates	EO dates	CGLS dates	EO dates	CGLS dates	EO dates	CGLS dates	EO dates
		2016-04-03	2016-04-01	2016-03-13	2016-03-18	2016-05-03	2016-05-08	2016-06-13	2016-06-13
		2016-04-13	2016-04-11	2016-04-03	2016-05-05	2016-05-13	2016-05-13	2016-06-23	2016-06-23
		2016-04-23	2016-04-21	2016-05-13	2016-05-13	2016-05-24	2016-05-24	2016-07-03	2016-07-03
		2016-05-03	2016-05-01	2016-05-24	2016-05-24	2016-06-03	2016-06-03	2016-07-13	2016-07-13
		2016-05-13	2016-05-08	2016-06-03	2016-06-06	2016-06-13	2016-06-09	2016-07-24	2016-07-24
		2016-05-24	2016-05-24	2016-06-13	2016-06-13	2016-06-23	2016-06-23	2016-08-03	2016-08-03
		2016-06-13	2016-06-09	2016-06-23	2016-06-23	2016-07-03	2016-07-03	2016-08-13	2016-08-13
		2016-09-13	2016-09-13	2016-07-03	2016-07-03	2016-07-13	2016-07-13	2016-08-24	2016-08-24
		2016-09-23	2016-09-25	2016-07-13	2016-07-13	2016-08-13	2016-08-12	2016-09-03	2016-09-04
		2016-10-03	2016-10-05	2016-08-24	2016-08-25	2016-08-24	2016-08-28	2016-09-13	2016-09-13
		2016-11-03	2016-10-31	2016-09-03	2016-09-10	2016-10-13	2016-10-15	2016-09-23	2016-09-23
		2016-12-03	2016-12-04	2016-12-03	2016-11-29	2016-11-03	2016-10-31	2016-10-24	2016-10-24
CGLS dates	EO dates	CGLS dates	EO dates	CGLS dates	EO dates	CGLS dates	EO dates	CGLS dates	EO dates
2017-03-13	2017-03-26	2017-02-13	2017-02-15	2017-03-24	2017-03-28	2017-01-24	2017-01-19	2017-06-13	2017-06-13
2017-03-24	2017-05-05	2017-03-24	2017-03-27	2017-04-23	2017-04-20	2017-02-13	2017-02-15	2017-06-23	2017-06-23
2017-05-03	2017-06-06	2017-04-13	2017-04-09	2017-05-13	2017-05-10	2017-03-24	2017-03-27	2017-07-03	2017-07-03
2017-06-03	2017-07-04	2017-05-03	2017-05-06	2017-05-24	2017-05-27	2017-04-13	2017-04-09	2017-07-13	2017-07-13
2017-07-03	2017-07-13	2017-05-24	2017-05-26	2017-07-13	2017-07-09	2017-04-23	2017-04-19	2017-07-24	2017-07-24
2017-07-13	2017-07-19	2017-06-03	2017-06-03	2017-07-24	2017-07-19	2017-05-13	2017-05-09	2017-08-03	2017-08-03
2017-07-24	2017-08-13	2017-06-13	2017-06-13	2017-08-03	2017-08-08	2017-06-23	2017-06-18	2017-08-13	2017-08-13
2017-08-13	2017-09-02	2017-06-23	2017-06-23	2017-08-13	2017-08-13	2017-07-13	2017-07-18	2017-08-24	2017-08-24
2017-09-03	2018-10-27	2017-07-13	2017-07-17	2017-08-24	2017-08-23	2017-08-24	2017-08-29	2017-09-03	2017-09-04
2017-10-24	2017-11-21	2017-08-24	2017-08-29	2017-09-03	2017-09-04	2017-11-03	2017-11-07	2017-09-13	2017-09-13
2017-11-23	2017-12-16	2017-11-03	2017-11-07	2017-09-13	2017-09-13	2017-11-23	2017-11-22	2017-09-23	2017-09-23
2017-12-13	2017-03-26	2017-12-13	2017-12-17	2017-10-13	2017-10-17	2017-12-13	2017-12-12	2017-10-24	2017-10-24
CGLS dates	EO dates	CGLS dates	EO dates	CGLS dates	EO dates	CGLS dates	EO dates	CGLS dates	EO dates
2018-03-24	2018-03-21	2018-02-03	2018-02-07	2018-04-03	2018-04-07	2018-01-13	2018-01-14	2018-06-03	2018-06-03
2018-04-03	2018-04-05	2018-02-22	2018-02-22	2018-04-23	2018-04-20	2018-02-22	2018-02-25	2018-06-13	2018-06-13
2018-04-13	2018-04-15	2018-03-24	2018-03-19	2018-05-03	2018-05-05	2018-04-23	2018-04-19	2018-06-23	2018-06-23
2018-05-13	2018-05-15	2018-04-23	2018-04-21	2018-05-24	2018-05-20	2018-05-03	2018-05-04	2018-07-03	2018-07-03
2018-05-24	2018-05-25	2018-05-13	2018-05-08	2018-07-03	2018-06-29	2018-07-24	2018-07-25	2018-07-13	2018-07-13
2018-06-13	2018-06-09	2018-05-24	2018-05-26	2018-07-24	2018-07-19	2018-08-03	2018-08-02	2018-07-24	2018-07-24
2018-07-13	2018-07-09	2018-06-23	2018-06-27	2018-08-03	2018-08-03	2018-08-24	2018-08-19	2018-08-03	2018-08-03
2018-08-13	2018-08-12	2018-07-13	2018-07-15	2018-08-13	2018-08-13	2018-09-03	2018-09-01	2018-08-13	2018-08-13
2018-08-24	2018-08-21	2018-08-03	2018-08-06	2018-08-24	2018-08-22	2018-09-13	2018-09-11	2018-08-24	2018-08-24
2018-09-13	2018-09-07	2018-09-13	2018-09-13	2018-09-13	2018-09-12	2018-09-23	2018-09-26	2018-09-03	2018-09-03
2018-10-13	2018-10-17	2018-10-13	2018-10-10	2018-09-23	2018-09-27	2018-10-13	2018-10-11	2018-09-13	2018-09-13
2018-10-24	2018-10-27	2018-12-03	2018-12-04	2018-10-13	2018-10-12	2018-10-24	2018-10-21	2018-09-23	2018-09-23

US-DRA		US-FPK		US-NR1		US-PSU		US-TBL	
CGLS dates	EO dates	CGLS dates	CGLS dates	CGLS dates	EO dates	CGLS dates	EO dates	CGLS dates	EO dates
2017-01-13	2017-01-11	2017-03-13	2017-03-18	2017-06-13	2017-06-11	2017-01-03	2017-01-01	2017-02-21	2017-02-21
2017-01-24	2017-01-24	2017-03-24	2017-03-26	2017-06-23	2017-06-23	2017-02-21	2017-02-18	2017-04-03	2017-04-02
2017-02-03	2017-02-03	2017-05-03	2017-05-05	2017-07-03	2017-07-01	2017-03-03	2017-03-06	2017-05-13	2017-05-12
2017-02-13	2017-02-13	2017-06-03	2017-06-06	2017-07-13	2017-07-16	2017-03-24	2017-03-22	2017-06-23	2017-06-21
2017-03-03	2017-03-02	2017-07-03	2017-07-04	2017-07-24	2017-07-24	2017-04-23	2017-04-23	2017-07-03	2017-07-01
2017-04-13	2017-04-14	2017-07-13	2017-07-13	2017-08-03	2017-08-03	2017-05-13	2017-05-09	2017-08-03	2017-07-31
2017-05-03	2017-05-04	2017-07-24	2017-07-19	2017-08-13	2017-08-13	2017-05-24	2017-05-24	2017-08-24	2017-08-20
2017-06-13	2017-06-13	2017-08-13	2017-08-13	2017-08-24	2017-08-27	2017-09-23	2017-09-21	2017-09-13	2017-09-09
2017-07-24	2017-07-23	2017-09-03	2017-09-02	2017-09-03	2017-09-03	2017-10-13	2017-10-16	2017-10-03	2017-10-04
2017-08-24	2017-08-27	2017-10-24	2018-10-27	2017-09-13	2017-09-13	2017-11-23	2017-11-20	2017-10-24	2017-10-24
2017-09-13	2017-09-16	2017-11-23	2017-11-21	2017-10-24	2017-10-24	2017-12-03	2017-12-03	2017-11-13	2017-11-13
2017-10-03	2017-10-06	2017-12-13	2017-12-16	2017-11-03	2017-11-03	2017-12-24	2017-12-20	2017-12-13	2017-12-13

CGLS dates	EO dates	CGLS dates	CGLS dates	CGLS dates	EO dates	CGLS dates	EO dates	CGLS dates	EO dates
2018-01-24	2018-01-21	2018-03-24	2018-03-21	2018-05-24	2018-05-26	2018-01-24	2018-01-19	2018-03-03	2018-03-03
2018-02-13	2018-02-10	2018-04-03	2018-04-05	2018-06-03	2018-06-03	2018-02-13	2018-02-13	2018-03-13	2018-03-13
2018-03-13	2018-03-17	2018-04-13	2018-04-15	2018-06-13	2018-06-11	2018-03-03	2018-03-05	2018-04-13	2018-04-12
2018-04-13	2018-04-09	2018-05-13	2018-05-15	2018-06-23	2018-06-21	2018-03-24	2018-03-25	2018-04-23	2018-04-27
2018-05-13	2018-05-09	2018-05-24	2018-05-25	2018-07-03	2018-07-01	2018-04-13	2018-04-14	2018-06-13	2018-06-11
2018-06-13	2018-06-08	2018-06-13	2018-06-09	2018-07-13	2018-07-11	2018-05-13	2018-05-09	2018-06-23	2018-06-21
2018-07-24	2018-07-20	2018-07-13	2018-07-09	2018-07-24	2018-07-24	2018-05-24	2018-05-24	2018-07-03	2018-07-01
2018-08-13	2018-08-17	2018-08-13	2018-08-12	2018-08-03	2018-08-03	2018-06-03	2018-06-03	2018-07-13	2018-07-11
2018-09-13	2018-09-11	2018-08-24	2018-08-21	2018-08-13	2018-08-13	2018-06-13	2018-06-13	2018-07-24	2018-07-21
2018-10-13	2018-10-08	2018-09-13	2018-09-07	2018-08-24	2018-08-20	2018-06-23	2018-06-23	2018-08-03	2018-07-31
2018-10-24	2018-10-23	2018-10-13	2018-10-17	2018-09-03	2018-08-30	2018-07-13	2018-07-08	2018-08-13	2018-08-15
2018-12-13	2018-12-10	2018-10-24	2018-10-27	2018-09-13	2018-09-14	2018-10-24	2018-10-19	2018-09-13	2018-09-14

Table 13. HR-EO availability between 01/01/2016 and 31/12/2018 for individual sites.

Site	Time range	HR-EO data available (12 p.a.)	Missing data
US-BON	2017-2018	Landsat8, Sentinel2	4/24
US-DRA	2017-2018	Sentinel2	0/24
US-FPK	2017-2018	Landsat8, Sentinel2	1/24
US-GCM	2017-2018	Landsat8, Sentinel2	0/24
US-PSU	2017-2018	Landsat8, Sentinel2	0/24
US-TBL	2017-2018	Sentinel2	0/24
US-SXF	2017-2018	Landsat8, Sentinel2	0/24
AU-CPR	2017-2018	Sentinel2	0/24
AU-TUM	2017-2018	Sentinel2	0/24
BE-BRA	2017-2018	Landsat8, Sentinel2	3/24
DE-HAI	2016-2018	Landsat8, Sentinel2	9/36
FR-GRI	2016-2018	Landsat8, Sentinel2	6/36
GF-GUY	2016-2018	Sentinel2	2/36
IT-REN	2016-2017	Landsat8, Sentinel2	2/24
US-NR1	2017-2018	Landsat8, Sentinel2	10/24
US-ARM	2017-2018	Sentinel2	0/24
NM-GOB	2016-2018	Landsat8, Sentinel2	0/36
NO-NYA	2017-2018	Sentinel2	7/24
NL-CAB	2016-2018	Landsat8, Sentinel2	4/36

5.1.2 Atmospheric correction

EO satellites measure radiance from which reflectance at the TOA can be derived in several narrow bands. In order to obtain the surface reflectance, the effect of the atmosphere on the recorded signal needs to be considered. These effects include Rayleigh scattering, scattering by aerosols and absorption mainly by Ozone, water vapour and Carbon Dioxide. This atmospheric correction process can be performed using the Second Simulation of the Satellite Signal in the Solar Spectrum (6S) radiative transfer code. 6S was developed by Vermote et al. (1997), following earlier versions developed by Tanré et al (1990). The 6S model simulates the effects on the radiation transferred through the atmosphere in the spectral range 0.25-4.00µm. The required input information includes the optical depth (transparency) and the observation/illumination geometry. The optical depth data can be obtained, where available, from the Aerosol Robotic Network (AERONET), otherwise it has to be estimated from the inferred direct-to-diffuse ratio.

For Sentinel-2 (and Landsat-8), atmospherically corrected surface reflectance is already provided in the Level-2A products (Vuolo et al., 2016). Figure 17 shows an example of Sentinel-2 RGB composite of TOA reflectance (left) and TOC-R after atmospheric correction (right) over the FLUXNET Hainich site. An assessment of different atmospheric correction methods is included in Doxani et al. (2018)

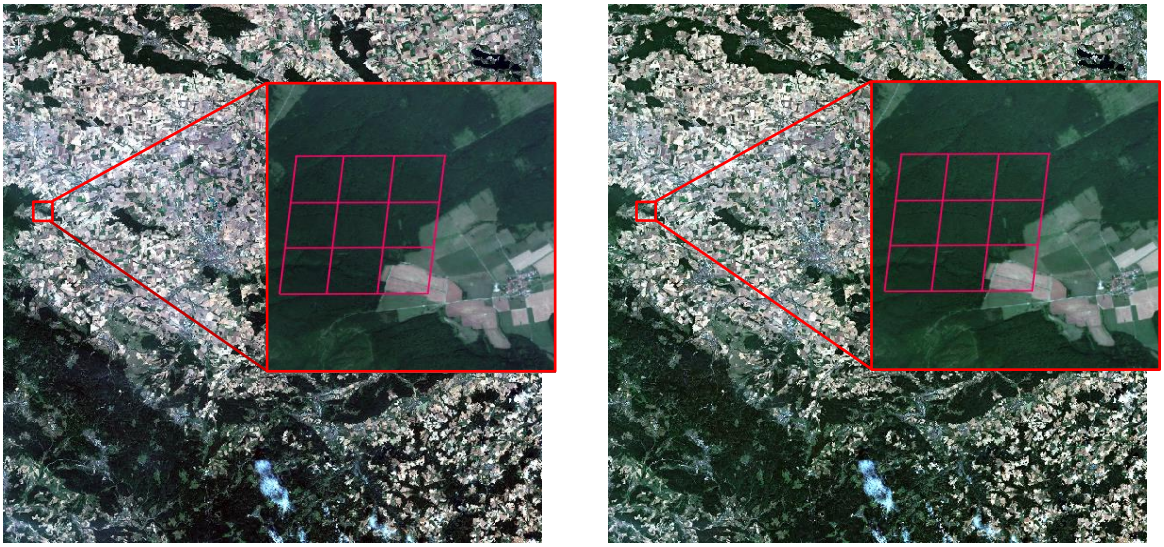

Figure 17.Sentinel-2 TOA reflectance (left) and TOC-R (right) at band b2 (490 nm) over Hainich, Germany. The pink grid indicates the MODIS 1 km by 1km grid.

5.1.3 Narrow-to-broadband conversion.

Sentinel-2 has a spatial resolution of 10m, 20m and 60 for products from different bands. In the method proposed here, the results from Liang (2000) are used to convert the Sentinel-2

narrow band TOC-R into broad band TOC-R using measurements from 5 different bands. The narrow-to-broadband coefficients for different satellites are concluded in Table. 8:

Table 14. Narrow-to-broadband coefficients for different satellites.

Satellite	Narrow-to-broad band conversion
Landsat-7	$\alpha = 0.356b_2 + 0.130b_3 + 0.373b_4 + 0.085b_5 + 0.072b_7 - 0.0018$ (Liang, 2000)
Landsat-8	$\alpha = 0.356b_2 + 0.130b_4 + 0.373b_5 + 0.085b_6 + 0.072b_7 - 0.0018$ (Liang, 2000)
Sentinel-2	$\alpha = 0.356b_2 + 0.130b_4 + 0.373b_8 + 0.085b_{11} + 0.072b_{12} - 0.0018$ (Naegeli et al., 2017)
SPOT	$-0.0022 + 0.3512b_1 + 0.1629b_2 + 0.3415b_3 + 0.1651b_4$ (Liang, 2000)

where b_2, b_4, b_8, b_{11} and b_{12} represent narrow bands at 490 nm, 665 nm, 865 nm, 1610 nm and 2190 nm, respectively.

5.1.4 Projection of tower albedometer FOV.

The height of tower and vegetation at Hainich site are 42 m and 9 m respectively. The albedometer has a FOV of 170°. The footprint of tower measurements can be estimated using these parameters (Eq. (22)), which is here given by a 750m diameter footprint.

$$D = \tan\left(\frac{FOV}{2}\right) * (h_{tower} - h_{toc}) * 2 \qquad (22)$$

where h_{tower} and h_{toc} are the height of tower and averaged height of vegetation, respectively. To be consistent when comparing the tower measurements and HR-EO TOC-R, the TOC-R from the tower is calculated using the derived BRDF function, along with the same viewing and solar geometry as the Sentinel-2 observation. For this case, the observation date and time is 6th August 2015 at 10:20 local time. The viewing zenith and azimuth angle are 3° and 145°, respectively. The shortwave TOC-R estimated from the tower is 0.121. Figure 18 shows a histogram of the shortwave TOC-R measured from HR-EO TOC-R pixels in the tower's FOV.

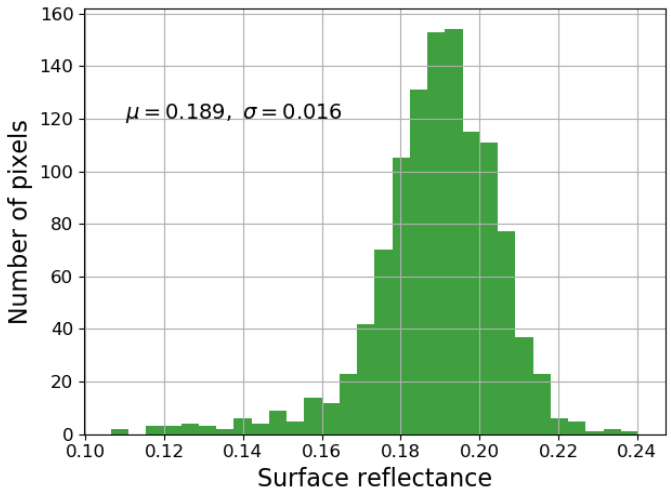

Figure 18.Shortwave TOC-R from HR-EO pixels in the tower's FOV.

5.2 The Sensor Invariant Atmospheric Correction (SIAC) method

This section introduces the SIAC atmospheric correction method, which is being used to produce atmospherically corrected Landsat-8 and Sentinel-2 data between 01/01/2017 and 31/12/2018. The SIAC method was developed by Feng Yin *et al*. from the UCL Department of Geography and being actively updated on Github[11]. In the GbOV project, the SIAC model was further developed into a streamlined version, which enables bulk atmospheric correction processing of Sentinel-2 and Landsat-8 on the server.

The idea of the SIAC method is to use a spectral BRDF dataset to describe the land surface anisotropy as a prior estimate of the atmospheric composition to solve an inverse problem.

The main steps of the SIAC method are summarised as following:

1) Using the 500m daily MODIS BRDF product (known as MCD43) to provide an expectation of the surface reflectance at the target sensor (Landsat-8 or Sentinel-2) acquisition geometry calculated at coarse resolution (500 m) and in the MODIS BRDF bands.

2) Using a set of linear transformations to convert the predicted reflectance from step 1) to the target sensor spectral bands. This yields an expectation of surface reflectance for the target geometry and spectral bands at coarse resolution.

3) The main assumption of the SIAC method is that the surface reflectances are strongly correlated with the TOA reflectances. Consequently, an empirical point spread function (PSF) model can be inferred by maximising the correlation between the TOA reflectance convolved with a Gaussian PSF and surface reflectance coarse resolution expectation.

[11] https://github.com/MarcYin/SIAC

4) Map the surface reflectances to the TOA using a radiative transfer (RT) model and estimates of atmospheric composition. These can be compared with the measured target sensor TOA reflectances convolved with the empirical PSF.

5) Exploiting the Copernicus Atmospheric 263 Monitoring Service (CAMS) data as an *a priori* estimate, an inverse solution can be constructed to retrieve aerosol optical thickness (AOT), total columnar water vapour (TCWV) and total columnar ozone (TCO3). Furthermore, a spatial regularisation is used under the assumption of smooth variation of atmospheric composition parameters.

6) The previous steps result in a complete inference of the *a posteriori* joint probability density function (pdf) of the atmospheric parameters, which can then be used to correct the original TOA reflectance data using a Lambertian surface-atmosphere coupling assumption.

The diagram in Figure 19 is used to show the processing chain of the SIAC atmospheric correction method.

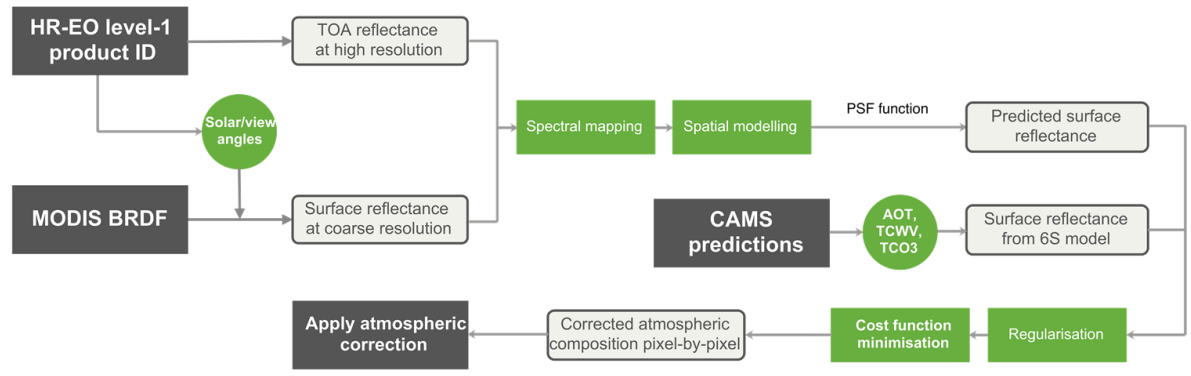

Figure 19.Flow diagram showing the SIAC processing chain.

Details about the implementation of spectral mapping, PSF modelling, atmospheric effect modelling and atmospheric composition retrievals are introduced in Yin et al. (2019).

The main differences between SIAC and other atmospheric correction approaches are as follows: 1) the use of an expectation of surface reflectance at coarse resolution; 2) the use of the CAMS data as a prior constraint; 3) the use of spatial regularisation in atmospheric composition parameters; 4) the use of state-of-the-art atmospheric radiative transfer models through Gaussian Process emulators (Gomez-Dans et al., 2016). An advantage of the SIAC method is the accurate retrieval of land surface reflectance along with uncertainty estimates for every single HR-EO pixel.

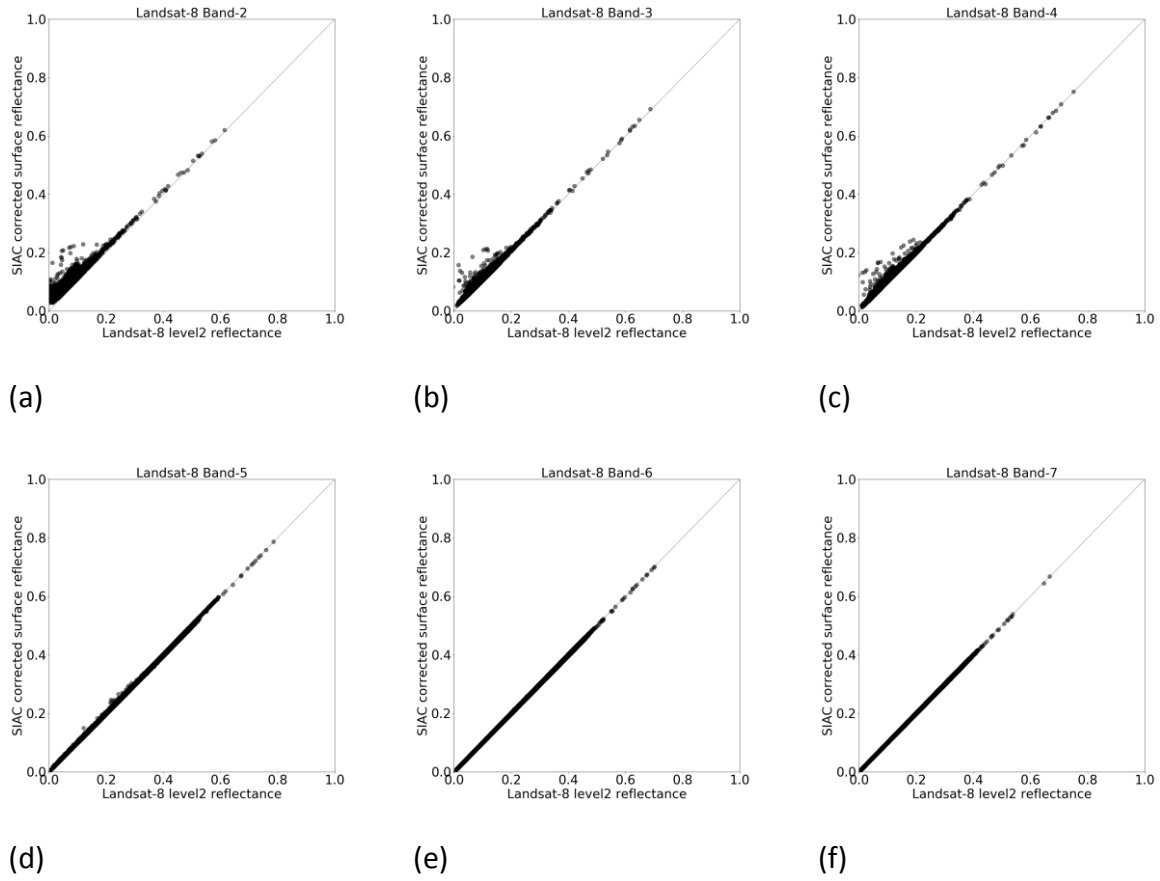

Figure 20.Comparison of Landsat-8 surface reflectances derived from a) Level-2 standard products and 2) atmospherically corrected Level-1 products using the SIAC.

In Figure 20, six 2D scatterplots are used to illustrate the intercomparison results of employing the SIAC method to atmospherically correct Landsat-8 Level-1 TOA reflectance data for different spectral bands. It is found that the surface reflectances derived from SIAC atmospheric correction have a very high correlation with the Landsat-8 Level-2 products, except for some differences for low-reflectance values in band-2 (450 – 510 nm), band-3 (530 – 590 nm) and band-4 (640 – 670 nm). The aforementioned paper (ibid) shows many site comparisons between 6S atmospheric corrections using AERONET data as the "aerosol truth".

To validate the use of the SIAC method in Sentinel-2 dataset, different atmospheric correction approaches are employed and intercompared. They are the SIAC method, the 6Sv model and the Sen2Cor model. The 6Sv[12] is the vector version of the 6S model which accounts for the radiation polarization. Sen2Cor is a processor for Sentinel-2 Level 2A product generation and formatting; it performs the atmospheric-, terrain and cirrus correction of Top-Of- Atmosphere Level 1C input data. Here the Sen2Cor processer is only used to create surface reflectance

[12] http://6s.ltdri.org/

(Bottom of Atmospheric reflectance). The Sen2Cor v2.8[13] employed was released on February 21, 2019 for this intercomparison.

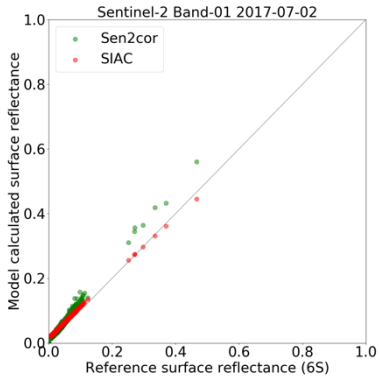

(a)

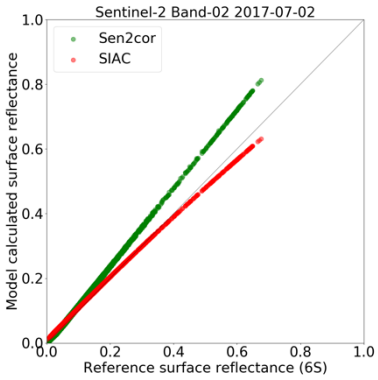

(b)

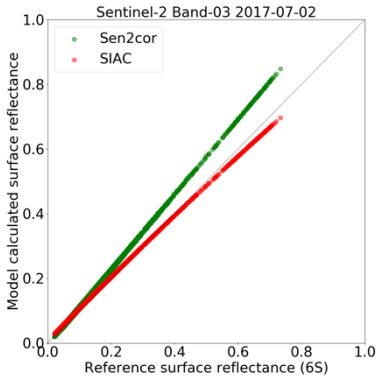

(c)

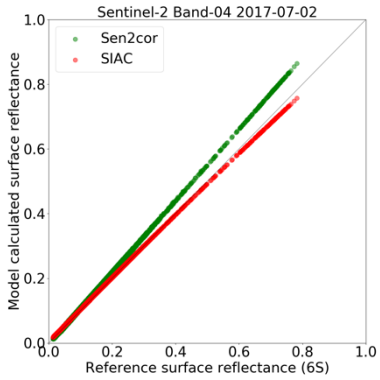

(d)

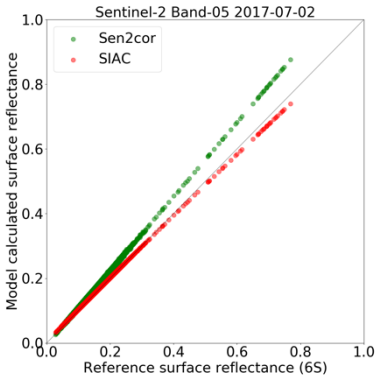

(e)

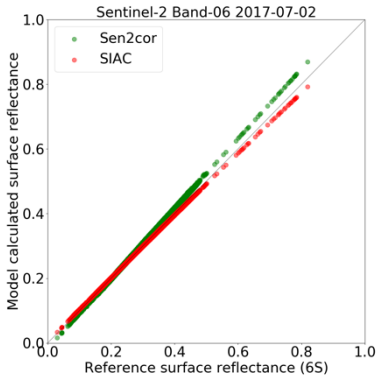

(f)

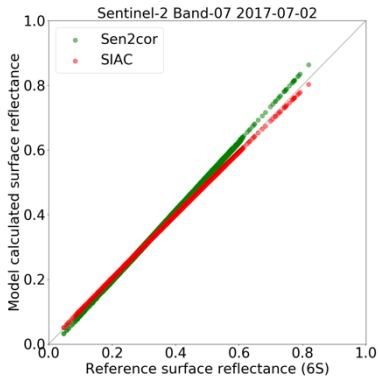

(g)

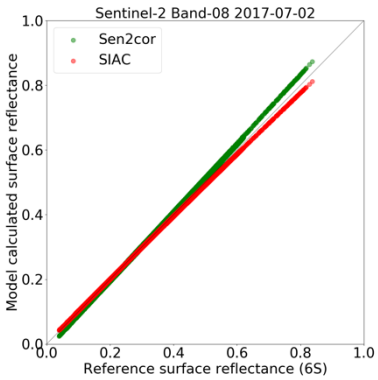

(h)

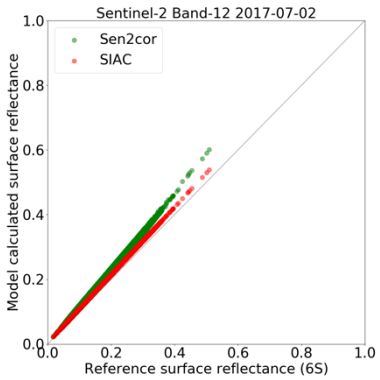

(i)

[13] http://step.esa.int/main/third-party-plugins-2/sen2cor/sen2cor_v2-8/

Figure 21.Comparison of surface reflectances retrieved from the Sen2Cor, SIAC and 6Sv atmospheric correction approaches. This example is taken from Sentinel-2 data at the Sioux Falls site on 2nd July 2017.

The intercomparison results of atmospherically corrected surface reflectances are shown in Figure 21 for Sentinel-2 bands at the Sioux Falls site on 2nd July 2017. The Sioux Falls site has near-real-time Aerosol Optical Depth (AOD) data measured from Aerosol Robotic Network (AERONET). The aerosol-truth measurements of the AOD can be used as input parameters for the 6Sv atmospheric correction and retrieve highly accurate surface reflectances. It is clearly seen that the surface reflectances retrieved from the SIAC method have a better correlation with the reference reflectances than those retrieved from Sen2Cor method. An example of TOA reflectances and SIAC retrieved surface reflectance is shown in Figure 22.

(a) (b)

*Figure 22.Example of TOA reflectances and SIAC retrieved surface reflectances at the Penn State University site on 24th May 2018. The figure shows a 10 * 10 km region with the tower in the centre.*

5.3 HR-BRF to CGLS (SW)

After TOC-R from tower measurements and HR-EO shortwave BRFs are estimated, a "calibration factor" can be calculated by comparing the single value from the tower albedometer and the averaged value from multiple pixels within the tower FOV within the HR-EO SW-BRFs. This "calibration factor" can then be used to upscale the high-resolution HR-EO SW-BRFs to the coarse CGLS grid. To verify the upscaled TOC-R at the coarse grid, the MODIS BRDF product is used to generate the TOC-R product under the same viewing and solar geometry for the same tower pixel. The adopted MODIS BRDF function has a spatial resolution of 1 km, which is nearly the same as the upscaled product. The result of this intercomparison is shown in Figure 23 for the shortwave TOC-R.

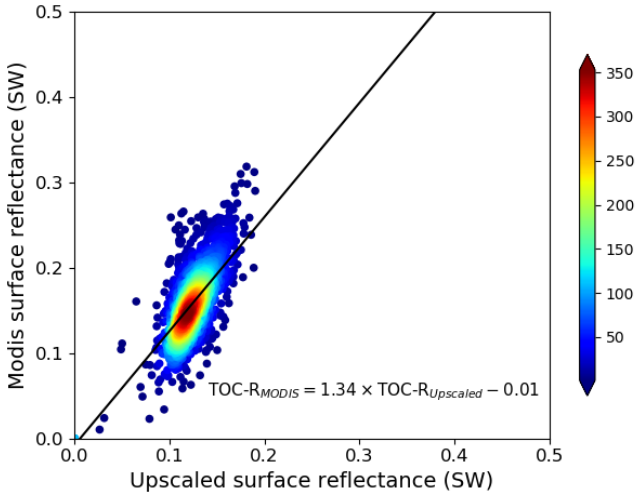

Figure 23.Inter-comparison of upscaled TOC-R product with MODIS equivalent for SW.

In comparison, Figure 24 shows a comparison of Sentinel-2 and MODIS spectral surface reflectance. The Sentinel-2 data are aggregated to the MODIS resolution (500 m) to ensure the reflectance values are compared at the same spatial scale.

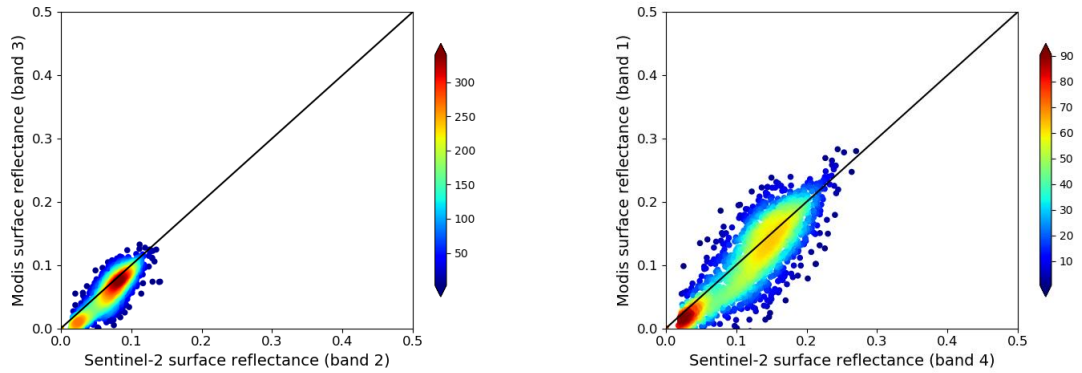

(a) (b)

Figure 24.Comparison of Sentinel-2 and MODIS spectral surface reflectance. Panel (a) shows Sentinel-2 band-2 (490 nm) compared with MODIS band-3 (459 – 479 nm), and panel (b) shows Sentinel-2 band-4 (665 nm) compared with MODIS band-3 (620 – 670 nm).

5.4 Albedo from LP2 at tower to CGLS (SW)

The evaluation of coarse-scale albedo products through a direct comparison with *in situ* data is feasible in three cases according to Wu et al. (2016). If the land surface is sufficiently homogeneous, *in situ* based measurements can be considered to be spatially representative and can be directly used (e.g. Cescatti et al., 2012). If the land surface is heterogeneous, the coarse-scale albedo products and *in situ* measurements are generally scale unmatched. A direct comparison between *in situ* measurements and coarse-scale albedo products is only valid under two circumstances: the footprint of the *in situ* observation is close to or larger than the range value of the surface albedos within the coarse pixel (Román et al., 2009; Wang et

al., 2012; Cescatti et al., 2012; Román et al., 2013; Wang et al., 2014). This range, a geostatistical attribute, defines the distance from the tower location beyond which there is no correlation of a biophysical property. In this case, the *in situ* measured albedo is spatially representative of the satellite albedo. The other is that the footprint of the *in situ* measurement is comparable with the spatial resolution of the satellite coarse pixel (Román et al., 2009). For example, some *in situ* observations collected from field towers have the projected FoVs of several hundred metres so that they can be directly compared with satellite coarse-resolution pixels.

Firstly, the projected FoV of the tower albedometer needs to be calculated. Employing the method described in Wu et al. (2016) shown in Figure 25 below, the FoV can be calculated by multiplying the height above the canopy by 8.7. However, this is the ideal case when the tower is nested inside a single coarse resolution pixel. It also produces a FoV which is less than that calculated for example, for the Hainich site (287 cf 750m). This is now the reference albedo and can be located by assuming that the albedometer measures a circular area from the top of the tower. This circular area can then be found by integrating the pixels within a HR-EO SW-albedo product.

This high resolution albedo product can then be derived using the methods described in Liang (2003) and Qu et al., (2016) for the Chinese HJ satellite sensor. Their method used early machine learning (neural networks) based on numerous radiative transfer simulations. Our method employs as input atmospherically corrected BRFs from HR-EO which were described in the previous section alongside BRFs predicted from a larger area derived from a MODIS BRDF climatology. A non-linear regression is used to establish the relationship between BRF and shortwave albedos to assign each pixel around the tower pixel with a corresponding BRDF. It is based on the assumption that over a large area, different high resolution mosaics of pixel BRFs will contribute to a range of BRFs when compared with BRFs calculated from BRDFs of coarse resolution pixels in an area. After aggregating the pixels for the corresponding area of the reference albedometer measurements, the “calibration factor” can be calculated between the albedo calculated from the HR-EO and that of the albedometer. This factor can then be applied to upscale the HR-EO albedos to the CGLS product.

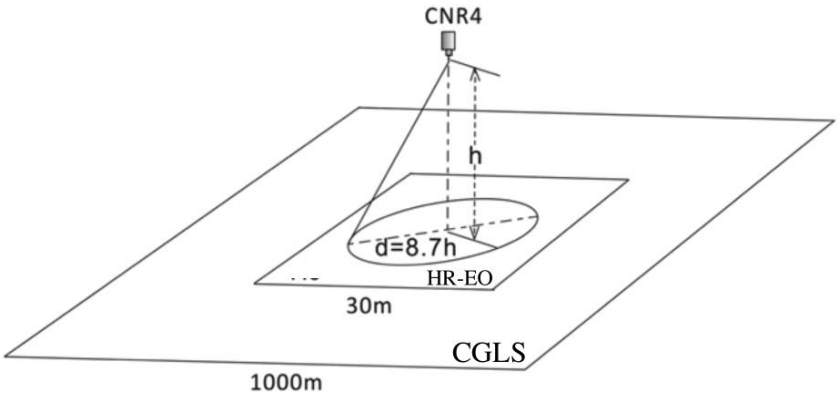

Figure 25.Schematic of relationship between albedometer FoV, a 30m pixel and the coarse-scale 1km FoV for an idealised case taken from Qu et al.,(2016) .

5.4.1 Retrieval of high-resolution (HR-EO) shortwave albedo

We first employ the method proposed by Shuai et al. (2011) to retrieve high-resolution shortwave albedo from Landsat high-resolution reflectance and coarse-resolution MODIS BRDF measurements. The MODIS BRDF is derived from a kernel-driven BRDF model and is here represented by $R_m(\lambda,\ \theta_{in},\ \theta_{out},\ \varphi)$. Taking the Sentinel-2 observations for example: the DHR at Sentinel-2 solar zenith angle and the BHR are denoted as follows,

$$DHR_m(\theta_{in}) = \frac{1}{\pi}\int_0^{2\pi} d\,\varphi \int_0^1 R_m(\lambda,\ \theta_{in} = \text{Sentinel\_}\theta_{in},\ \theta_{out},\ \varphi)\, u_v du_v \qquad (23)$$

$$BHR_m = \frac{1}{\pi}\int_0^{2\pi} d\,\varphi \int_0^1 DHR_m(\theta_{in})\, u_s du_s \qquad (24)$$

where m denotes MODIS 500-m spatial resolution, u_v(=$\sin\theta_{out}$) and u_s(=$\sin\theta_{in}$) are the variables of integration. The Bi-directional Reflectance at MODIS resolution for the Sentinel-2 viewing and illumination geometry is given by,

$$\mathrm{R_m}(\Omega_\mathrm{S}) = R_m(\lambda,\ \theta_{in} = \text{Sentinel\_}\theta_{in},\ \theta_{out} = \text{Sentinel\_}\theta_{out},\ \varphi = \text{Sentinel\_}\varphi) \quad (25)$$

where Ω_S is the Sentinel-2 viewing and solar geometry. Then, the ratios between the albedo and reflectance at Sentinel-2 viewing and solar geometries at MODIS resolution can be computed as,

In the processing chain (Figure 26), Sentinel-2 data are reprojected from UTM to MODIS (sinusoidal) projection, and then aggregated from 20-m to 500-m

$$\alpha_D = DHR_m(\theta_{in})/\mathrm{R_m}(\Omega_\mathrm{S}) \quad \alpha_B = BHR_m/\mathrm{R_m}(\Omega_\mathrm{S}) \qquad (26)$$

Suppose that we have a pure homogeneous area that covers all the Sentinel-2 pixels for a particular MODIS pixel(s), the ratios of albedo and reflectance should be similar at MODIS and Sentinel-2 resolution. Based on this assumption, the DHR and BHR at Sentinel-2 spatial resolution can be computed with

$$DHR_S(\theta_{in}) = \sum_{i=1}^{n} w_i \alpha_{D_i} \mathrm{R_S}(\Omega_S) \qquad BHR_S(\theta_{in}) = \sum_{i=1}^{n} w_i \alpha_{B_i} \mathrm{R_S}(\Omega_S) \qquad (27)$$

where n is the number of pure endmembers, α_{D_i} is the ratio between DHR and reflectance for the i*th* pure component, w_i is the weighting of the i*th* component in the target Sentinel-2 pixel.

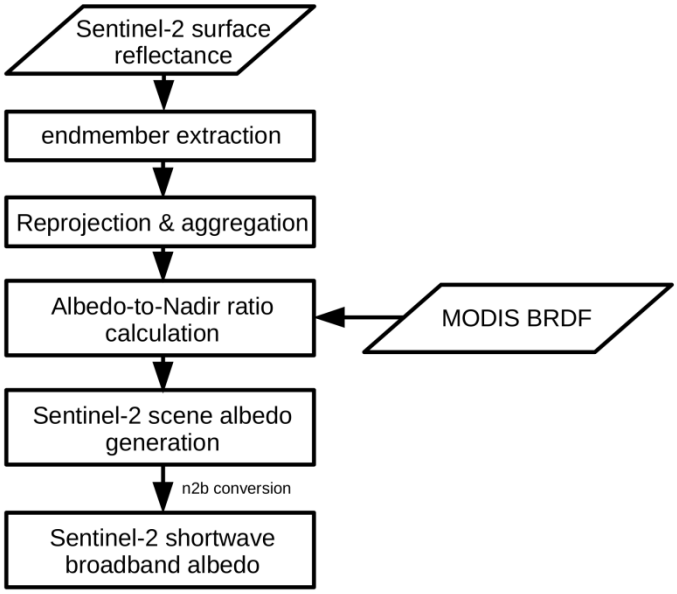

Figure 26.Processing chain of calculating high-resolution albedo from HR-EO surface reflectance and MODIS BRDF data.

Using the N-FINDR endmember extraction algorithm (Schowengerdt, 1997) and fully constrained least squares (Heinz et al., 1999) linear unmixing method, the proportion of classes within each MODIS pixel is calculated. Figure 27 shows the proportions of two dominant classes for the aggregated data over the Hainich site.

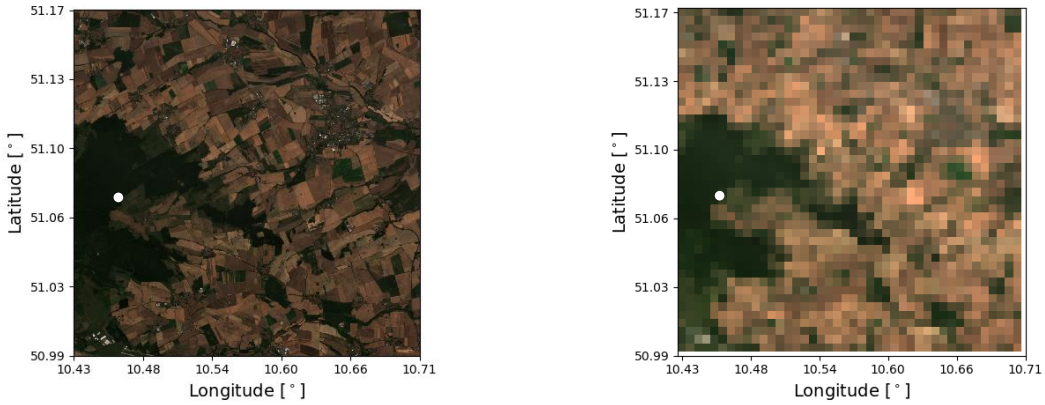

(a) (b)

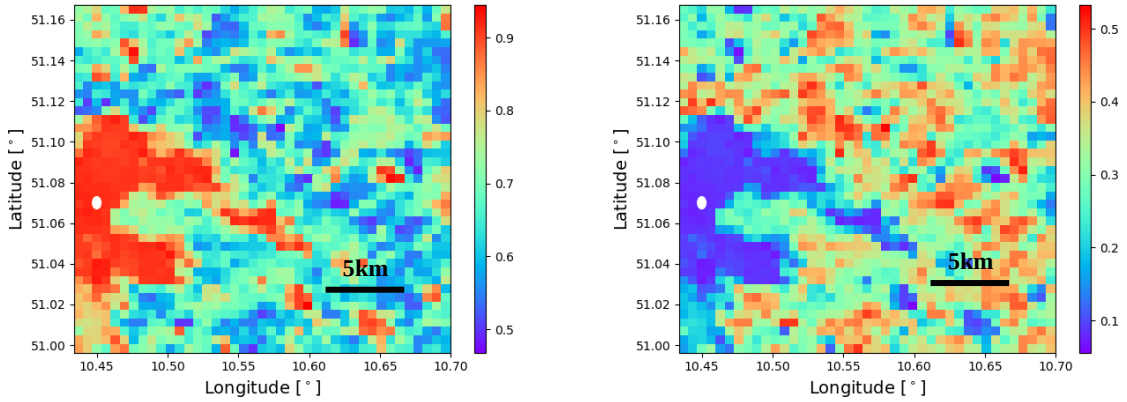

(c) (d)

Figure 27.RGB composite of surface shortwave reflectance over the Hainich site in (a) Sentinel-2 resolution (20 m), and after aggregated to (b) MODIS resolution (500m). The proportion of two dominant classes for each pixel derived from the endmember algorithm is

For each class, the pixels with the proportion value larger than a threshold (e.g. 0.9 for the first dominant class of Figure 27) can be regarded as pure pixels. For theses pure pixels, the DHR, BHR and reflectance at Sentinel-2 viewing and solar geometries can be computed using the MODIS BRDF function. Then, the α_D and α_B for a given class can be calculated from the averaged mean of all the pure pixels. Finally, albedo at Sentinel-2 spatial resolution can be determined by the weighted sum of α_D (or α_B) for different classes. As the albedo at Sentinel-2 resolution is calculated for different bands separately, Eq. (22) should be used to obtain the shortwave albedo. Figure 28 gives the high-resolution albedo (DHR and BHR) calculated for Sentinel-2 viewing and solar geometries on 6th August, 2015.

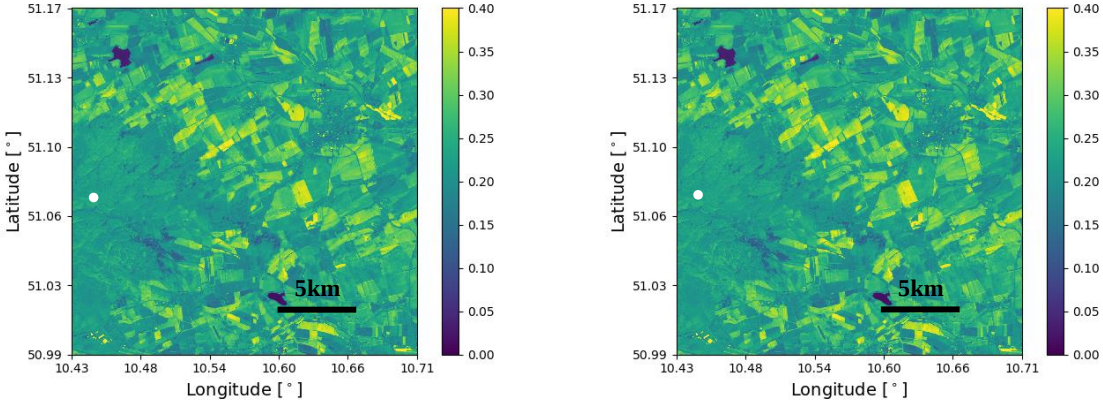

(a) (b)

Figure 28.Calculated high-resolution DHR (a) and BHR (b) over the Hainich site on 6th August, 2015. The white dots indicate the location of the tower.

In Figure 29, the steps for upscaling high-resolution albedo to the CGLS pixel size is shown.

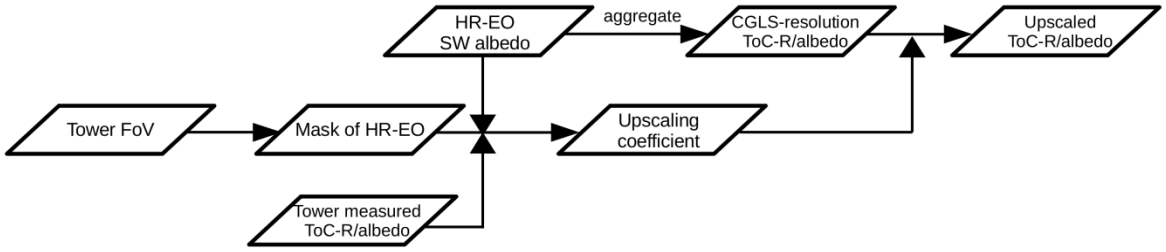

Figure 29.Steps of upscaling high-resolution albedo/ToC-R to CGLS pixel size. The process of calculating HR-EO SW albedo is illustrated in Fig. 26.

5.4.2 Upscaling of albedo from tower to CGLS

For the Hainich site, the *in situ* DHR and BHR can be calculated from the BRDF function, which is based on continuous tower measurements. The upscaling factor is calculated as the ratio between the *in situ* DHR (or BHR) and the averaged high-resolution DHR (or BHR) within the tower's FOV. Then, this factor is used to upscale the high-resolution albedo to coarse-resolution (1/112˚) albedo. The process of upscaling albedo is the same as the process of upscaling TOC-R, which was introduced in Section 5.2 above. Figure 30 shows the comparison between upscaled DHR and DHR derived from MODIS BRDF function.

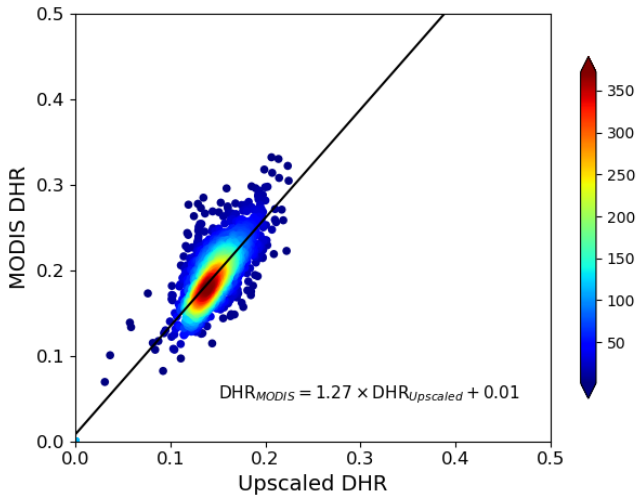

Figure 30.Comparison between upscaled DHR and DHR derived from MODIS BRDF function.

5.5 Validation of LP1 and LP2

In this section, the upscaled LP1 and LP2 products are compared with the CGLS products. First of all, examples at the US-PSU site are used to show the comparison between upscaled LP1/LP2 (12 products per annum) and CGLS products between 01/01/2012 and 31/12/2016. The LP2 (upscaled DHR and BHR) time-series comparisons show a good agreement between upscaled values and CGLS albedo products. The discrepancies between LP1 (upscaled ToC-R) and CGLS ToC-R products are due to insufficient cloud-free albedometer measurements which are essential for the angular BRDF modelling.

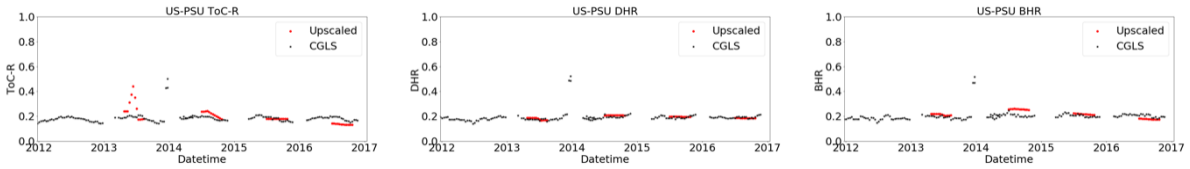

Figure 31.Comparison between LP1/2 and CGLS products ToC-R/albedo product at the US-PSU site.

In addition, the DHRs and BHRs retrieved from tower data were upscaled to a larger area ($\approx 20 * 20$ km) at CGLS resolution and compared with CGLS products to assess the performance of this upscaling strategy. Scatter plots between the upscaled LP2 and CGLS 1-km albedo are displayed in Figure 32 for LP2-DHR comparisons and Figure 33 for LP2-BHR comparisons, respectively.

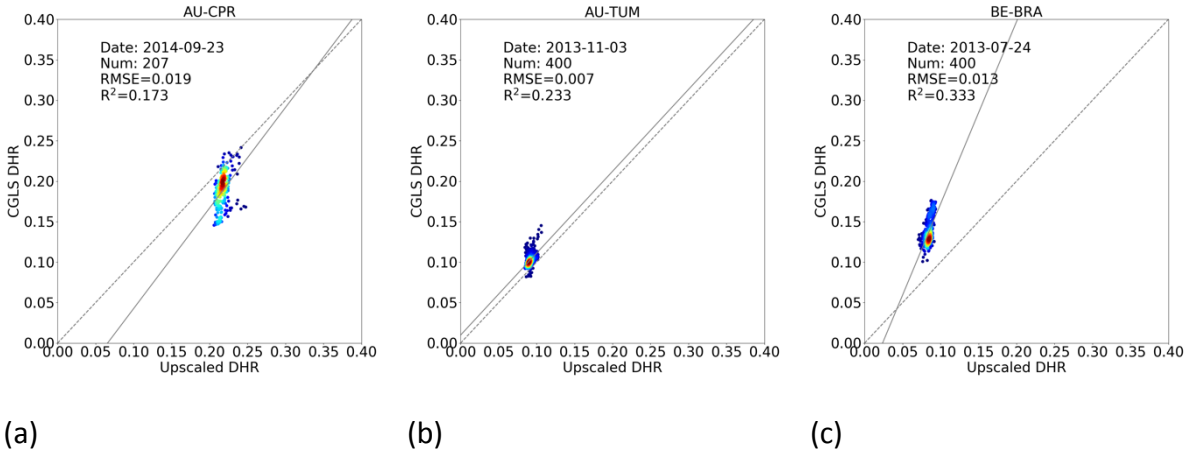

(a) (b) (c)

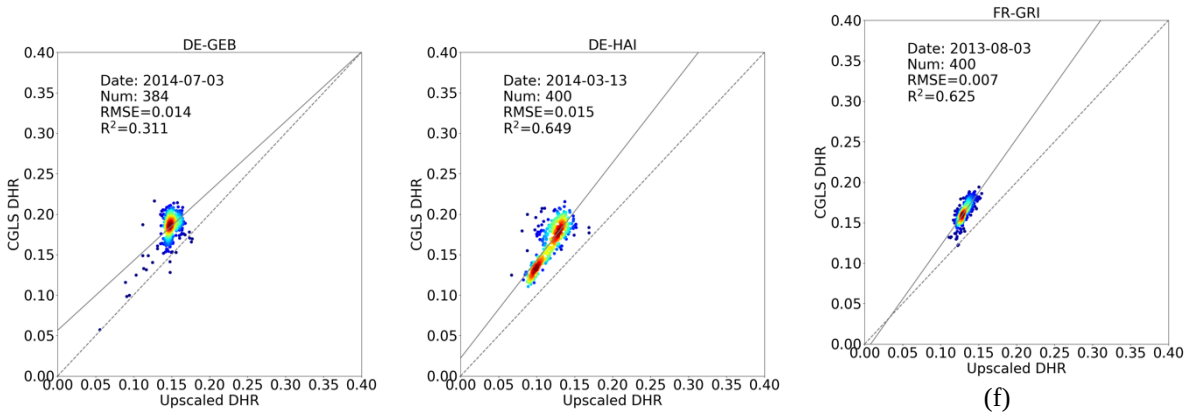

(d) (e) (f)

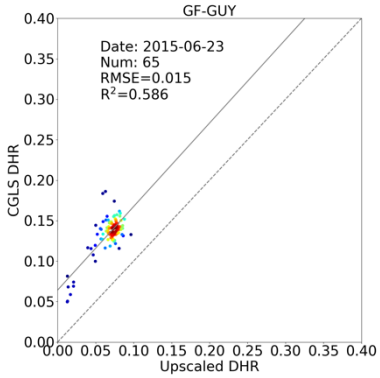

(g)

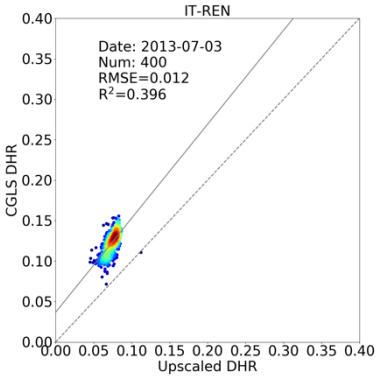

(h)

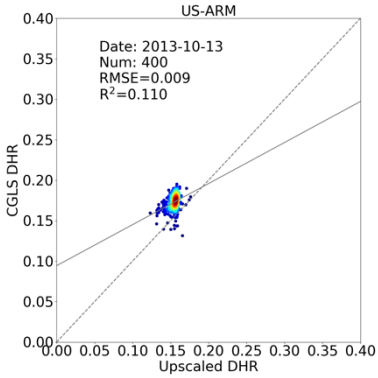

(i)

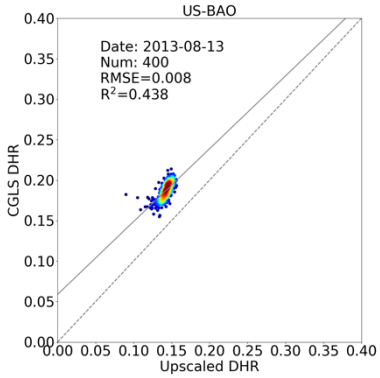

(j)

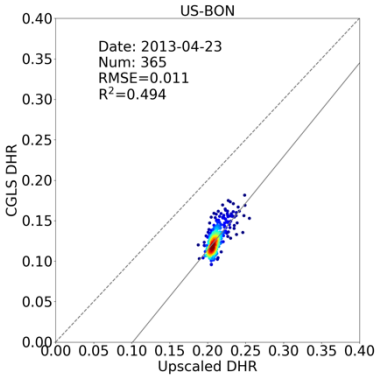

(k)

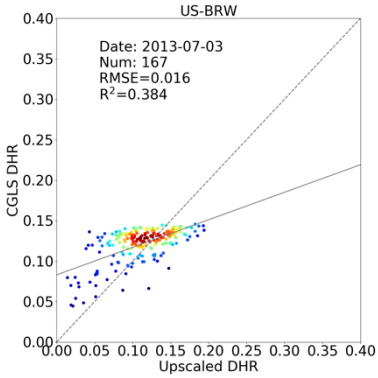

(l)

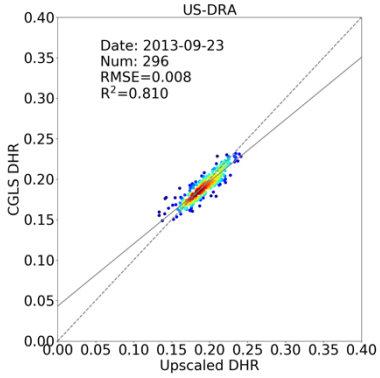

(m)

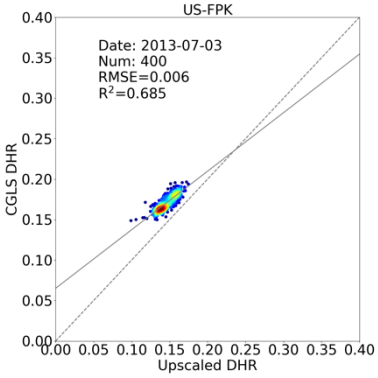

(n)

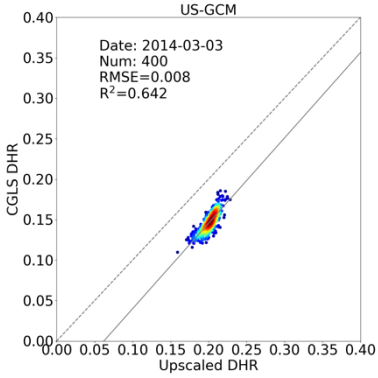

(o)

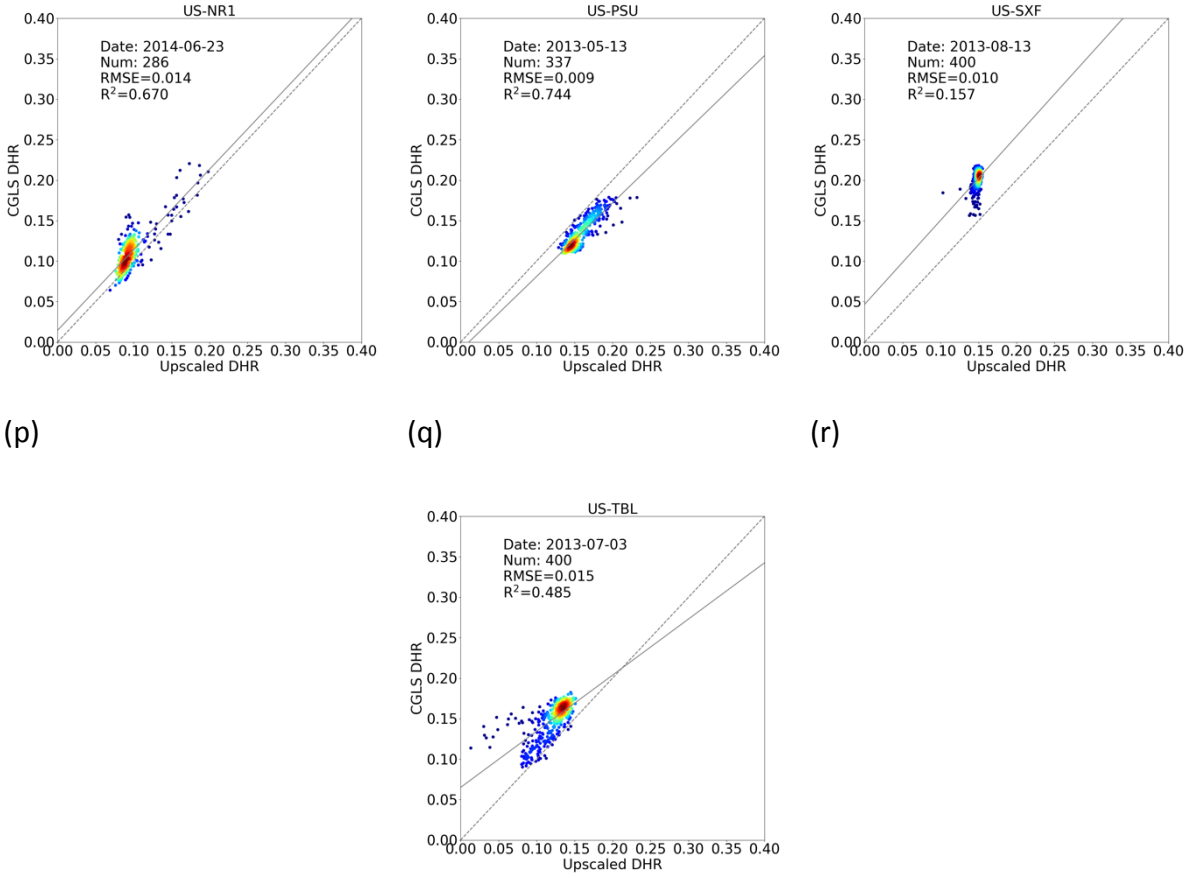

(p) (q) (r)

(s)

Figure 32.Comparison between LP1-DHR and CGLS products.

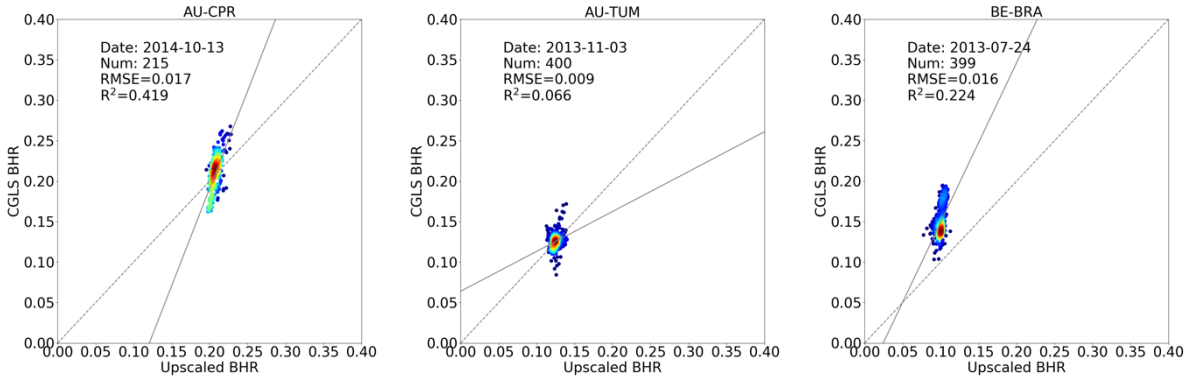

(a) (b) (c)

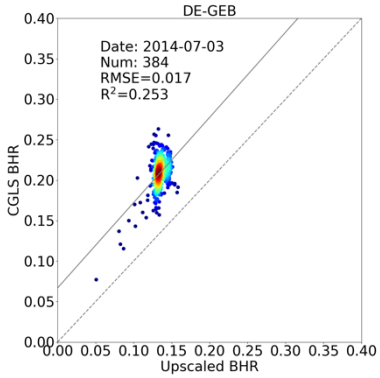

(d)

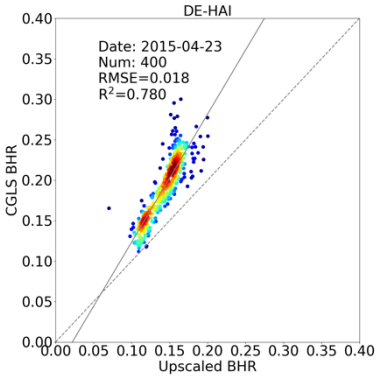

(e)

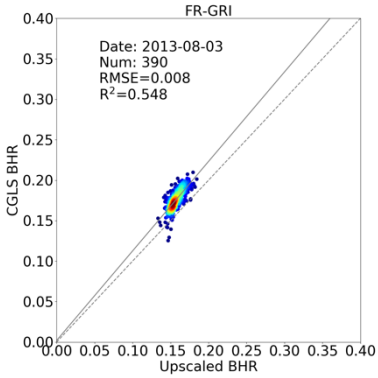

(f)

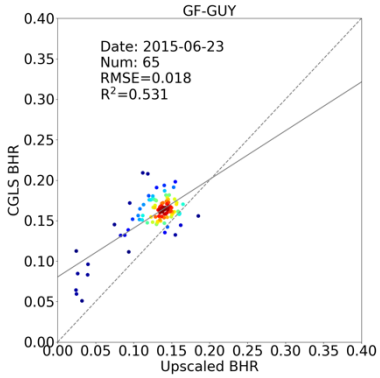

(g)

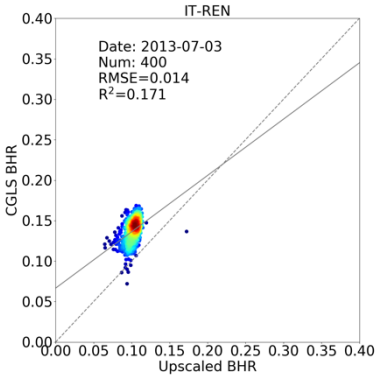

(h)

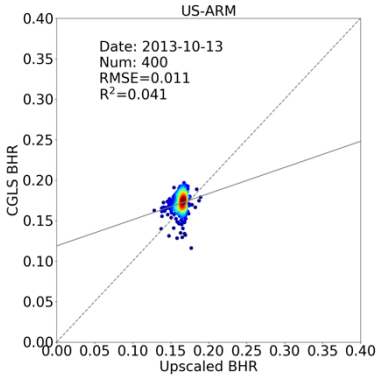

(i)

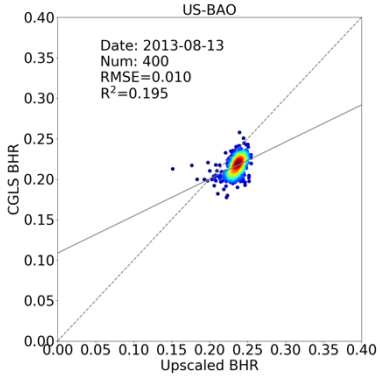

(j)

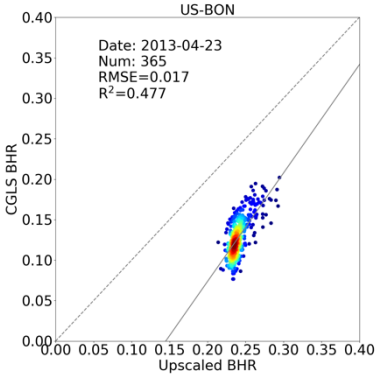

(k)

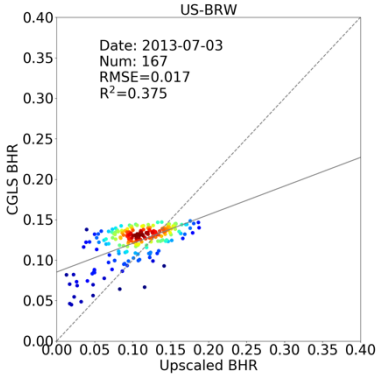

(l)

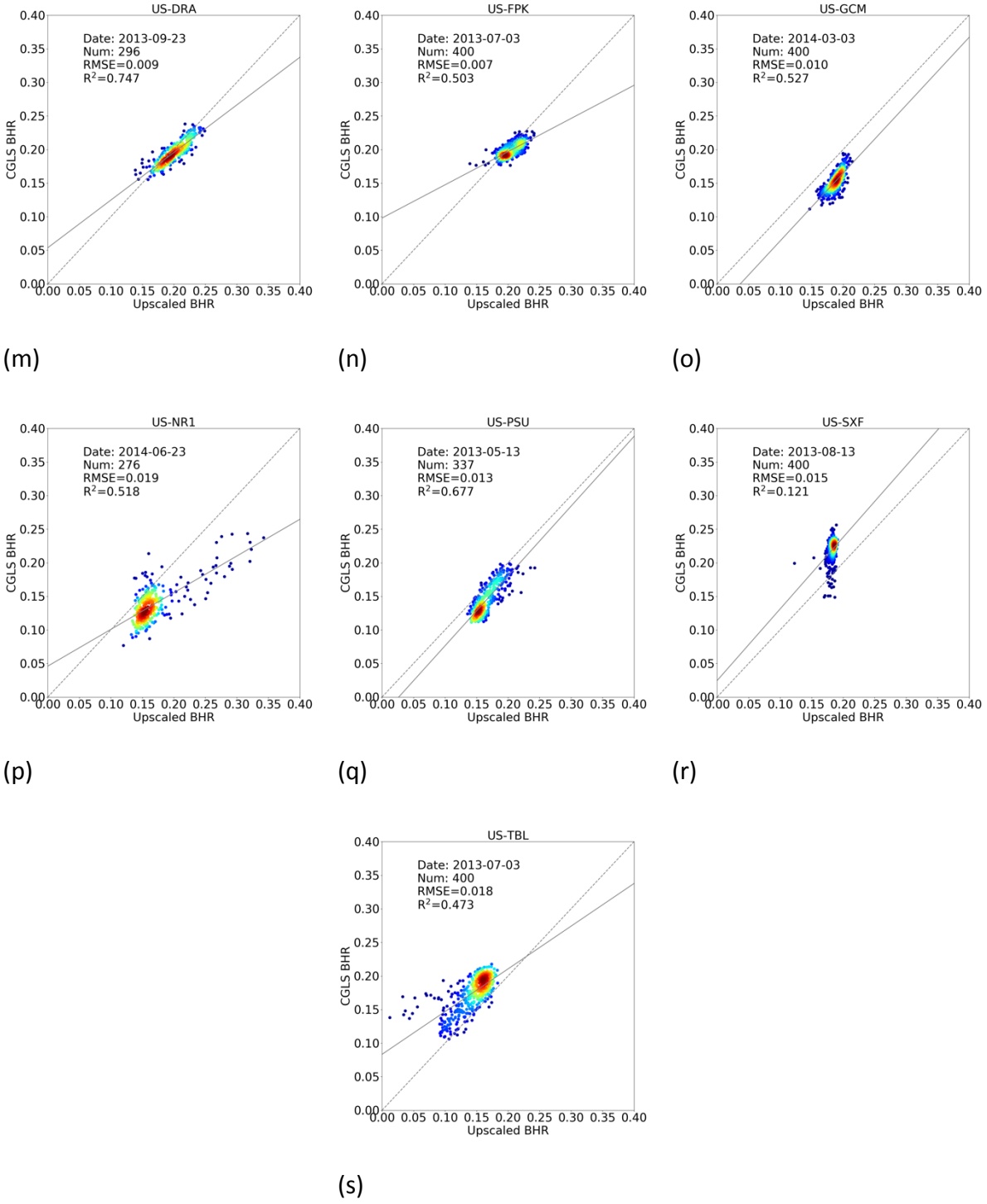

Figure 33.Comparison between LP1-BHR and CGLS products.

For example, at the Fort Peck site, the upscaled DHRs are well correlated with the CGLS DHRs, with a R-squared ($\boldsymbol{R^2}$) of 0.685 and root-mean-square-error (RMSE) of 0.006. The Brasschaat site shows a bias in the "point-to-pixel" time series analysis, but the upscaled scaled DHRs show a better correlation with CGLS values, with a $\boldsymbol{R^2}$ of 0.333 and RMSE of 0.013. The Barrow site has fewer pixels upscaled to coarse resolution than the other sites, and the upscaled DHRs

show larger differences with CGLS for the pixels with smaller albedo values due to melt-ponds and tundra in this region. At the Tumbarumba site, most pixels are clustered around the 1:1 line because of the good agreement in "point-to-pixel" time series analysis. But the upscaled DHRs have a relatively small value of $\boldsymbol{R^2}$ $(\mathbf{0.233})$ when compared with CGLS DHRs, which suggests that the upscaling coefficient is not suitable for upscaling to a region covering 20*20 pixels around the tower. The BHR upscaling results are close to the DHR upscaling results in terms of $\boldsymbol{R^2}$ and RMSE.

6 LP1 and LP2 uncertainties

This section gives an overview of the processing logic to infer the final LP1 and LP2 uncertainties from the model. In essence, this involves the calculation of uncertainties that propagate from uncertainties in the tower albedometers up to coarse satellite resolutions. The uncertainties of HR-EO at pixel-level need to be considered because the HR-EO is used as a transfer function while upscaling the tower measurements to coarse spatial resolutions.

In this project, the tower albedometers at selected sites have a daily uncertainty (σ_{daily}) of 5% at the 95% confidence level. Because in our method, the BRDF multi-angular modelling combines albedometer measurements over a fixed time window, the calculated ToC-R, DHR and BHR values have a much smaller uncertainty which can be estimated as following:

$$\sigma_{in-situ} = \frac{\sigma_{daily}}{\sqrt{N}} \quad (28)$$

where σ_{daily} is the tower albedometer daily uncertainty, and N is the number of days within the fixed time window which is 30 in this case.

While upscaling the LP1 and LP2 from tower derived values up to the CGLS spatial scale, HR-EO measurements are used as a transfer function so that the uncertainties of HR-EO pixel reflectances need to be known. The spectral surface reflectance values derived from the streamlined SIAC model have estimated uncertainties for every single pixel in each individual spectral band, which can be combined to calculate the uncertainties of the derived shortwave broadband using the same equations listed in Table 14 by replacing the spectral reflectance values with the spectral reflectance uncertainties. An example of calculating the absolute uncertainty of the shortwave broadband reflectance for a Sentinel-2 pixel is as following:

$$\sigma_{SW_{absolute}} = 0.356\sigma_{b2} + 0.130\sigma_{b4} + 0.373\sigma_{b8} + 0.085\sigma_{b11} + 0.072\sigma_{b12} - 0.018 \quad (29)$$

where $\sigma_{SW_{absolute}}$ is the absolute uncertainty of shortwave broadband reflectance value, and σ_{b2}, σ_{b4}, σ_{b8}, σ_{b11}, σ_{b12} are the uncertainties of Sentinel-2 band 2 (490 nm), band 4 (665 nm), band 8 (865 nm), band 11 (1610 nm) and band 12 (2190 nm). The relative uncertainty of shortwave broadband reflectance is:

$$\sigma_{SW_{relative}} = \frac{\sigma_{SW_{absolute}}}{BRF_{SW}} \quad (30)$$

where BRF_{SW} is the shortwave broadband surface reflectance value derived from the SIAC processing and narrow-to-broadband conversion.

The final coarse-resolution LP1 and LP2 are generated by aggregating the HR-EO values to the coarse CGLS resolution and then correcting the aggregated values using the calibration factor. The final relative uncertainty consists of two parts, which are the tower albedometer uncertainty and the HR-EO uncertainty as mentioned above. The final uncertainty is:

$$\sigma = \sigma_{in-situ} + \sigma_{SW_{relative}} \quad (31)$$

Figure 34 - Figure 36 show examples of upscaled BHR, DHR and ToC-R values along with the estimated uncertainties at the US-DRA site.

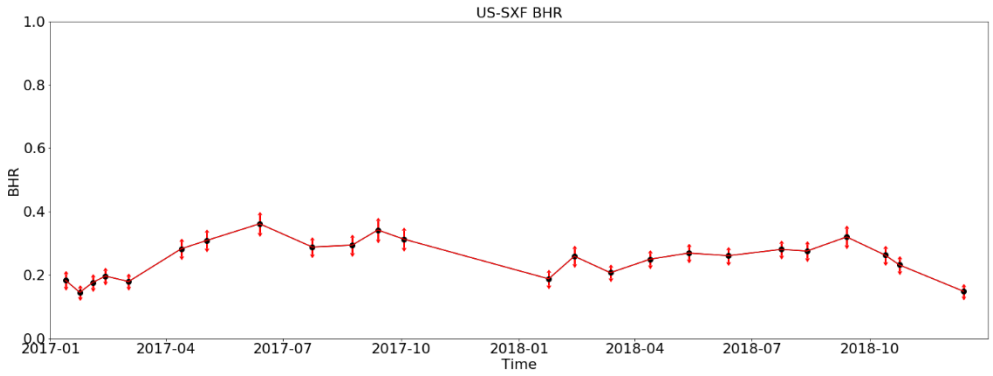

Figure 34. Example of upscaled BHR and uncertainty values at the US-DRA site.

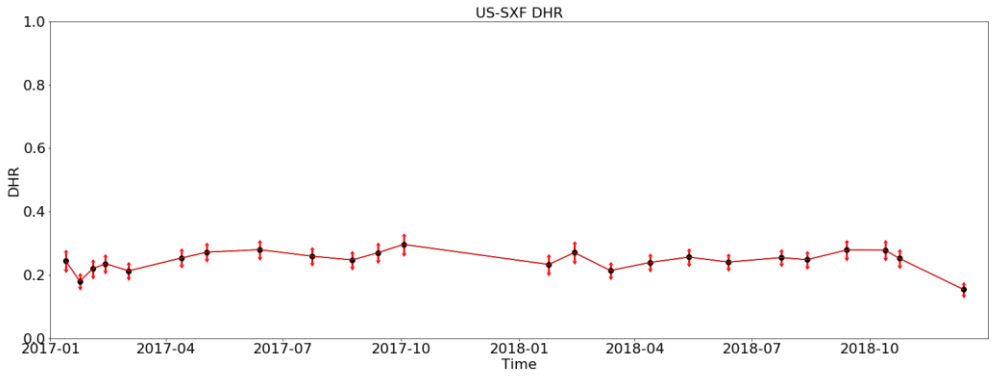

Figure 35. Example of upscaled DHR and uncertainty values at the US-DRAsite.

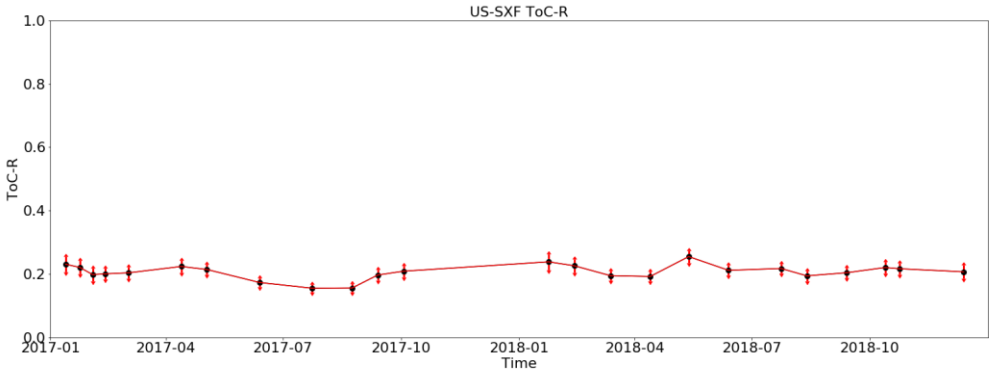

Figure 36. Example of upscaled ToC-R and uncertainty values at the US-DRA site.

7 Software development

The processing chain introduced in Chapters 4 and 5 for producing RM1, LP1 and LP2 products is built up based on Python 2.7 code. In Table 15, all the functions and open-source packages used in each processing stage are listed. The steps and relevant functions for producing upscaled TOC-R, DHR and BHR are illustrated in Figure 37.

Table 15. List of functions and Python packages for each processing stage of RM1, LP1 and LP2.

Processing stage	Function name	Python packages
Calculation of diffuse radiation	cal_diff_radiation()	numpy[14], datetime[15]
Calculation of DHR	cal_dhr()	numpy, timezonefinder [16] , astral[17], pytz[18]
Calculation of BHR	cal_bhr()	numpy, timezonefinder, astral, pytz
Calculation of TOC-R	cal_tocr()	numpy, timezonefinder, astral, pytz
SIAC streamline	cal_correction()	SIAC[19]
Upscaling of TOC-R	upscale_tocr()	numpy, scipy[20], netCDF4[21]
Calculation of HR-albedo	cal_hr_albedo()	Numpy, scipy, netCDF4, pypstools[22]
Upscaling of albedo	upscale_albedo()	numpy, scipy, netCDF4

[14] http://www.numpy.org/
[15] https://docs.python.org/2/library/datetime.html
[16] https://pypi.org/project/timezonefinder/
[17] https://astral.readthedocs.io/en/latest/
[18] https://pypi.org/project/pytz/
[19] https://github.com/MarcYin/SIAC
[20] https://www.scipy.org/
[21] http://unidata.github.io/netcdf4-python/
[22] https://pypi.org/project/pypstools/

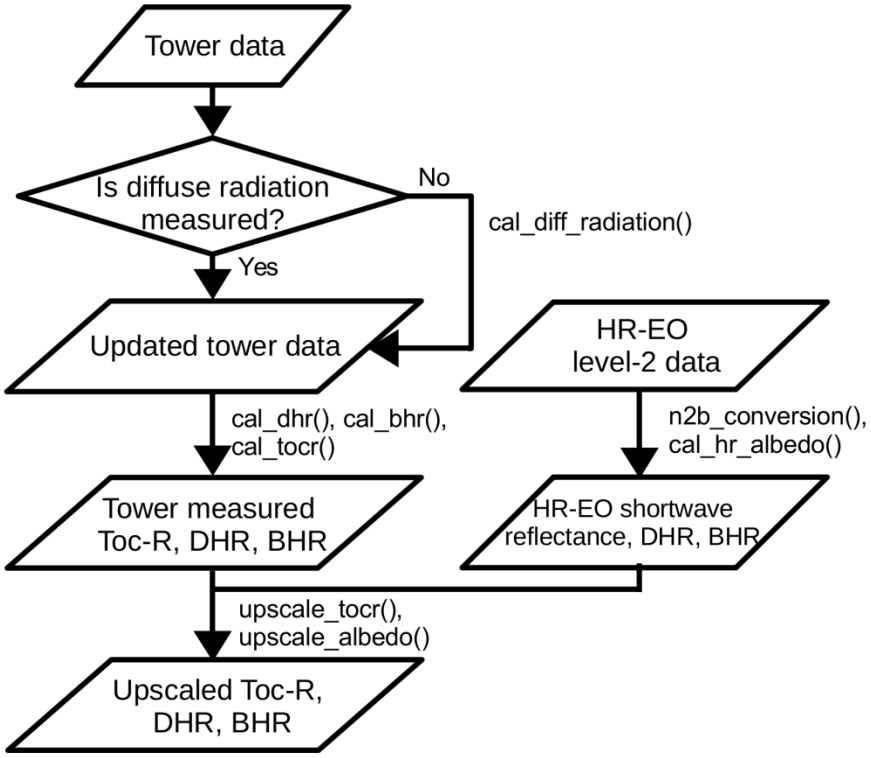

Figure 37.Steps and functions for producing upscaled TOC-R, DHR and BHR.

8 References

Camacho, F: Gio Global Land Component Lot 1 (GIO-GL Lot 1): Validation Report: TOC-R SPOT/VGT V1. ccc. "ccc." 3333, 2015.

Cescatti, A., Marcolla, B., Vannan, S. K. S., Pan, J. Y., Román, M. O., Yang, X., Ciais, P., Cook, R. B., Law, B. E., Matteucci, G., Migliavacca, M., Moors, E., Richardson, A. D., Seufert, G., and Schaaf, C. B.: Intercomparison of MODIS albedo retrievals and in situ measurements across the global FLUXNET network, *Remote Sensing of Environment*, 121, 323 - 334, doi:10.1016/j.rse.2012.02.019, 2012.

Doxani, G., E. Vermote, J.-C. Roger, F. Gascon, S. Adriaensen, D. Frantz, O. Hagolle, A. Hollstein, G. Kirches, F. Li, J. Louis, A. Mangin, N. Pahlevan, B. Pflug, and Q. Vanhellemont.: Atmospheric Correction Inter-Comparison Exercise, *Remote Sensing*, 10(3), 352, doi:10.3390/rs10020352, 2018.

Gomez-Dans, J. L., Lewis, P. E., and Disney, M.: Efficient emulation of radiative transfer codes using gaussian processes and application to land surface parameter inferences. *Remote Sensing*, 8(2):119, doi: 10.3390/rs8020119, 2016.

Heinz, D., Chang, C. I. and Althouse, M. L. G.: Fully constrained least-squares based linear unmixing hyperspectral image classification, *Geoscience and Remote Sensing Symposium*, 1999. IGARSS '99 Proceedings. IEEE 1999 International, Hamburg, pp. 1401-1403 vol.2., 1999.

Lacaze, R.: Gio Global Land Component Lot 1 (GIO-GL Lot 1): Algorithm Theoretical Basis Document: Surface Albedo, 2014.

Liang, S.: Narrowband to broadband converions of land surface albedo: I Algorithms, *Remote Sensing of Environment*, 76, 213–238, doi:10.1016/S0034-4257(00)00205-4, 2000.

Liang, S.: A direct algorithm for estimating land surface broadband albedos from MODIS imagery, *IEEE Transactions on Geoscience and Remote Sensing*, 41(1), 136–145, doi: 10.1109/TGRS.2002.807751, 2003.

Lucht, W., Schaaf, C.B., Strahler, A.H.: An algorithm for the retrieval of albedo from space using semiempirical BRDF models, *IEEE transactions on geoscience and remote sensing*, 38, 977-998, doi: 10.1109/36.841980, 2000.

Lewis, P., J-P Muller et al: GlobAlbedo Algorithm Theoretical Basis Document, 2011.

Naegeli, K.; Damm, A.; Huss, M.; Wulf, H.; Schaepman, M.; Hoelzle, M. Cross-Comparison of Albedo Products for Glacier Surfaces Derived from Airborne and Satellite (Sentinel-2 and Landsat 8) Optical Data, *Remote Sens.*, 9, 110, doi: 10.3390/rs9020110, 2017.

Qu, Y., Liang, S., Liu, Q., He, T., Liu, S., & Li, X.: Mapping surface broadband albedo from satellite observations: A review of literatures on algorithms and products. Remote

Sensing, 7(1), 990–1020, doi: 10.3390/rs70100990, 2015.

Reda, I. : Method to calculate uncertainties in measuring shortwave solar irradiance using thermopile and semiconductor solar radiometers, Tech. Rep. NREL/TP-3B10-52194, 20 pp., Natl. Renewable Energy Lab., Golden, Colo., doi:10.2172/1021250, 2011.

Román, M.O., C. B. Schaaf, C. E. Woodcock, A. H. Strahler, X. Yang, R. H. Braswell, P. S. Curtis, K. J. Davis, D. Dragoni, M. L. Goulden, L. Gu, D. Y. Hollinger, T. E. Kolb, T. P. Meyers, J. W. Munger, J. L. Privette, A. D. Richardson, T. B. Wilson, and S. C. Wofsy,: The MODIS (Collection V005) BRDF/albedo product: Assessment of spatial representativeness over forested landscapes, *Remote Sensing of Environment*, 113(11), 2476 - 2498, doi: 10.1016/j.rse.2009.07.009, 2009.

Román, M. O., C. B. Schaaf, P. Lewis, F. Gao, G. P. Anderson, J. L. Privette, A. H. Strahler, C. E. Woodcock, M. Barnsley.: Assessing the coupling between surface albedo derived from MODIS and the fraction of diffuse skylight over spatially characterized landscapes, *Remote Sensing of Environment,* 114, 738-760, doi: 10.1016/j.rse.2009.11.014, 2010.

Román, M. O., Gatebe, C. K., Shuai, Y. M., Wang, Z. S., Gao, F., Masek, J. G., He, T., Liang. S.L., Schaaf, C. B.: Use of in situ and airborne multiangle data to assess MODIS- and Landsat-based estimates of directional reflectance and albedo. *IEEE Transactions on Geoscience and Remote Sensing*, 51(3), 1393 - 1404 doi:10.1109/TGRS.2013.2243457, 2013.

Roujean J.-L., Leroy M., Deschamps P.-Y.: A Bidirectional Reflectance Model of the Earth's Surface for the Correction of Remote Sensing Data, *Geophysical Research Letters*, doi: 10.1029/92JD01411, 1992.

Roujean, J-L.: Gio Global Land Component Lot 1 (GIO-GL Lot 1): Algorithm Theoretical Basis Document: TOP OF CANOPY NORMALIZED REFLECTANCE (TOC-R), 2014.

Sanchez, J.: Gio Global Land Component Lot 1 (GIO-GL Lot 1): Assessment Report: Quality Surface Albedo V1, 2015.

Schaepman-Strub, Gabriela, et al.: Reflectance Quantities in Optical Remote Sensing: Definitions and Case Studies, *Remote Sensing of Environment* 103(1), 27-42, doi:10.1016/j.rse.2006.03.002, 2006.

Schowengerdt, R. A.: Remote Sensing: Models and Methods for Image Processing, 2nd ed. New York: Academic Press, 1997.

Shuai, Y., Masek, J. G., Gao, F., and Schaaf, C. B.: An algorithm for the retrieval of 30-m snow-free albedo from Landsat surface reflectance and MODIS BRDF, *Remote Sensing of Environment*, 115, 2204 - 2216, doi: 10.1016/j.rse.2011.04.019, 2011.

Song, R., Muller, J.-P., Kharbouche, S., Woodgate, W.: Intercomparison of Surface Albedo Retrievals from MISR, MODIS, CGLS Using Tower and Upscaled Tower Measurements, Remote Sens, 11, 644, doi: 10.3390/rs11060644, 2019.

Strahler, A.H., Muller, J.P., Lucht, W., Schaaf, C., Tsang, T., Gao, F., Li, X., Lewis, P., Barnsley, M.J.: MODIS BRDF/albedo product: algorithm theoretical basis document version 5.0. MODIS documentation, 1999.

Tanré, D., Deroo, C., Duhaut, P., Hermanc, M., Morcrette, J. J., Perbos, J., and Deschamps, P. Y.: Technical note Description of a computer code to simulate the satellite signal in the solar spectrum: the 5S code, *International Journal of Remote Sensing*, 11, 659 - 668, doi:10.1080/01431169008955048, 1990.

Vermote, E. F., Tanre, D., Deuze, J. L., Herman, M., and Morcette, J. J.: Second Simulation of the Satellite Signal in the Solar Spectrum, 6S: an overview, *IEEE Transactions on Geoscience and Remote Sensing*, 35, 675 - 686, 1997.

Vuolo, F., M. Zoltak, C. Pipitone, L. Zappa, H. Wengg, M. Immitzer, M. Weiss, F. Baret, and C. Atzberger,: Data Service Platform for Sentinel-2 Surface Reflectance and Value-Added Products: System Use and Examples, *Remote Sensing*, 8, 938 doi: 10.3390/rs8110938, 2016.

Wang, Z., Schaaf, C. B., Strahler, A. H., Chopping, M. J., Román, M. O., Shuai, Y., Woodcock, C. E., Hollinger, D. Y., Fitzjarrald, D. R.: Evaluation of MODIS albedo product (MCD43A) over grassland, agriculture and forest surface types during dormant and snow-covered periods. *Remote Sensing of Environment*, 140, 60 - 77, doi: 10.1016/j.rse.2013.08.025, 2014.

Wu, X. D., Wen, J. G., Xiao, Q., Liu, Q., Peng, J. J., Dou, B. C., Li, X. H., You, D. Q., Tang, Y., and Liu, Q. H.: Coarse scale in situ albedo observations over heterogeneous snow-free land surfaces and validation strategy: A case of MODIS albedo products preliminary validation over northern China, *Remote Sensing of Environment*, 184, 25 - 39, doi: 10.1016/j.rse.2016.06.013, 2016.

Yin, F., Lewis, P. E., Gomez-Dans, J., and Wu, Q. (2019, February 21). A sensor-invariant atmospheric correction method: application to Sentinel-2/MSI and Landsat 8/OLI. doi: 10.31223/osf.io/ps957

9 Comparison of blue-sky-albedo (BSA) between CGLS products and in-situ retrievals

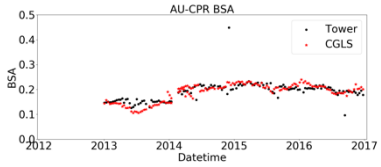

(a)

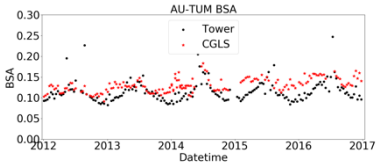

(b)

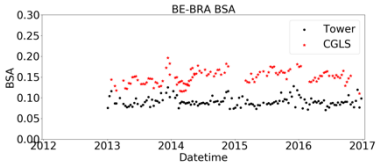

(c)

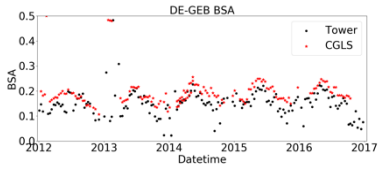

(d)

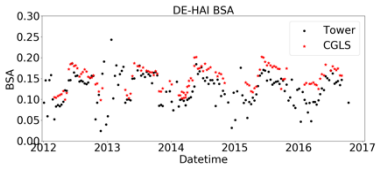

(e)

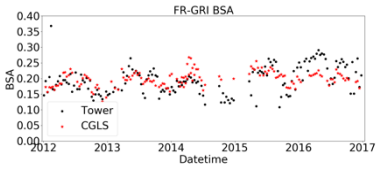

(f)

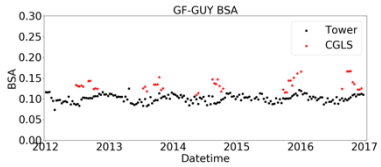

(g)

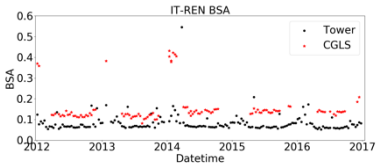

(h)

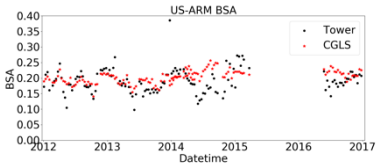

(i)

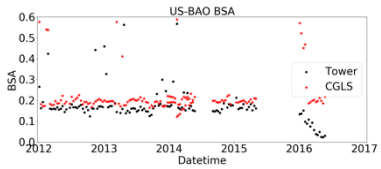

(j)

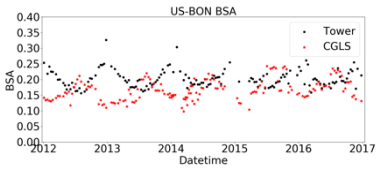

(k)

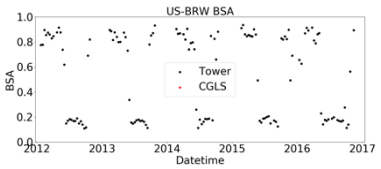

(l)

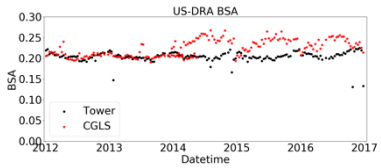

(m)

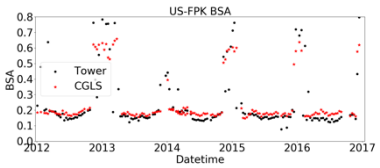

(n)

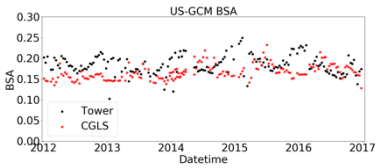

(o)

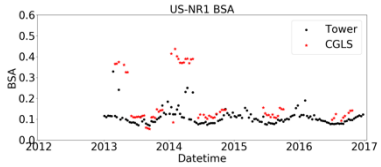

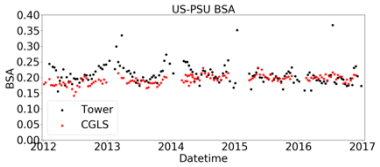

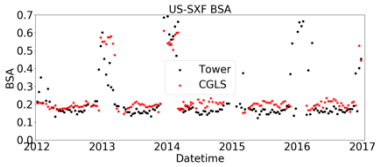

(p) (q) (r)

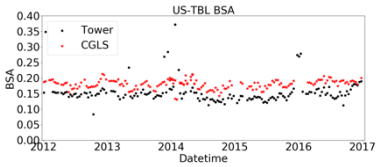

(s)

End of Document